

University of Nevada, Reno

**Human Endothelial Progenitor Cells:
A Novel and Promising Cellular Therapy
for Regenerative Medicine**

A dissertation submitted in partial fulfillment of
the requirements for the degree of Doctor of Philosophy in
Cellular and Molecular Biology

By

Joshua A. Wood, MS

Dr. Graça Almeida-Porada, MD, PhD / Dissertation Advisor

May, 2009



University of Nevada, Reno
Statewide • Worldwide

THE GRADUATE SCHOOL

We recommend that the dissertation
prepared under our supervision by

JOSHUA A. WOOD, MS

entitled

**Human Endothelial Progenitor Cells:
A Novel and Promising Cellular Therapy for Regenerative Medicine**

be accepted in partial fulfillment of the
requirements for the degree of

DOCTOR OF PHILOSOPHY

Graca Almeida-Porada, MD, PhD, Advisor

Esmail Zanjani, PhD, Committee Member

Christopher D. Porada, PhD, Committee Member

Luis Gomez-Raya, PhD, Committee Member

Marsha Urban, PhD, Graduate School Representative

Marsha H. Read, Ph. D., Associate Dean, Graduate School

May, 2009

Abstract

Endothelial progenitor cells represent a novel and promising therapy for a myriad of tissues and conditions including diseases and disorders of the liver and small intestine. Cirrhosis and other diseases have created a need for a readily available supply of hepatocytes and supporting cells in diseased and scarred liver. Following chemo/radiation therapy and inflammatory bowel disease, the cell populations of the small intestine are diminished and a cell therapy for the replenishment of these populations is needed. Additionally, the cellular markers to identify both EPCs and mesenchymal stem cells (MSCs) have been defined in the literature but a debate remains as to the heterogenic vs. homogenic nature of the cell populations. This dissertation investigates the engraftment potential of EPCs in the liver when transplanted (Tx) *In Utero* into the pre-immune sheep model via two routes of injection, Intra-hepatic (IH) and Intra-peritoneal (IP). Upon finding engraftment, the contribution of these cells to vasculature and parenchymal tissue as well as their differentiative potential in contribution to the developing liver was investigated. Tx EPCs engraft albeit at low levels but preferentially associate with vasculature. In addition to their association with vasculature, the EPCs maintain the expression of endothelial markers in addition to expressing markers ranging from fully differentiated hepatic cells to liver stem cells. In addition to their contribution to the liver, EPCs not only engraft into the small intestine but do so in a preferential manner in the area containing the crypts of Lieberkühn (above the muscularis mucosa and below the crypt-villus junction). Upon transplantation, these cells actively engraft and differentiate into both intestinal stem cells (ISCs) and into the supporting cell types of the ISC niche as well as mature cells of the intestinal

parenchyma. Finally, LAM-PCR and LM-PCR were employed to identify vector integration sites in both MSCs and EPCs transfected with a variety of retroviruses. These experiments are designed to address the existence of a heterogeneous or homogenous population in both the EPC and MSC populations. Further testing on an experimental sample reveals the presence of chimeric DNA in the sample and successful amplification of integration sites in this sample is pending further investigation.

ACKNOWLEDGEMENTS

Thank you to my mentor, Graça Almeida-Porada, MD, PhD whose unending dedication to my advancement as a scientist made this dissertation possible. I would also like to thank Evan J. Colletti, PhD for his continuous training and guidance in the pursuit of my dreams.

Thank you to the members of my committee, Dr. Esmail Zanjani, Dr. Christopher D. Porada, Dr. Luis Gomez-Raya, and Dr. Marsha Urban for your continued dedication to my progression and ongoing guidance.

Thank you to the past and present members of the Almeida-Porada and Porada Labs, for your daily input that made this work possible. As many of you already know, the success of a lab and its scientists is a team effort, and I would not be here otherwise.

Thank you to my wife. Brittany, without your emotional and intellectual support and understanding I would not be who I am today. Your love is a pillar in my life and a key to my success.

Thank you to all of you that listened as I told you about my research. I cannot count the hours that friends and family have tolerantly listened to me and provided both input and emotional support. It is genuinely appreciated.

TABLE OF CONTENTS	PAGE
Chapter 1: Introduction	1
Embryonic Stem Cells	5
Adult Stem Cells	7
Mesenchymal Stem Cells	8
Endothelial Progenitor Cells	13
Study Model Systems	20
Discosoma Red	22
Retroviral Integration	25
References	28
Chapter 2: Human Cord Blood Derived Endothelial Progenitor Cells Engraft Following <i>In Utero</i> Transplantation, Integrate into the Developing Cytoarchitecture and Contribute to Ongoing Vasculogenesis in the Liver	32
Abstract	33
Introduction	34
Results	39
Discussion	48
Methods and Materials	49
References	54
Chapter 3: Human Endothelial Progenitor Cells: A Novel and Promising Cellular Therapy for Regenerating Intestinal Mucosa	58
Abstract	59
Introduction	61
Results	66

Discussion	74
Methods and Materials	76
References	81
Chapter 4: Retroviral Integration Site Analysis of HIV and MSCV in MSCs & EPCs	85
Abstract	86
Introduction	86
Results	93
Discussion	101
Methods and Materials	103
References	114
Chapter 5: Conclusions	116
References	124
Glossary of Cellular Proteins and Labels	125
References	132

LIST OF FIGURES AND TABLES

FIGURE/TABLE	PAGE
Chapter 2	
Tbl. 2.1 EPCs engraft in the bone marrow of transplanted animals.	40
Fig. 2.1. EPCs engraft into the liver and preferentially contribute to vasculature based on the route of engraftment.	41
Fig. 2.2 In Situ labeling of EPCs.	42
Fig. 2.3 Engrafted EPCs maintain CD31 and vWF positivity in the liver based on the route of engraftment.	44
Fig. 2.4 EPCs participate in the cytoarchitecture of the chimeric liver.	46
Fig. 2.5 Engrafted EPCs contribute to the development and function of the liver.	47
Fig. 2.6 Outline of experimental protocol	50
Chapter 3	
Fig. 3.1 EPCs retain DsRed expression and preferentially engraft near the crypts of Lieberkühn.	67
Fig. 3.2 In Situ Labeling of Engrafted EPCs	69
Fig. 3.3 EPCs contribute to the intestinal stem cell (ISC) population.	71
Fig. 3.4 EPCs contribute to the intestinal stem cell niche.	72
Fig. 3.5 EPCs contribute to the intestinal cell population.	73
Fig. 3.6 Outline of experimental protocol	76
Chapter 4	
Fig. 4.1 Linear amplification mediated (LAM)-PCR.	89
Fig. 4.2 Linker Mediated (LM)-PCR.	91

Fig. 4.3	TOPO cloning of 2 nd Nested PCR products.	92
Fig. 4.4	Bands identified in the positive control sample to be TOPO cloned.	95
Fig. 4.5	Positive control HIV-based vector positive control vector integration site.	97
Fig. 4.6	Vector integration sites identified using LM-PCR on the HIV-based positive control MSC DNA.	99
Fig. 4.7	LM-PCR of MSCV positive control and chimeric samples.	100
Fig. 4.8	2288 Intestine DNA can be amplified and is chimeric.	101
Tbl. 4.1	Standard PCR reaction program for LAM-PCR.	104
Fig. 4.9	Outline of Linear Amplification Mediated (LAM)-PCR protocol.	106
Tbl. 4.2	Standard DNA digestion for LM-PCR.	108
Tbl. 4.3	Standard Linker Cassette Ligation.	109
Tbl. 4.4	Standard PCR reaction program for LAM-PCR.	110
Fig. 4.10	Outline of Linker Mediated (LM)-PCR.	110

Chapter 1: Introduction
Stem Cells and Retroviruses

The goal of the projects and experiments presented in this dissertation is to study the engraftment and differentiative potential of two types of adult stem cells: mesenchymal stem cells (MSCs) and endothelial progenitor cells (EPCs). In contrast to embryonic stem cells that are collected from the blastula, adult stem cells are collected from several adult tissues including MSCs and EPCs as well as a variety of other stem cell types. While the role of EPCs in vasculogenesis is currently being studied by several investigators, very little research is being done to determine any additional roles these cells may play in the body. To further explain the role of EPCs, these cells were transplanted into the fetal sheep model (please see description of the model below). Following collection of the tissue, immunofluorescent techniques were employed to examine the chimeric fetal tissue to determine the role of EPCs in the liver and small intestine of the developing sheep fetus. In contrast to EPCs, a great deal of research about the engraftment and differentiative potential of mesenchymal stem cells has been conducted. However, there remains a debate as to the heterogeneity of this cell population. Specifically, it is still unclear as to whether a population of MSCs contains a mixture of different types of stem cells with unique differentiative abilities or a homogeneous mixture of stem cells where the entire population has the same capabilities. In an effort to elucidate this question, a PCR technique known as linear amplification mediated polymerase chain reaction (LAM-PCR) was employed.

LAM-PCR was initially developed to track retroviral integration sites into cellular DNA following concerns of insertional mutagenesis in a gene therapy trial.^{1,2} Several children were given a retroviral vector containing the gene to replace their absent gamma-common chain of the interleukin-2 receptor gene.^{3,4} The clinical symptoms of

the absent gene are severe combined immunodeficiency which results in death by two years of age unless the child is raised in an essentially sterile environment. The gene therapy trial was initially successful in that all but one of the children in the study experienced restoration of the interleukin-2 receptor and elimination of the immunodeficiency; some of the children in the study then experienced the onset of leukemia.⁵ LAM-PCR analysis revealed that the retroviral vector had integrated into the DNA of the afflicted children upstream of the LMO-2 oncogene. The result of this integration was the activation of the oncogene and the onset of leukemia in addition to the expression of the functional interleukin 2 gene and correction of the immunodeficiency. The leukemia was effectively treated using chemotherapy and the gene therapy trial was ultimately considered a success, but the safety of gene therapy was questioned.⁶

While LAM-PCR analysis in our studies of engrafted MSCs is not primarily intended to answer safety questions, the question would be addressed by the successful sequencing of vector integration sites. The primary goal is to take advantage of the semi-random nature of retroviral integration. It is highly unlikely that two retroviruses will integrate between the same two base pairs in different cells. Therefore, each retroviral integration site serves as a unique identifier of the cell it is contained in. Identification of these retroviral integration sites provides the opportunity to track engrafted MSCs and their daughter cells at the clonal level. By identifying individual cells and their progeny, the heterogeneity vs. homogeneity question that was previously proposed can be addressed. If the integration sites found in one tissue source are not in common with the integration sites found in another tissue source then there is evidence that different sub-

populations of what we commonly refer to as MSCs may exist. However, if integration sites are found in common across the various tissue sources then there is strong evidence that the currently defined populations of MSCs are homogeneous. The role of the genes found immediately downstream of these integration sites can then be used to analyze the risks of insertional mutagenesis when using these vectors in gene therapy.

While LAM-PCR and LM-PCR are employed to investigate the integration sites of MSCs, a much more fundamental question is posed for the investigation of EPCs. Previous work has demonstrated the role of EPCs in vessel formation both *In vitro* and *In vivo*. These cells have also been shown to result in the process of *de novo* blood vessel formation or vasculogenesis.⁷⁻⁹ However, the role of endothelial cells in the body is much greater than simply blood vessel lining and this evidence suggests that EPCs may play a greater role in the body as well. In light of this knowledge we proposed to investigate the role of these cells throughout the body. To answer this question we performed an *In utero* transplantation of human EPCs into the pre-immune fetal sheep model. In order to effectively identify engrafted EPCs, we first transduced these cells with a vector that expresses the red fluorescent protein, DsRed. Following transplantation, the tissues were collected and preserved for later analysis. In order to analyze engraftment, the preserved tissues were sectioned. Following the identification of engraftment, the roles these cells were playing in the various cellular microenvironments in which they were found were investigated.

The investigation of the engraftment and differentiative potential of EPCs in the body began with the liver. The regenerative capabilities of the liver have been previously demonstrated and an active population of stem cells is known to be present in this organ.

In investigating the population of stem cells that lead to liver regeneration, we wanted to know what role, if any, EPCs play in the liver. We already know that there is a large amount of vascularization in the liver and hypothesized that the human EPCs would contribute to the vasculature in the developing liver at a minimum.

It is also known that there is a large population on epithelial and endothelial cells in the small intestine. Furthermore, depletion of the small intestine occurs as a side effect of chemo/ radiation therapy and depletion of the small intestine occurs directly as a result of diseases such as inflammatory bowel disease or as a result of eating disorders such as anorexia. A readily available supply of stem cells that could be transplanted to restore the cell populations in the small intestine would represent a novel breakthrough in the treatment of these side effects, diseases, and disorders.^{10,11} Consequently, we studied the engraftment and differentiation of EPCs in the small intestine.

Embryonic Stem Cells

Adult stem cells such as MSCs and EPCs have a great deal of differentiative potential but embryonic stem cells possess essentially unlimited differentiative potential. First isolated and cultured in 1998 by James Thomson, ESCs come from the blastocyst that forms approximately five days following fertilization.^{12,13} At this point in development the blastocyst is composed of an inner cell mass, where the ESCs are derived from, and an outer ring of cells called the trophoblast.^{14,15} The trophoblast later gives rise to the placenta while the pluripotent ESCs that compose the inner cell mass give rise to the fetus.¹⁵ ESCs are known to be truly pluripotent because they can differentiate into any cell type across the three germ layers. ESCs are also capable of essentially unlimited self-renewal. The three germ layers are distinguishable at later

developmental stages after some level of differentiation of the ESCs has occurred. These three germ layers are the endoderm, mesoderm, and ectoderm. The endoderm is responsible for giving rise to the liver, pancreas, lungs, thyroid, and gastrointestinal tract.¹⁶ In contrast, the mesoderm gives rise to the skeleton, muscles, heart, spleen, and kidney.¹⁷ Finally, the ectoderm gives rise to the nervous system, lenses of the eyes, tooth enamel, and the epidermal skin layer.¹³ ESCs can undergo both symmetric and asymmetric division.¹⁸ In symmetric division, one ESC divides into two daughter ESCs but in asymmetric division, an ESC divides into a daughter ESC and a daughter progenitor cell.¹⁸ This progenitor cell then proceeds down a path of differentiation ultimately resulting in a specific cell type in a specific tissue or organ.^{12,13,15} In the past there has been a great deal of controversy surrounding the source of ESCs.

Originally, these cells could only be extracted from the blastocyst of a fertilized embryo and the process resulted in the destruction of the embryo.¹⁸ The primary source for human ESCs is subsequently the fertilized embryos that would otherwise be discarded from fertility clinics.¹⁸ The ethics of deriving ESCs from this source has led to a great deal of public controversy. As a result of this controversy, federally funded ESC research in the United States had been limited to cell lines that were cultured before the legislation was passed in 2001 until President Obama recently lifted the ban.^{19,20} Given these limitations, science has advanced to the point where ESCs are being derived from the morphologically earlier blastomere without destroying the blastomere or the eventual blastocyst and from disaggregated blastocysts that will never form an embryo and are unsuitable for transfer.¹⁸ Additionally, ESCs are being derived from bioengineered embryo-like artifacts, reprogramming of somatic cells back to pluripotency, and non-

harmful biopsy of living *In vitro* fertilized embryos.^{21,22} While progress is being made, the promised potential of ESCs has yet to be realized.²¹

A more fundamental problem with ESCs is that they may be too primitive. The ability to successfully differentiate ESCs into adult tissue in the clinical setting has yet to be fully realized. The microenvironment from which these cells are being taken is very early (i.e. embryonic) in development and the microenvironment in which they are required to function in the clinical setting is fetal at the earliest but more commonly it is adult. The difference in microenvironments is different enough that direct transplant of ESC into the adult environment often results in the formation of teratomas and other tumors.^{23,24} To address these issues, ESCs are often differentiated *In vitro* prior to transplant. This procedure has its own limitations and associated risks.²⁵ In contrast to differentiated ESCs, a readily available supply of adult stem cells is often available.

Adult Stem Cells (ASCs)

Alternative to ESCs, ASCs exist in a variety of tissues and can be obtained from adult tissue sources. By obtaining these cells from adult sources, all of the controversy surrounding the source of ESCs is negated. ASCs are more differentiated cells and thus perform better in an adult cellular environment. Teratomas do not result following adult stem cell transplantation.^{22,26} These cells can also be difficult to isolate and culture depending on the tissue source desired. For instance, neural stem cells (NSCs) can be obtained from the brains of adult patients but this procedure is rather invasive. However, populations of more potent stem cells exist in more easily accessed sources. For example, mesenchymal stem cells (MSCs), are derived from the bone marrow and have been shown to give rise to neurons and neural stem cells *In vivo* in a xenotransplantation

model.^{27,28} Additionally, readily accessible adult stem cells like MSCs are now being isolated and dedifferentiated into ESC-like cells. Through the introduction the *Oct4*, *Klf4*, and *Sox* genes, differentiated adult cells can be dedifferentiated into ESC like cells. These induced pluripotent stem cells (iPS) must then be differentiated into the desired cell type but the cells can be collected allogeneically and immune rejection can be avoided.²⁹

Doubts were raised in 2002 that fusion rather than actual differentiation was occurring.¹³ In this argument investigators suspected that the engrafted stem cell was fusing to a differentiated cell in the tissue it engrafted in. The result of this fusion, according to the investigators, was that the stem cell appears to have contributed to the local cellular environment through differentiation because the fused cell exhibited both stem cell and differentiated cell characteristics but the stem cell had not actually made a contribution because true differentiation had not occurred.¹³ While this argument is still not completely laid to rest, our lab and others have demonstrated that fusion is not occurring upon stem cell transplantation and engraftment in our model of transplantation.³⁰⁻³³

Mesenchymal Stem Cells (MSCs)

Cohnheim performed what are perhaps the earliest experiments with MSCs when he found that fibroblasts that produce collagen during wound repair may have come from the bone marrow.³² McCulloch and Till described the clonal nature of cells extracted from bone marrow in the 1960's.^{34,35} The original term for MSCs, colony-forming unit-fibroblasts (CFU-f), was then coined by Friedenstein in the 1970's in a paper reporting the clonogenic potential of multipotent bone marrow cells using an *ex-vivo* assay.^{33,36,37}

To date, the CFU-f culturing technique of plating ficoll-purified bone marrow monocytes in cell culture flasks is still employed.^{32,38} Ficoll-purification simply separates the cells based on density during centrifugation allowing the isolation of the mononuclear cells from red-blood cells.³² However, STRO-1+ cells are often selected before plating and are considered pure MSCs. In either case, the adherent cells following 24-48hrs of culturing are considered the MSC population.^{33,38}

The traditional appearance of an MSC is that of a small cell body with a few thin but long extensions. The cell body is inherently long and thin but features a round nucleus with a visible nucleolus.³² Traditionally, MSCs express CD105 and CD73 (the SH2 and SH3/4 domains), as well as CD44, CD90, CD71, CD106, and Stro-1. Isolation of MSCs involves ficoll separation of the mononuclear cell layer followed by selection of the Stro-1⁺, Gly A⁻, & Lin⁻ cell population.³⁰ MSCs do not express cell markers that are related to hematopoietic cells such as CD34 or CD45 they also do not express the endothelial cell marker CD31.³² The definition and significance of these markers can be found in the glossary of terms. MSCs are a very diverse population of stem cells that have been classically shown to give rise to tissues of the mesoderm layer. These tissues include osteoblasts, chondrocytes, myocytes, and adipocytes.^{32,39} Like any other stem cell, MSCs are capable of both symmetric (producing two daughter stem cells) and asymmetric (producing one stem cell and one progenitor cell) division.²⁶ Recently, our lab and others have shown that MSCs are also capable of giving rise to tissues including brain, liver, kidney, lung, spleen, thymus, pancreas, intestine, heart, and the hematopoietic system.^{26,28,39} These cells are primarily collected from bone marrow though MSCs and MSC-like cells have been found in other sources such as cord blood,

amniotic fluid, and even adipose tissue.³² Therefore, MSCs have potential in the treatment of diseases related to degradation of a myriad of tissues.

The oldest applications of MSCs have been in the generation of bone. Several labs have previously demonstrated the ability of MSCs to give rise to bone *In vitro* and clinical use of MSCs in trials to correct osteogenesis imperfecta are currently being conducted.⁴⁰ Along similar lines, MSCs have also been used to produce cartilage and combined with their ability to produce bone; these cells show promising results in the treatment of a myriad of skeletal disorders.⁴¹ MSCs have also been used to generate myocytes and to engraft and restore dystrophin expression in the mouse muscular dystrophy (mdx) model.²⁸

With respect to the ability of MSCs to differentiate into cell types outside the mesenchymal layer, MSCs have been found to give rise to cells of both the neural and glial cell types. These findings make MSCs important in the treatment of central nervous system (CNS) disorders including demyelination and in mediating repair following spinal cord injury.⁴² In addition to the ability of MSCs to give rise to neural tissues, MSCs have also been shown to give rise to cardiomyocytes and to endothelium thus making them promising candidates in the treatment of heart disease and in blood vessel formation.⁴³ MSCs have also been used to produce pancreatic islet beta cells that are capable of producing insulin.³⁹ As a result MSCs are being investigated for the use in treatment of type I diabetes. Our lab and others have also shown that MSCs are capable of giving rise to hepatocytes and thus these cells also show promise in the treatment of liver diseases and in liver regeneration.^{44,45} Finally, MSCs are also easily transduced and expanded *In vitro* making them ideal candidates to serve as gene delivery vehicles. Ultimately, MSCs

are a very promising candidate for treatment of a variety of disorders and for use in gene therapy.²⁸

While MSCs represent many novel and promising therapies, they are only a very small fraction of the nucleated cells isolated from bone marrow. MSCs compose only 0.001%-0.01% of this population of cells.⁴⁶ It is the high efficiency with which they can be expanded that enables them to be used so effectively.^{28,46} In addition to their ability to expand, their ability to home to injury sites has been demonstrated by several investigators and is critical to the therapeutic potential of MSCs. The ability of MSCs to home to the site of an injury has been demonstrated through intravenous injection following bone fracture, myocardial infarction, and ischaemic cerebral injury. MSCs have also been shown to repair the meniscus and cartilage following intraarticular injection after traumatic injury.⁴⁶

Following the irradiation of mice, MSCs have been shown to home to the bone marrow and spleen again demonstrating their migration to the site of injury. The exact mechanism of homing has yet to be fully elucidated.⁴⁶ It is known that the critical step in homing and adherence is rolling. Rolling is the process by which a cell begins to bind with low affinity to vascular endothelium in a shear resistant manner. This process slows the cell effectively separating it from the more rapidly circulating cells. CD44 has recently been discovered to be critical in this process. CD44 is a large family of adhesion molecules containing transmembrane glycoproteins. Furthermore, the glycosylation pattern on the surface markers affects its binding and this results in effective binding signatures for specific homing.⁴⁷ Additionally, Wang et al. demonstrated that the chemokine monocyte chemoattractant protein-1 (MCP-1) up-regulated the engraftment of

MSCs following cerebral ischaemic injury. MCP-1 is not normally present but appears following injury and was shown to be chemotactic for MSCs.⁴⁶

As important as homing, MSCs self-renewal and maintenance is also not completely understood. Self-renewal is the ability of the stem cell to maintain an undifferentiated state. One of the key players in self-renewal is thought to be leukemia inhibitory factor (LIF) as it not only helps maintain the dedifferentiated state but also represses osteoblast and osteoclast activities. Fibroblast growth factor 2 (FGF2) also contributes to maintaining the stemness of an MSC though its mechanism is also unknown. Additionally, recent evidence suggests that mammalian homologues of the *Drosophila* wingless (Wnts) may play a role in maintaining stemness. Particularly, Wnt3a increased long-term *In vitro* culture of MSCs.²⁶

The maintenance of MSC and control of either symmetric or asymmetric division is the product of the local cellular and extracellular environment the cells reside in. This environment is referred to as the niche or in this case, the MSC niche. The idea of a niche was first introduced by Schofield in 1978 and is meant to encompass all of the elements surrounding a stem cell. Recent evidence indicates the MSC niche is perivascular in nature. MSC are commonly found lining vessels and this location allows them to easily enter circulation. Additionally, many cell surface markers common to perivascular cells are expressed on MSCs including alpha smooth muscle actin. Additionally, the local extracellular environment in the bone marrow is inherently hypoxic. The hypoxic environment has been found to increase the proliferative ability of MSCs in culture and increased expression of oct-4 and rex-1 (genes commonly expressed

in ESCs). However, no specific soluble or insoluble extracellular matrix proteins have been found that contribute to the MSC niche.²⁶

While a great deal remains to be discovered in the control, self-renewal, migration, and engraftment of MSCs, these cells represent a promising cellular therapy option for the treatment of a large number of diseases and disorders ranging from neuron formation to non-hematopoietic bone marrow repopulation. Additionally, MSCs are found in a variety of tissue ranging from bone marrow where they were first characterized to liver and lung where they have only recently been discovered. Despite the limited number of MSCs that exist in any tissue, the ease with which they can be expanded in culture lends them to autologous transplantation.^{26,28,32,39} Furthermore, as the supporting MSC niche continues to be elucidated, their ability to expand and differentiate in culture will only increase.⁴⁸

Endothelial Progenitor Cells (EPCs)

Endothelial progenitor cells (EPCs) are a population of cells responsible for *de novo* blood vessel synthesis. Traditionally, as EPCs differentiate they become endothelial cells which are the cells that are responsible for lining the blood vessels. Endothelium controls the delivery of hormones, vasoactive autocooids, proliferative signals and circulating cells to the appropriate targets.⁴⁹ Endothelium also forms a continuous layer between blood and tissue and the endothelial cells are thought to turnover every 1-3 years in major vessels.⁴⁹ Initially, EPCs cells were thought only to exist in the developing embryo as the vast majority of *de novo* or new blood vessel synthesis occurs during this stage. *De novo* synthesis of vasculature has subsequently been termed “vasculogenesis.” However, in the 1990’s a population of adult circulating

EPCs was discovered and first characterized by Ashara and colleagues⁷. Ashara also found that the adult populations of EPCs are derived from the bone marrow.

The first observation of endothelial cell differentiation was found in yolk sac blood islands 100 years ago. The idea that circulating cells give rise to endothelial cells has been published as far back as 1932. In the same year, capillary like structures were documented in cultures of leukocytes.⁵⁰ The following year the development of organized vessels in blood vessel cultures was reported, and in 1950 it was found that blood vessels can form from cultured bone marrow. In 1985 and 1987, two separate studies concluded that endothelial cells are derived from blood cells as opposed to the cells composing the blood vessel walls.⁵⁰ In 1994, a group studying polytetrafluoroethylene pieces suspended in the aorta of dogs found that a population of circulating cells with possible stem cell characteristics left the pieces covered with endothelial cells, smooth muscle cells, macrophages, monocytes, and capillary-like structures.⁵⁰

When Ashara and colleagues reported the isolation of EPCs from human peripheral blood in 1997 they found evidence that hemangioblasts may be present in blood.^{7,50} Hemangioblasts are a hematopoietic stem cell and endothelial progenitor cell precursor thought to exist in the embryo but disputed in adults.^{50,51} The term was coined in the early 1900s when Sabin postulated that hematopoietic and endothelial lineages must have a common progenitor based on their spatial and temporal proximity.⁵² That is to say, in the blood islands of the embryo hematopoietic stem cells are known to develop in the center and EPCs are known to develop from the periphery. While a great deal of indirect evidence has supported the existence of the hemangioblast, mostly based on

expression of endothelial and hematopoietic markers during development, no *In vivo* evidence that directly identifies the hemangioblast has been observed.^{52,53} For this reason the existence of the hemangioblast is disputed.⁵² As an alternative, EPCs are proposed to originate from the angioblast which is simply a primitive cell on the periphery of the embryonic blood islands that gives rise to EPCs.⁵²

Further controversy has surrounded EPC research in the form a dispute over the culturing techniques. A commercially available kit became commonly used for the isolation of EPCs from bone marrow mononuclear cells separate by centrifugation on a ficoll density gradient. In the commercially available method the mononuclear cells were then plated on fibronectin coated plates and the non-adherent cells were collected and replated. In a Blood 2007 paper by Yoder et al., these cells were termed colony forming unit-endothelial cells (CFU-EC). Yoder et al. then clearly demonstrates that these cells give rise to fibroblasts and macrophages but do not give rise to endothelial cells. This finding is consistent with the clinical evidence observed as a short benefit in the patients blood system is observed but no long term benefit nor blood vessel formation was found.⁸ However, it should be noted that the author's who coined the term "CFU-EC" dispute that what they defined as CFU-EC are in fact a population of EPCs and while they do not dispute the findings Yoder et al. makes, they argue that the cells isolated from the commercial kit should be named after the kit's designer and thus should be named CFU-Hill to avoid confusion with what they define as CFU-ECs.⁵⁴

In contrast to CFU-EC, Yoder et al. defines a population of endothelial colony forming cells (ECFCs). ECFCs are derived using the same mononuclear cell layer described in the isolation of CFU-ECs but these cells are instead plated on collagen I.

The non-adherent cells are then removed and the adherent cells form colonies and compose the ECFCs. Yoder et al. not only demonstrates that ECFC express all of the classic endothelial cell markers but form chimeric blood vessels when transplanted *In vivo* as well.⁸ The ECFC provided by Dr. Yoder are the cells employed in all of the EPC experiments presented and discussed in later chapters with the exception that the EPCs used in the experiments discussed were isolated from umbilical cord blood and peripheral blood where EPCs have also been found.⁵⁵

In the majority of cases EPCs have been used to study vessel formation particularly in following ischemic injury. These cells promote the revascularization and evidence indicates that they help improve organ function following a period of oxygen deprivation (ischemic injury) to the tissue. The mobilization and recruitment of EPCs to the wound site is promoted through elevated levels of vascular endothelial cell growth factor (VEGF), stromal cell-derived factor (SDF-1), granulocyte colony-stimulating factor (GCSF), and granulocyte-monocyte colony-stimulating factor (GM-CSF). Intravenous administration is sufficient to introduce EPCs to a wound site but improved engraftment was found when more targeted delivery was applied. This was mostly due to the fact that intravenous dosing results in some level of trapping and sequestration in various organs.⁹

The level of contribution by EPCs and their progenitors to vessel formation ranged from 1-25% depending on the study and angiogenesis was also observed to increase contributing evidence to the idea the EPCs promote vasculogenesis. This evidence also suggests that hormone secretion may be occurring in a paracrine manner thus supporting local angiogenesis. In the corresponding clinical trials following cardiac

ischemic injury, increases were observed in the left ventricular ejection fraction corresponding to a decrease in endsystolic volume and shrinkage of the infarct size. Thickening of the left ventricular wall and improvement in exercise capacity have been observed as well.⁹

EPCs have also been documented exhibiting vasculogenic capabilities in the lung. While vasculogenesis in the adult non-injury model is not readily observed, a population of highly proliferative microvascular EPCs has been observed.⁴⁹ Due to the high demand for cellular turnover in vascular homeostasis and repair in the lung, the microvascular EPC identified in the lung have the most proliferative capability documented to date.⁴⁹ This discovery indicate that EPCs may be important in the treatment of pulmonary occlusive disease, idiopathic interstitial pneumonia, and a host of other pulmonary diseases.⁴⁹

In addition to their contribution following ischemic injury, EPCs are also involved in the vascularization of tumors. In particular, these cells have been studied with respect to angiogenesis. Studies have demonstrated the recruitment of endothelial cells to tumor cites and that circulating EPCs are increased during the angiogenic phase of breast cancer.⁹ However, the specific dependence of tumor vasculature on recruited EPCs remains disputed. The level of dependence has ranged from 0% to 90% depending on the model in animal model studies. The contribution of recruited EPCs to tumors in human patients averaged 4.8% and ranged from 1% to 12%. Furthermore, certain populations of EPCs have been isolated that contribute to lymphatic growth. When these cells are depleted tumor growth retardation is also observed. The evidence that EPCs may target tumors had lead to their development as gene or cell therapy vehicles. In mice, EPCs

carrying a suicide gene resulted in a reduction in tumor volume and lung metastasis though human studies have not yet been performed.⁹

EPCs have also been employed in the vascularization of engineered tissue. Current research is using EPCs to seed small-diameter prosthetic bypass grafts as their previous failures have been primarily attributed to thrombosis caused by delayed endothelization. Bone marrow (BM) derived cells (possibly including MSCs and HSCs) were shown to increase the endothelization of Dacron vascular grafts in dogs.⁹ The mobilization of leukocytes resulted in similar endothelization of grafts as well.⁹

EPCs also have a role in *In utero* therapy due to the fact that they can incorporate into developing vasculature. Vasculogenesis occurs during the early neonatal periods of normal organs and has not been observed in adult organs. This evidence indicates that *In utero* transplantation of EPCs may be used to correct vasculogenesis in congenital diseases.⁹ However, EPCs first appear in appreciable levels in the cord blood of later gestation infants, around 37-40 weeks. This is in contrast to MSCs and HSCs which are known to appear much earlier in gestation.⁵⁶

Directly defining the EPC population can be challenging due to the fact that hematopoietic stem cells (HSCs) express many of the same cellular markers. One of the key differences between HSCs and EPCs is the expression of the cell marker CD45 which is present only on cells of a hematopoietic lineage. EPCs commonly express the cellular markers: CD141, CD105, CD146, von Willebrand Factor (vWF), CD34, CD133, and CD117. However, CD34, CD133, and CD117 are also known to be expressed on HSCs.⁵⁵ While ECFCs are the cells employed in all of the experiments performed by our lab, multiple sub-populations of EPCs exist and have been defined. The major EPC sub-

types described to date are separated based on whether they are circulating or resident in the local blood vessel wall. Within the resident group there are: conduit-intima-derived EPCs, conduit-vessel wall-derived EPCs, and Microcirculation derived EPCs. Within the circulating EPC group there are: CFU-EC (CFU-Hill), ECFC, and multipotent adult progenitors.⁴⁹

All of the EPC populations express the cell markers CD31, CD34, vascular endothelial growth factor receptor 2 (VEGFR2), and vWF. Additionally, all of these cells types are capable of vasculogenesis except for the CFU-ECs which also happen to be positive for the leukocyte marker CD45. However, the conduit-vessel wall derived EPCs are also CD45 positive but engage in vasculogenesis indicating that CD45 does not guarantee an EPC is incapable of vascular contribution. CD133 expression remains unknown on many of the EPC subsets though they are known to be expressed on ECFCs.⁴⁹

Ultimately, the EPC population with the ability to contribute to vasculature and demonstrate the most undifferentiated state are those cells isolated by Dr. Yoder and termed ECFCs. These cells classically express CD31, CD34, vWF, and CD133 but not CD45. EPCs are responsible for the generation of the endothelium which is responsible for the homing of circulating cells and hormones involved in a myriad of processes in the body. EPCs are known to originate from embryonic blood islands, but the existence of the hemangioblast is disputed.⁵² In any case, EPCs can be isolated from bone marrow, peripheral blood, and umbilical cord blood. In the non-injury model, EPCs are responsible for the natural turnover of macrovessels every 1-3 years and much more frequently in microvasculature. EPCs have classically been studied with respect to

treatment of ischemic injury though they have also shown some potential in the treatment of pulmonary disease. EPCs are also important in the angiogenic and vasculogenic phases of cancer and have been studied as potential gene and cellular therapy vehicles. Furthermore, studies are beginning to be conducted that employ EPCs for the endothelialization of engineered vessels and tissues and in the ability to treat vasculogenic disorders *In utero*.

Study Model Systems

In an effort to study the potential of any stem cell host animal (*In vivo*) and cell culture (*In vitro*) models are necessary. *In vitro* models are employed by our labs and most others prior to *In vivo* transplantation models. In *In vitro* models, investigators employ culturing media along with incubation to determine the potential of stem cells. During *In vitro* testing the markers of stem cells are also determined as well as how to best purify a population. For example, Dr. Yoder first isolated, cultured, and characterized EPCs before any transplantation studies were conducted.⁵⁵ Furthermore, Dr. Yoder and other labs performed *In vitro* tests to determine the ability of EPCs to give rise to *de novo* blood vessels in matrix-gel assays.^{9,57,58} Unfortunately, *In vitro* testing cannot answer all questions surrounding the potential of a stem cell and it does not perfectly recreate the cellular environment in a living system. For these reasons, *In vivo* testing is necessary to determine the safety and efficacy on any stem cell.

In performing *In vivo* tests there are several options as to how the specific test will be performed. Cultured cells can be transplanted along with supporting structure or cellular chemicals that drive transplantation. For example, matrix-gel plugs containing EPCs have been transplanted in mice to demonstrate that the EPCs alone can give rise to

blood vessels and that these vessels will profuse with the blood of the animal. In addition to supporting media or structures, the type of transplantation must be decided. In autologous transplantation cells from an animal are extracted, expanded in culture, and transplanted back into the same animal. This technique has been used in bone marrow transplants successfully in human patients. Its advantages are that immune rejection is not a problem and engraftment is therefore the highest it can be. The disadvantage is that a healthy autologous supply of cells to extract and culture is not always available. In this case allogeneic transplantations can be employed. In allogeneic transplantations, cells from an immune matched donor are used for culturing and transplantation. While this technique has again been successful in bone marrow transplantations, complete immune tolerance remains an issue and immune suppressors must continue to be administered. Both of these techniques allow the study of cells a specific animal species to be studied within the same species. However, for safety reasons, xenotransplantation models precede any testing of human cells in humans.

Xenotransplantation is the transplantation of cells or tissue from one animal into another. This system is employed by our lab and many others to study the potential of human cells before clinical testing is attempted. Selecting the animal to employ in such studies ultimately is based on the arguments suggesting that animal most closely resembles the human physiological and cellular environment. However, the animal model employed is also based on cost and social concerns. For instance, a mouse or sheep model will often be employed before testing in a non-human primate model. Animal models for xenotransplantation of cells are very diverse and range from mice to chimps and include: dogs, sheep, cats, and a host of other species.

The sheep model is the most appropriate balance of accurate simulation of human physiology and cellular environments available to. Sheep are very similar anatomically and physiologically, excluding of course that they are ruminants. Sheep are very similar in size to humans and their general anatomy is very similar to that of humans as well. Sheep produce a similar number of offspring to humans, especially when compared to dogs, cats, or mice, and this is of particular importance because many studies are performed *In utero*. *In utero* studies employed to avoid immune rejection. By injecting our cells at 50-60 days of gestation we obtain optimal engraftment but are still in the period of time prior to complete immune system development. This means that as the immune system develops it does not distinguish our injected cells from the sheep cells and thus the cells are tolerated. In mice, animals lacking an immune system are available⁵⁹ but this has not yet been engineered in sheep and thus this option is not available to us. Therefore, our animal model for studies of stem cell potential and engraftment is the fetal sheep model following *In utero* xenotransplantation.

Discosoma Red

Discosoma Red (DsRed) is a 28-kDa fluorescent protein that provides the red coloration around the oral disk of a coral from the *Discosoma* genus.⁶⁰ In its natural state, DsRed occurs as a tetramer, four DsRed proteins joined together.⁶¹ The discovery of DsRed allowed the use of a red fluorescent label to be detected in immunofluorescence and other colorimetric applications in counter part to the more famous green fluorescent protein (GFP) which was isolated from the jellyfish, *Aequorea victoria*. In most fluorescent proteins the important motifs are several 11-stranded β -barrels. In GFP, Tyrosine (Tyr)-66 and Glycine (Gly)-67 along with Arginine (Arg)-96 and Glutamate

(Glu)-222 are important residues that contribute to the green chromophore. In the DsRed protein, it was found that the 11-stranded β -barrels were conserved as were the key residues though they had been shifted to Tyr-67, Gly-68, Arg-95, and Glu-215, respectively.^{60,62} Further study also revealed that Glutamine (Gln)-66 contributes to the formation of the chromophore.⁶¹

The results of these changes shifted the absorption and emission of the DsRed protein to 558 and 583nm, respectively.⁶⁰ The obvious result is that DsRed appears red rather than green. The difference between the emission and absorption spectrum of a given fluorophore is known as the Stokes shift and reflects the loss of vibrational energy in the excited state. DsRed is known to have a slightly larger Stokes shift than GFP but it is not as large as other red variants like mRFP or mPlum which absorb at 588nm but emit at 607nm and 649nm, respectively. However, it is important to note that mRFP is the monomeric version of the tetrameric DsRed and mPlum is a mutation of the monomeric DsRed.⁶³ This demonstrates that DsRed is capable of mutation that changes both the Stokes ratio and shifting the emission into the deep red spectrum. The extinction coefficient, which is the amount of light that can be absorbed at a particular wavelength, is documented $75,000 \text{ M}^{-1}\text{cm}^{-1}$ at the 558nm absorption which is much higher than previously thought. This evidence indicates that its emission is much stronger than previously observed. DsRed has also been shown to be relatively resistant to photobleaching though it is not impossible to photobleach.⁶⁰

An interesting characteristic of DsRed is that it actually proceeds through a green maturation phase during development.^{60,61} The formation of the chromophore is the result of a cyclization reaction followed by two subsequent dehydrogenation reactions.⁶¹

Due to the cyclization reaction, the initial absorption and emission of the DsRed protein is 475 and 499nm, respectively. As the dehydrogenation reactions proceeds, the color shift fully progresses and emission in the green spectrum is not longer observed. In the native protein this process takes up to two days but mutations in modified forms of DsRed have reduced the period greatly.^{60,61,64} The shift in emission is the result of an extension to the π -system through the dehydrogenations.^{60,61} Furthermore, while mutation of the Lysine (Lys)-83 to Met shifts the emission from 583nm to 602nm resulting in an even deeper red emission; mutating the Lys-83 to Arg results in the prevention of the color change from green to red and thus the protein appears green.⁶⁰ Further mutation experiments that tested a variety of amino acid substitutions resulted in proteins with emission spectrums that ranged from deep purple (18nm) to red including variants of blue, green, and yellow emissions.^{60,61} The shifting in color emission is related to electrostatic interactions of the chromophore to various amino acid substitutions. Further studies using non-natural amino acids and various side chain groups revealed a number of other fluorescent shift so ranging as deep red as 615nm.⁶¹

Other important characteristics of DsRed are that it appears to be pH resistant from pH=4.5 to pH=12. However, at acidic pHs below 4.5 the emission spectrum disappears and no red fluorescence is detected.⁶⁰ Additionally, like GFP, DsRed is found to form aggregates though DsRed forms tetramers as opposed to GFPs dimmers but further mutations in the DsRed sequence have lead to the development of DsRed monomers.^{60,61} Furthermore, evidence early forms of DsRed were found to form oligomers to other proteins and may have resulted in activation of unintended signal

transduction pathways *In vivo*.⁶⁰ Mutations in the DsRed sequence have also corrected the oligomer formation problem.^{60,61}

Ultimately, DsRed is a red fluorescent protein discovered in the *Discosoma* species of coral. The initial green fluorophore is primarily the result of the cyclization of Gln66, Tyr67, and Gly68. Two subsequent dehydrogenation reactions result in the extension of the π -bond resonance and the color shift proceeds from an emission at 499nm to 583nm essentially changing from green to red. Rapidly developing variants have been developed as have variants that do not form oligomers or form tetramers. The rapidly developing monomer is the form employed in our experiments. It is also important to note that while DsRed is not overly pH sensitive, it does have a green intermediate phase and it is highly related to the other color variations of fluorescent proteins. DsRed is also readily susceptible to manipulation through electrostatic interactions with the chromophore which can result in changes in its spectrum of emission.

Retroviral Integration

The gene for the DsRed protein is often introduced into a host cell through the use of retroviruses. Retroviruses are an integral part of molecular biology and gene therapy as they allow for the incorporation of DNA into the genome of the host cell. In gene therapy, retroviruses are often used to implant a beneficial gene into the host genome. In molecular biology, retroviruses are often used to confer the expression of a marker gene such as DsRed into the DNA of a cell population of interest. Upon infection, retroviral RNA reverse transcribes into viral DNA and this DNA then integrates into the host genome. Once integrated, the viral DNA is then passed down to each daughter cell as the

cells divides. The process of retroviral integration is of extreme importance to gene therapy for two reasons: first, it allows the permanent integration of a corrective gene into the genome of the patient; second, integration into certain locations of the host genome can have deleterious results.

Perhaps the most famous instance of gene therapy involving retroviral integration is a clinical trial resulting in leukemia after a therapeutic retrovirus integrated upstream of the LMO2 proto-oncogene.^{3,5,6,65} In two separate trials, 20 patients have been treated with gene therapy vectors to insert a functional copy of the gamma-common chain of the IL-2 receptor. In the French trial, four patients contracted leukemia as a result of insertional mutagenesis upstream of the LMO-2 proto-oncogene. Three of the four patients were successfully treated using conventional anti-leukemic chemotherapy.^{3,5,6,65} The fourth patient has only recently been diagnosed and the outcome of that patient's treatment remains unpublished as does the integration sites of the gene therapy vector employed. The incidence on leukemia in these trials brought the identification of retroviral integration sites to the forefront of gene therapy.⁶⁵

Since these trials several investigators have shown evidence that retroviral integration is a semi-random process. This means that while no two vectors are statistically likely to integrate between the same two base pairs in different cells, each different type of retrovirus will integrate preferentially into certain areas of the genome. Human immunodeficiency virus (HIV) has been shown to preferentially integrate into active genes (those that are replicating regularly). Another vector, murine leukemia virus (MLV) preferentially engrafts near transcription start sites.⁶⁶ Ultimately, the tracking of retroviral integration sites has become extremely important. Several techniques have

evolved in order to sequence the integration site of retrovirus. The most recent and through method of mapping retroviral integration sites is called pyro-sequencing. This technique essentially sequences thousands of individual genomes and tracks the integration sites in each. While thorough, this technique is not necessary or economically feasible for many of our experiments. For these reasons we employed Linker Mediated (LM)-polymerase chain reactions (PCR). LM-PCR allows us to identify the exact integration site of retroviruses using the long terminal repeated (LTR) regions of the retrovirus as a primer binding site. The exact technique will be described in later chapters.

References

1. Schmidt M, Kohn HGMWGHKOSSDCJFTCLHHCEDH-PKSKDB. Efficient Characterization of Retro-, Lenti-, and Foamyvector-Transduced Cell Populations by High-Accuracy Insertion Site Sequencing. *Annals of the New York Academy of Sciences*. 2003;996:112-121.
2. Schmidt M, Zickler P, Hoffmann G, et al. Polyclonal long-term repopulating stem cell clones in a primate model. *Blood*. 2002;100:2737-2743.
3. Hacein-Bey-Abina S, Le Deist F, Carlier F, et al. Sustained Correction of X-Linked Severe Combined Immunodeficiency by ex Vivo Gene Therapy. *New England Journal of Medicine*. 2002;346:1185-1193.
4. Handgretinger R, Koscielniak E, Niethammer D, Cavazzana-Calvo M, Hacein-Bey-Abina S, Fischer A. Gene Therapy for Severe Combined Immunodeficiency Disease. *New England Journal of Medicine*. 2002;347:613-614.
5. Hacein-Bey-Abina S, Von Kalle C, Schmidt M, et al. LMO2-Associated Clonal T Cell Proliferation in Two Patients after Gene Therapy for SCID-X1. *Science*. 2003;302:415-419.
6. Baum C, von Kalle C, Staal FJT, et al. Chance or necessity? Insertional Mutagenesis in Gene Therapy and Its Consequences. *Mol Ther*. 2004;9:5-13.
7. Asahara T, Murohara T, Sullivan A, et al. Isolation of Putative Progenitor Endothelial Cells for Angiogenesis. *Science*. 1997;275:964-966.
8. Yoder MC, Mead LE, Prater D, et al. Redefining endothelial progenitor cells via clonal analysis and hematopoietic stem/progenitor cell principals. *Blood*. 2007;109:1801-1809.
9. Young PP, Vaughan DE, Hatzopoulos AK. Biologic Properties of Endothelial Progenitor Cells and Their Potential for Cell Therapy. *Progress in Cardiovascular Diseases*. 2007;49:421-429.
10. Walker MR, Stappenbeck TS. Deciphering the 'black box' of the intestinal stem cell niche: taking direction from other systems. *Current Opinion in Gastroenterology*. 2008;24:115-120.
11. Yen T-H, Wright N. The gastrointestinal tract stem cell niche. *Stem Cell Reviews*. 2006;2:203-212.
12. Thomson JA, Itskovitz-Eldor J, Shapiro SS, et al. Embryonic Stem Cell Lines Derived from Human Blastocysts. *Science*. 1998;282:1145-1147.
13. Krogh D. *Biology: A Guide to the Natural World* (ed 3rd). Upper Saddle River, NJ: Pearson Education Inc; 2005.
14. Martin GR. Isolation of a pluripotent cell line from early mouse embryos cultured in medium conditioned by teratocarcinoma stem cells. *PNAS*. 1981;78:7634-7638.
15. Raven PH, Johnson GB. *Biology: Times Mirror/Mosby College*; 1986.
16. Tremblay KD, Zaret KS. Distinct populations of endoderm cells converge to generate the embryonic liver bud and ventral foregut tissues. *Developmental Biology*. 2005;280:87-99.
17. Thiery JP, Sleeman JP. Complex networks orchestrate epithelial-mesenchymal transitions. *Molecular Cell Biology*. 2006;7:131-142.

18. Sills E, Takeuchi T, Tanaka N, Neri Q, Palermo G. Identification and isolation of embryonic stem cells in reproductive endocrinology: theoretical protocols for conservation of human embryos derived from in vitro fertilization. *Theoretical Biology and Medical Modeling*. 2005;2:25.
19. Wertz D. Embryo and stem cell research in the United States: history and politics. *Gene Therapy*. 2002;9:674-678.
20. BBC. Obama ends stem cell funding ban. *BBC News*. 2009.
21. Schulman A. The search for alternative sources of human pluripotent stem cells. *Stem Cell Reviews*. 2005;1:291-292.
22. Bioethics PsCo. White Paper: Alternative Sources of Human Pluripotent Stem Cells; 2005.
23. Nussbaum J, Minami E, Laflamme MA, et al. Transplantation of undifferentiated murine embryonic stem cells in the heart: teratoma formation and immune response. *FASEB*. 2007;21:1345-1357.
24. Qing He PTTMSJLPZEBMD-DFHAKDMMEJ. Fate of undifferentiated mouse embryonic stem cells within the rat heart: role of myocardial infarction and immune suppression. *Journal of Cellular and Molecular Medicine*. 2009;13:188-201.
25. Unger C, Skottman H, Blomberg P, Sirac Dilber M, Hovatta O. Good manufacturing practice and clinical-grade human embryonic stem cell lines. *Human Molecular Genetics*. 2008;17:R48-53.
26. Kolf CM, Cho E, Tuan RS. Biology of adult mesenchymal stem cells: regulation of niche, self-renewal and differentiation. *Arthritis Research & Therapy*. 2007;9:204.
27. Phinney DG, Prockop DJ. Concise Review: Mesenchymal Stem/Multipotent Stromal Cells: The State of Transdifferentiation and Modes of Tissue Repair Current Views. *Stem Cells*. 2007;25:2896-2902.
28. Porada CD, Zanjani ED, Almeida-Porada G. Adult Mesenchymal Stem Cells: A Pluripotent Population with Multiple Applications. *Current Stem Cells Research & Therapy*. 2006;1:231-238.
29. Nakagawa M, Koyanagi, Tanabe K, et al. Induction of pluripotent stem cells from adult human fibroblasts by defined factors. *Cell*. 2007;131:861-872.
30. Colletti EJ, Airey JA, Liu W, et al. Generation of tissue-specific cells from MSC does not require fusion or donor to host mitochondrial/membrane transfer. *Stem Cell Research*. 2009;2:125-138.
31. Almeida-Porada G, Porada C, Gupta N, Torabi A, Thain D, Zanjani ED. The human-sheep chimeras as a model for human stem cell mobilization and evaluation of hematopoietic grafts' potential. *Experimental Hematology*. 2007;35:1594-1600.
32. Chamberlain G, Fox J, Ashton B, Middleton J. Concise Review: Mesenchymal Stem Cells: Their Phenotype, Differentiation Capacity, Immunological Features, and Potential for Homing. *Stem Cells*. 2007;25:2739-2749.
33. Deans RJ, Moseley AB. Mesenchymal stem cells: Biology and potential clinical uses. *Experimental Hematology*. 2000;28:875-884.
34. Becker A, McCulloch E, Till J. Cytological Demonstration of the Clonal Nature of Spleen Colonies Derived from Transplanted Mouse Marrow Cells. *Nature*. 1963;197:452-454.

35. Siminovitch L, McCulloch E, Till J. The distribution of colony-forming cells among spleen colonies. *The Journal of Cellular and Comparative Physiology*. 1963;62:327-336.
36. Friedenstein AJ, Gorsaja JF, Kulagina NN. Fibroblast precursors in normal and irradiated mouse hematopoietic organs. *Experimental Hematology*. 1976;4:267-274.
37. Friedenstien AJ, Deriglasova U, Kulagina N, et al. Precursors for fibroblasts in different populations of hematopoietic cells as detected by the in vitro colony assay method. *Experimental Hematology*. 1974;2:83-92.
38. Wan C, He Q, McCaigue M, Marsh D, Li G. Non adherent cell population of human marrow culture is a complementary source of mesenchymal stem cells (MSCs). *Journal of Orthopaedic Research*. 2006;24:21-28.
39. Chen L-B, Jiang X-B, Yang L. Differentiation of rat marrow mesenchymal stem cells into pancreatic islet beta-cells. *World J Gastroenterol*. 2004;10:3016-3020.
40. Horwitz EM, Gordon PL, Koo WKK, et al. Isolated allogeneic bone marrow-derived mesenchymal cells engraft and stimulate growth in children with osteogenesis imperfecta: Implications for cell therapy of bone. *Proc Natl Acad Sci USA*. 2002;99:8932-8937.
41. Prockop DJ. Marrow Stromal Cells as Stem Cells for Nonhematopoietic Tissues. *Science*. 1997;276:71-74.
42. Park HC, Shim YS, Ha Y, et al. Treatment of Complete Spinal Cord Injury Patients by Autologous Bone Marrow Cell Transplantation and Administration of Granulocyte-Macrophage Colony Stimulating Factor. *Tissue Engineering*. 2005;11:913-922.
43. Silva GV, Litovsky S, Assad JAR, et al. Mesenchymal Stem Cells Differentiate into an Endothelial Phenotype, Enhance Vascular Density, and Improve Heart Function in a Canine Chronic Ischemia Model. *Circulation*. 2005;111:150-156.
44. Chamberlain J, Yamagami T, Colletti E, et al. Efficient generation of human hepatocytes by the intrahepatic delivery of clonal human mesenchymal stem cells in fetal sheep. *Hepatology*. 2007;46:1935-1945.
45. Sato Y, Araki H, Kato J, et al. Human mesenchymal stem cells xenografted directly to rat liver are differentiated into human hepatocytes without fusion. *Blood*. 2005;106:756-763.
46. Barry FP, Murphy JM. Mesenchymal stem cells: clinical applications and biological characterization. *The International Journal of Biochemistry & Cell Biology*. 2004;36:568-584.
47. Khaldoyanidi S. Directing Stem Cell Homing. *Cell Stem Cell*. 2008;2:198-200.
48. He Q, Wan C, Li G. Concise Review: Multipotent Mesenchymal Stromal Cells in Blood. *Stem Cells*. 2007;25:69-77.
49. Alvarez DF, Huang L, King JA, ElZarrad MK, Yoder MC, Stevens T. Lung microvascular endothelium is enriched with progenitor cells that exhibit vasculogenic capacity. *American Journal of Physiology - Lung Cellular and Molecular Physiology*. 2008;294:L419-430.
50. Ribatti D. The discovery of endothelial progenitor cells: An historical review. *Leukemia Research*. 2007;31:439-444.
51. Yoder MC. Hemangioblasts: of mice and men. *Blood*. 2007;109:2667-2668.

52. Jin S-W, Patterson C. The Opening Act: Vasculogenesis and the Origins of Circulation. *Arterioscler Thomb Vasc Biol.* 2009;29:00-00.
53. Eguchi M, Masuda H, Asahara T. Endothelial progenitor cells for postnatal vasculogenesis. *Clin Exp Nephrol.* 2007;11:18-25.
54. Gehling UM, Ergun S, Fiedler W. CFU-EC: how they were originally defined. *Blood.* 2007;110:1073.
55. Ingram DA, Mead LE, Tanaka H, et al. Identification of a novel hierarchy of endothelial progenitor cells using human peripheral and umbilical cord blood. 2004;104:2752-2760.
56. Javed MJ, Mead LE, Prater D, et al. Endothelial Colony Forming Cells and Mesenchymal Stem Cells are Enriched at Different Gestational Ages in Human Umbilical Cord Blood. *Pediatric Research.* 2008;64:68-73.
57. Ingram DA, Krier TR, Mead LE, et al. Clonogenic Endothelial Progenitor Cells Are Sensitive to Oxidative Stress. 2007;25:297-304.
58. Ingram DA, Mead LE, Moore DB, Woodard W, Fenoglio A, Yoder MC. Vessel wall-derived endothelial cells rapidly proliferate because they contain a complete hierarchy of endothelial progenitor cells. 2005;105:2783-2786.
59. McCune JM, Namikawa R, Kaneshima H, Shultz LD, Lieberman M, Weissman IL. The SCID-hu mouse: murine model for the analysis of human hematolymphoid differentiation and function. *Science.* 1988;241:1632-1639.
60. Baird GS, Zacharias DA, Tsien RY. Biochemistry, mutagenesis, and oligomerization of DsRed, a red fluorescent protein from coral. 2000;97:11984-11989.
61. Goulding A, Shrestha S, Dria K, Hunt E, Deo SK. Red fluorescent protein variants with incorporated non-natural amino acid analogues. *Protein Engineering, Design & Selection.* 2008;00:1-6.
62. Matz MV, Fradkov AF, Labas YA, et al. Fluorescent proteins form nonbioluminescent Anthozoa species. *Nature Biotechnology.* 1999;17:969-973.
63. Abbyad P, Childs W, Shi X, Boxer SG. Dynamic Stokes shift in green fluorescent protein variants. *PNAS.* 2007;104:20189-20194.
64. Bevis BJ, Glick BS. Rapidly maturing variants of the *Discosoma* red fluorescent protein (DsRed). *Nature Biotechnology.* 2002;20:83-87.
65. Pike-Overzet K, van der Burg M, Wagemaker G, van Dongen JJM, Staal FJT. New Insights and Unresolved Issues Regarding Insertional Mutagenesis in X-linked SCID Gene Therapy. *Mol Ther.* 2007;15:1910-1916.
66. Mitchell RS, Beitzel BF, Schroder ARW, et al. Retroviral DNA Integration: ASLV, HIV, and MLV Show Distinct Target Site Preferences. *PLoS Biol.* 2004;2:1127-1137.

Chapter 2:
**Human Cord Blood-Derived Endothelial
Progenitor Cells Engraft Following *In Utero*
Transplantation, Integrate into the Developing
Cytoarchitecture and Contribute to Ongoing
Vasculogenesis in the Liver**

Abstract

Endothelial progenitor cells (EPC), whether isolated from the bone marrow (BM), peripheral (PB), or cord blood (CB), represent a promising tool for the development of novel cell therapies. EPC have been shown to contribute to re-endothelialization and neovascularization of damaged tissue and have been proposed to be some of the primary regulators of tissue regeneration in organs such as the liver. Many studies have looked at the role of EPC in vasculogenic processes, but very few, if any, have focused their efforts on determining the complete differentiative potential of EPC upon transplantation in an experimental model that permits the robust formation of donor-derived tissue-specific cells in the absence of selective pressure to drive differentiation towards a specific phenotype. To this end, CB-derived EPC were obtained as previously described¹, transduced with a retroviral vector expressing DsRed, and transplanted (Tx) into 55-60 days old fetal sheep recipients (n=13) at concentrations ranging from 1.1-2.6x10⁶cells/fetus. Recipients were then evaluated at 85 days post-transplant for the presence of donor (human)-specific cell types using flow cytometry and confocal microscopy. Using these methods, we found that EPC engraftment in liver, as detected by DsRed expression, co-localized with CD31 and vWF. Overall engraftment in animals receiving cells ranged from 0.013%±0.003% to 0.43%±0.03. Importantly, there was a preferential distribution of EPC around the vessels, with the EPC comprising 91.96% ± 6.97% of the cells located around the vascular and perivascular areas in animals receiving Intra-hepatic injection (IH) and 98.70% ±2.91% of the cells located around the vascular

and perivascular areas in animals receiving Intra-peritoneal (IP) injection. Furthermore, expression of Connexin-45 in engrafted EPC demonstrated that the EPC had not only engrafted but had also functionally integrated into the developing blood vessels. Flow cytometric analysis of BM and PB of the transplanted sheep demonstrated that EPC engrafted and proliferated in the BM, with cells expressing CD105 (6.2 ± 2.2) and CD146 (0.6 ± 0.1), and continued to circulate in the PB with cells positive for CD105 (1.4 ± 0.4) and CD146 (0.9 ± 0.2). Of interest is that a CD45 negative aminopeptidase N+ (APN/CD13) population was found in both BM (18 ± 7) and PB (5.6 ± 2). This is particularly interesting, since CD13/APN is a potent regulator of vascular endothelial morphogenesis during angiogenesis. In conclusion, CB derived EPC are able to engraft and proliferate in vivo, integrate into the developing cytoarchitecture, and establish a circulating EPC pool ensuring long-term contribution to ongoing vasculogenesis.

Introduction

Early endothelial progenitor cells form in the hemangioblast and appear in umbilical cord blood at highest levels from 33-36 weeks.^{2,3} These cells are critically involved in the budding of a variety of organs including heart, lung, gut, and liver.⁴ In the liver, early endothelial cells recruit mesenchymal cells and form the sinusoidal architecture during organogenesis and liver repair.^{4,5} Following recruitment of mesenchymal cells, bile ducts and vasculature develop.⁶

Originally, EPCs were discovered and shown to contribute to vasculogenesis following post ischemic injury and other vessel impacting damage.⁷⁻¹⁰ In 1985 and 1987, two separate studies concluded that endothelial cells are derived from blood cells as

opposed to the cells composing the blood vessel walls. In 1994, Scott *et al.* found that a population of circulating cells with possible stem cell characteristics left polytetrafluoroethylene pieces covered with endothelial cells, smooth muscle cells, macrophages, monocytes, and capillary-like structures while studying the pieces following suspension in the aorta of dogs.¹¹ Controversy has surrounded EPC research in the form a dispute over the culturing techniques. A commercially available kit became commonly used for the isolation of EPCs from bone marrow mononuclear cells separate by centrifugation on a ficoll density gradient. In the commercially available method the mononuclear cells were then plated on fibronectin coated plates and the non-adherent cells were collected and replated. In a Blood 2007 paper by Yoder *et al.*, these cells were termed colony forming unit-endothelial cells (CFU-EC). Yoder *et al.* then clearly demonstrates that these cells give rise to fibroblasts and macrophages but do not give rise to endothelial cells. This finding is consistent with the clinical evidence observed as a short benefit in the patients blood system but no long term benefit nor blood vessel formation was found.¹² However, it should be noted that the author's who coined the term "CFU-EC" dispute that what they defined as CFU-EC are in fact a population of EPCs and while they do not dispute the findings in Yoder *et al.*, they argue that the cells isolated from the commercial kit should be named after the kit's designer and thus should be named CFU-Hill to avoid confusion with what they define as CFU-ECs.¹³

In contrast to CFU-EC, Yoder *et al.* defines a population of endothelial colony forming cells (ECFCs). ECFCs are derived using the same mononuclear cell layer described in the isolation of CFU-ECs but these cells are instead plated on collagen I. The non-adherent cells are then removed and the adherent cells form colonies and

compose the ECFCs. Yoder et al. not only demonstrates that ECFC express all of the classic endothelial cell markers, but form chimeric blood vessels when transplanted *In vivo* as well.¹² EPCs are in higher circulation levels during the angiogenic phases of invasive breast cancer and pathways for their role in cancer related angiogenesis have been proposed.¹⁴⁻¹⁸ Since these studies, several other studies have demonstrated the existence of a variety of EPC populations that all have common cell markers but also have unique markers specific to each population.¹⁹ Additionally, EPCs have been found in a variety of tissues ranging from circulating peripheral blood to lung microvasculature.^{4,20,21} While there is a great deal of evidence for the role of EPCs in vasculogenic processes, there is little research as to the capabilities of EPCs in liver.^{8,16,18,21,22}

While vasoconstrictive and shunt therapies have been developed, liver transplantation is the classic treatment for cirrhotic conditions of the liver.²³ In lieu of whole organ transplantation, cell therapy has advantages over organ transplantation because small populations of cells can be transplanted as opposed to the entire organ which contains many more immunologically recognizable proteins and cell types.²⁴ Furthermore, several researchers have demonstrated that a critical number of functional hepatocytes must be maintained in order to sustain basic metabolic function and prevent mortality.²⁴⁻²⁷ Cell therapy allows the existing hepatocyte population to be maintained and in some cases allows for the autologous transplant of *ex vivo* expanded cells.

Current cell therapies include the transplantation of hepatocytes, hematopoietic stem cells (HSCs), mesenchymal stem cells (MSCs), and EPCs. Hepatocyte transplantation has been employed to repopulate the liver in fumarylacetoacetate

hydrolase (FAH) knockout mice indicating that hepatocytes possess some stem cell-like characteristics.²⁷⁻³⁰ Limitations to hepatocyte transplantation are mainly related to their poor *In vitro* expansion potential and their lack of availability.³¹ Donor derived hepatocytes also require a selective advantage in order to significantly contribute to repopulation of the liver.^{24,32} HSCs are capable of generating hepatocytes but also have much higher engraftment levels only when a selective advantage is given to the donor derived cells.³³ In contrast to hepatocytes, HSCs are readily available from the bone marrow and peripheral blood and can be expanded *In vitro*. However, the clinical potential of HSCs for the generation of hepatocytes is challenged by evidence that some of the hepatocyte generation by HSCs is through fusion to an existing hepatocyte rather than true differentiation.³⁴

Cohnheim performed what are perhaps the earliest experiments with MSCs when he found that fibroblasts that produce collagen during wound repair may have come from the bone marrow.³⁵ McCulloch and Till described the clonal nature of cells extracted from bone marrow in the 1960's.^{36,37} Isolation of MSCs involves ficoll separation of the mononuclear cell layer followed by selection of the Stro-1⁺, Gly A⁻, & Lin⁻ cell population.³⁸ MSCs are primarily collected from bone marrow though MSCs and MSC-like cells have been found in other sources such as cord blood, amniotic fluid, and even adipose tissue.³⁵ MSCs do not express cell markers that are related to hematopoietic cells such as CD34 or CD45 and they do not express the endothelial cell marker CD31.³⁵ MSCs are a very diverse population of stem cells that have been classically shown to give rise to tissues of the mesoderm layer. These tissues include osteoblasts, chondrocytes, myocytes, and adipocytes.^{35,39} MSCs are also capable of giving rise to albumin

producing hepatocytes.³⁹⁻⁴² Our lab and others have also shown that MSCs are capable of giving rise to hepatocytes and thus these cells also show promise in the treatment of liver diseases and in liver regeneration.^{40,43} Finally, MSCs are also easily transduced and expanded *In vitro* making them ideal candidates to serve as gene delivery vehicles for gene therapy in the liver.

While MSCs represent many novel and promising therapies, they are only a very small fraction of the nucleated cells isolated from bone marrow. MSCs compose only 0.001%-0.01% of this population of cells.⁴⁴ It is the high efficiency with which they can be expanded that enables them to be used so effectively.^{42,44} Recent evidence indicates the MSC niche is perivascular in nature. MSC are commonly found lining vessels and this location allows them to easily enter circulation. Additionally, many cell surface markers common to perivascular cells are expressed on MSCs including alpha smooth muscle actin.

In all but one subtype, EPCs have been shown to either contribute to, or are responsible for, *de novo* vasculogenesis.²¹ Endothelial progenitor cells, whether isolated from the bone marrow (BM), peripheral (PB), or cord blood (CB), represent a promising tool for the development of novel cell therapies.^{16,18,20,45} EPCs have been shown to contribute to re-endothelialization and neovascularization of damaged tissue and have been proposed to be some of the primary regulators of tissue regeneration in organs such as the liver^{9,22}. However, their differentiative potential in a large animal model and their full capabilities in the liver have yet to be fully elucidated.^{20,46}

Classically, vasculogenesis via EPCs has been demonstrated in relation to post-ischemic injury or other vascular diseases but little to no research has been published on

any other potential these cells may have.^{9,22,47} Recent evidence indicates that EPCs support hepatocyte regeneration by providing the supporting factors necessary for hepatocyte repair and growth. EPCs have also been shown to contribute to vascular repair and vasculogenesis in the liver.⁴⁸⁻⁵¹ Furthermore, endothelium controls the delivery of hormones, vasoactive autocooids, proliferative signals and circulating cells to the appropriate targets and EPCs have been shown to secrete hepatocyte growth factor.^{21,49-51} EPCs have also been shown to reduce liver fibrosis and stimulate hepatocyte growth following injection into a rat model of cirrhotic liver disease.⁴⁸⁻⁵¹ The regenerative properties of the liver have long been observed but the mechanisms and cell types that allow for this repair have yet to be fully elucidated. Thorough knowledge of the liver repair mechanisms may lead to innovative therapies for such diseases and disorders as cirrhosis, billiary cirrhosis, and gastroenterological disorders affecting the liver.^{23,52-54}

In this paper we have investigated the engraftment potential of EPCs in the liver when transplanted (Tx) *In Utero* into the pre-immune sheep model via two routes of injection, Intra-hepatic (IH) and Intra-peritoneal (IP). Furthermore, upon finding engraftment, we investigated the contribution of these cells to vasculature and parenchymal tissue as well as their differentiative potential in contribution to the developing liver. We found that Tx EPCs engraft albeit at low levels but preferentially associate with vasculature. In addition to their association with vasculature, the EPCs maintain the expression of endothelial markers in addition to expressing markers raging from fully differentiated hepatic cells to liver stem cells.

Results

EPC engraftment into the bone marrow of transplanted animals

Flow cytometric analysis of peripheral blood (PB) and bone marrow (BM) (n=9) was performed on both IH and IP injected animals using antibodies for CD105, CD146, CD45, and CD13. CD105 is a human endothelial cell-specific marker. CD146 is a human endothelial cell-specific adhesion marker. Detection of these markers provides evidence that human endothelial cells engrafted and are proliferating in the bone marrow of the transplanted sheep. Of interest is that a CD45 negative aminopeptidase N+ (CD13/APN) population was found in both BM and PB. CD13/APN is a potent regulator of vascular endothelial morphogenesis during angiogenesis¹⁷ (tbl. 2.1).

	Bone Marrow	Peripheral Blood
CD 105	6.2%±2.2	1.4%±0.4
CD146	0.6%±0.1	0.9%±0.2
CD13 / APN (CD 45 -)	18%±7.0	6.5%±2.0

Table 2.1. **EPCs engraft in the bone marrow of transplanted animals.** Flow cytometric analysis of peripheral blood (PB) and bone marrow (BM) (n=9) was performed using antibodies for CD105, CD146, CD45, and CD13. CD105 is a human endothelial cell-specific marker. CD146 is a human endothelial cell-specific adhesion marker. Detection of these markers provides evidence that human endothelial cells engrafted and are proliferating in the bone marrow of the transplanted sheep. Of interest is that a CD45 negative aminopeptidase N+ (CD13/APN) population was found in both BM and PB. CD13/APN is a potent regulator of vascular endothelial morphogenesis during angiogenesis.

EPC engraftment and contribution to vasculature

EPCs engraft into the liver and preferentially contribute to vasculature based on the route of engraftment. EPC engraftment ranges from 0.013%±0.003% to 0.43%±0.03% across all experimental animals. The integration level does not appear to be related cell dose based on a regression analysis (data not shown). Of the engrafted

population, overall contribution to vasculature ranges from 91.69%±6.97% (n=5) in IH injected animals and 98.70%±2.91% (n=10) in IP injected animals. The difference between the contributions to vasculature in the two routes of engraftment is significant and demonstrates that IP injection results in greater contribution to vasculature in the liver (fig. 2.1).

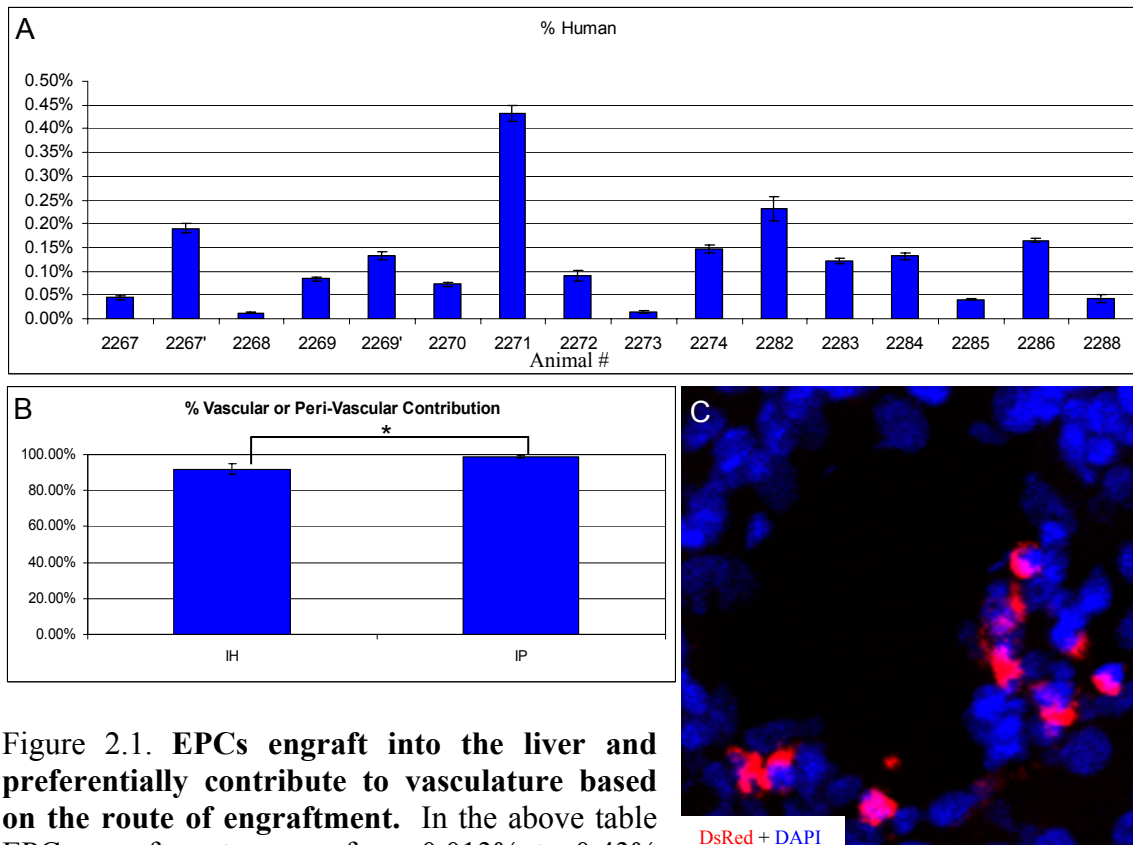


Figure 2.1. EPCs engraft into the liver and preferentially contribute to vasculature based on the route of engraftment. In the above table EPC engraftment ranges from 0.013% to 0.43% (A). Overall contribution to vasculature ranges from 91.69%±3.12% (n=5) in IH injected animals and 98.70%±0.92% (n=10) in IP injected animals (* p<0.05) (B). Representative image of DsRed+ EPCs engrafting into the vasculature of a chimeric sheep liver with DAPI labeling of both human and sheep nuclei(C). Data represented as mean ± standard error and all analysis employs two-tailed student's t-tests, (*p<0.05).

In Situ labeling of engrafted EPCs

To confirm the presence of human EPCs in the liver of transplanted animals, In Situ hybridization of a human specific probe was performed. Following hybridization,

the probe was found to label all nuclei in the human fetal liver. Additionally, hybridization of the human specific probe did not label any nuclei in animals that were not transplanted. Furthermore, In Situ hybridization of the human specific probe labeled only those nuclei that were expressing DsRed in the transplanted sheep liver. (fig 2)

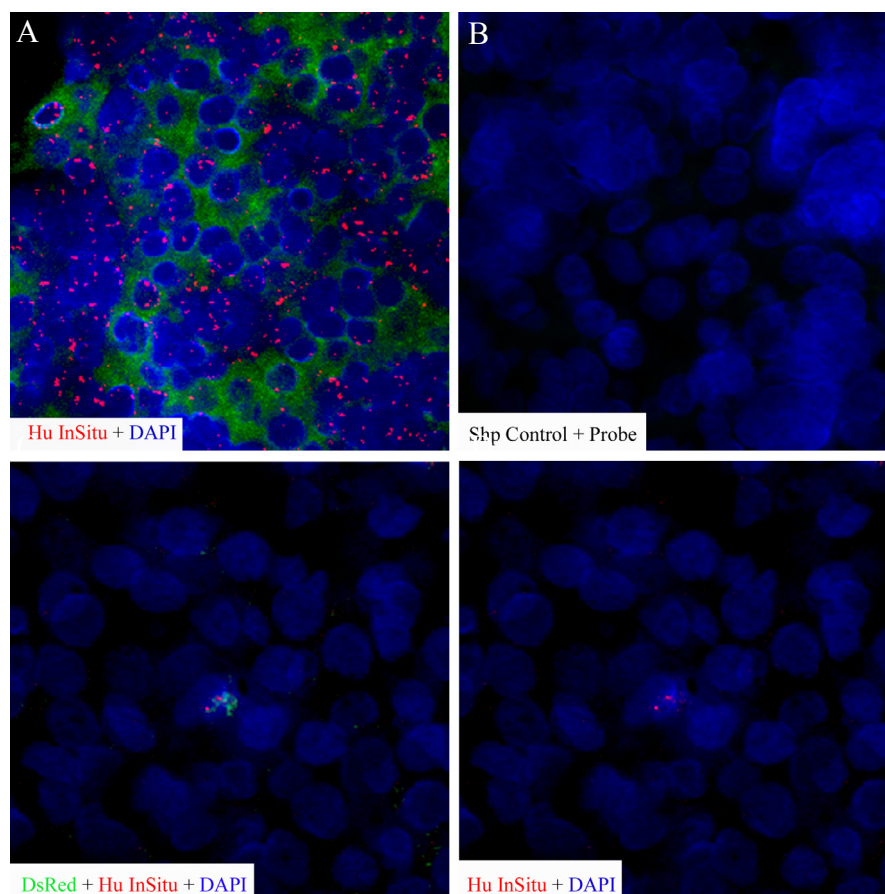


Figure 2.2. **InSitu labeling of EPCs.** In Situ labeling with a human specific probe labels all nuclei in human fetal liver (A) and does not label nuclei in fetal sheep liver (B). In chimeric fetal liver the human specific probe labels the DsRed positive human EPCs engrafted in the fetal sheep liver (C,D).

EPC expression of CD31 and vWF

Engrafted EPCs maintain CD31 and vWF positivity in the liver based on the route of engraftment. Regression analysis shows that CD31 and vWF expression vary significantly depending on the route of injection (data not shown). Liver engrafted EPCs continue to express CD31 at a level of $98.45\% \pm 0.47\%$ (n=5) when intrahepatic (IH) injection was performed and at a level of $91.25\% \pm 2.85\%$ (n=10) when intraperitoneal

(IP) injection was performed. The high level of CD31 expression in the IH engrafted cells demonstrates that these cells are remaining in a somewhat undifferentiated state. Liver engrafted EPCs continue to express vWF at a level of $97.73\% \pm 1.45\%$ (n=5) following IH injection and at a level of $88.80\% \pm 2.99\%$ (n=10) following IP injection. The continued expression of vWF by the IH engrafted EPCs is significantly greater than it is in the IP injected animals and concurs with the CD31 data that demonstrates that the IH route of engraftment leaves the EPCs less differentiated than the IP route of engraftment. Early passage EPCs demonstrated greater levels of both CD31 and vWF expression when compared to later passage EPCs. These levels of expression were $97.89\% \pm 0.77\%$ (n=10) and $97.76\% \pm 0.97\%$ (n=10) for CD31 and vWF, respectively in early passage EPCs as compared to $87.64\% \pm 4.07\%$ (n=6) and $83.18\% \pm 3.13\%$ (n=6) for CD31 and vWF, respectively in later passage EPCs. However, a student's two-tailed t-test revealed that only the difference in vWF expression levels were significant between cell passages. Furthermore, while no significant difference between early and late passage expression of CD31 in only IP injected cells was observed, a significant difference between early and late passage expression of vWF among IP injected cells was observed. In early passage IP injected cells, $97.24\% \pm 1.76\%$ of the EPCs expressed vWF as compared to $83.18\% \pm 3.13\%$ of the late passage IP injected cells. While early compared to late passage cells account for some of the difference in CD31 and vWF expression, early and late passage alone cannot conclusively account for all of the significant variation between the IH and IP injected animals as demonstrated by the lack of significance between the early and late CD31 levels. (fig. 2.3)

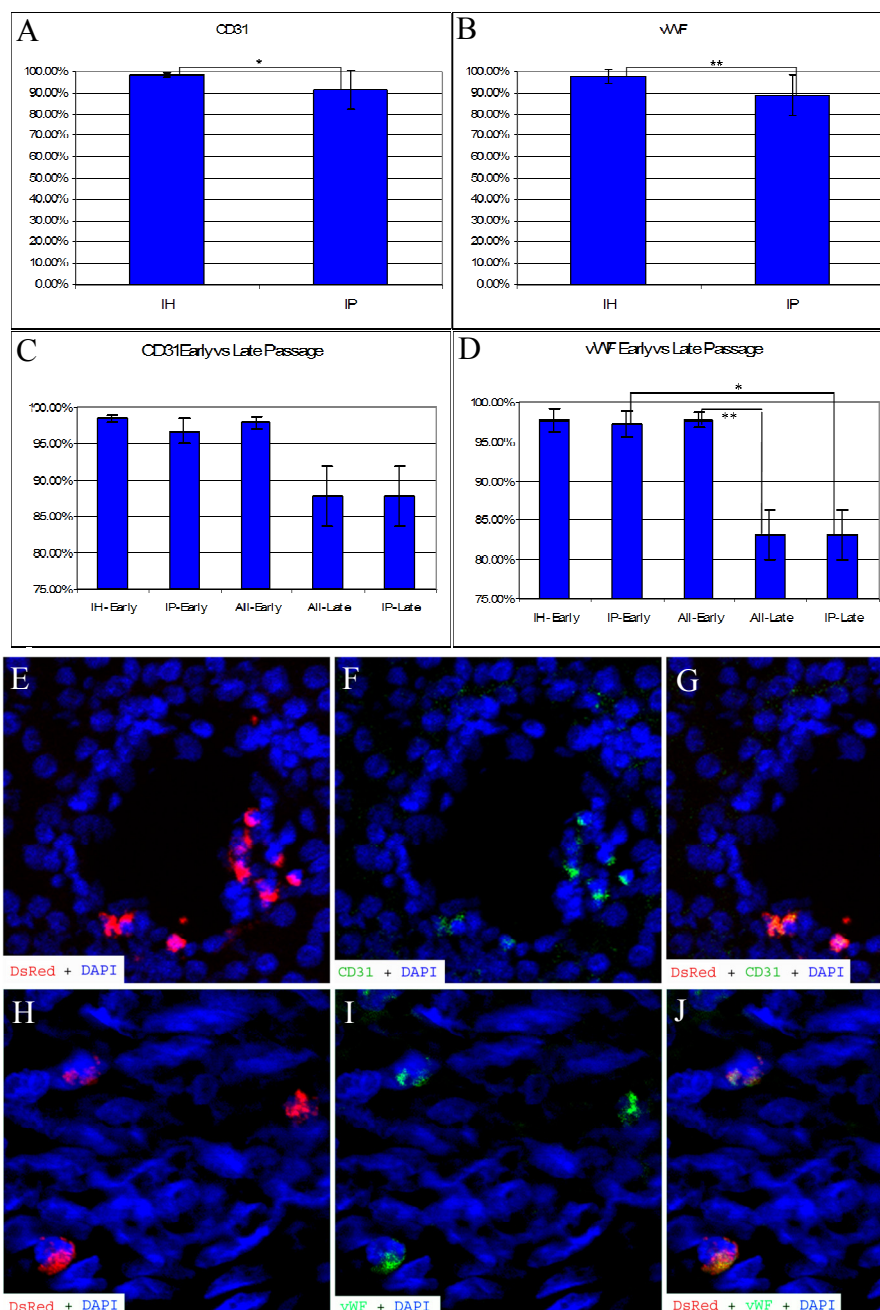


Figure 2.3. Engrafted EPCs maintain CD31 and vWF positivity in the liver based on the route of engraftment. Liver engrafted EPCs continue to express CD31 at a level of $98.45\% \pm 0.47\%$ ($n=5$) via IH injection and at a level of $91.25\% \pm 2.85\%$ ($n=10$) via IP injection, $p < 0.05$ (A). Liver engrafted EPCs continue to express vWF at a level of $97.73\% \pm 1.45\%$ ($n=5$) via IH injection and at a level of $88.80\% \pm 2.99\%$ ($n=10$) via IP injection, (B). Early passage EPCs express CD31 and vWF at levels of $97.89\% \pm 0.77\%$ ($n=10$) and $97.76\% \pm 0.97\%$ ($n=10$), respectively and late passage EPCs express CD31 and vWF at levels of $87.64\% \pm 4.07\%$ ($n=6$) and $83.18\% \pm 3.13\%$ ($n=6$), respectively (C,D). Representative staining of CD31 (E,F,G) and vWF (H,I,J) demonstrate colocalization of CD31 and vWF. Data represented as mean \pm SEM, (* $p < 0.05$, ** $p < 0.01$).

EPC contribution to liver cytoarchitecture and function

Engrafted EPCs actively participate in the cytoarchitecture of the liver. Engrafted EPCs actively form tight junctions with the surrounding liver tissue with either engraftment route as demonstrated by the expression of Con 45. Expression of Con 45 was observed in $97.56\% \pm 1.41\%$ (n=4) of the DsRed+ EPCs in the IH injected animals and $96.32\% \pm 1.10\%$ (n=9) of the DsRed+ EPCs in the IP injected animals. In addition to forming tight junctions, engrafted DsRed+ EPCs actively produced the clotting protein Factor VIII which was observed in $59.35\% \pm 6.86\%$ (n=4) of these cells in IH injected animals and $42.38\% \pm 7.39\%$ (n=9) of these cells IP injected animals. Furthermore, a somewhat smaller population of the engrafted EPCs produced the lymphocyte marker, CD45 which was expressed by $10.28\% \pm 2.49\%$ (n=4) of the cells in IH injected animals and $18.85\% \pm 2.22\%$ (n=9) of the cells in IP injected animals. Expression of CD45 is significantly higher in the EPCs delivered via IP injection and when taken in conjunction with the reduced CD31 and vWF levels in IP injected animals, indicates that these cells are engaging in greater differentiation than the EPCs delivered via IH injection. Though not statistically significant, early passage EPCs in both routes of injection expressed CD45 at lower levels than early passage IP injected cells alone, $12.44\% \pm 2.65\%$ as compared to $17.70\% \pm 3.48\%$. In combination with the significant difference in CD45 expression found between IH and IP injected cells, this demonstrates that the variation in CD45 is due to the route of injection rather than the passage of the EPCs. (fig. 2.4).

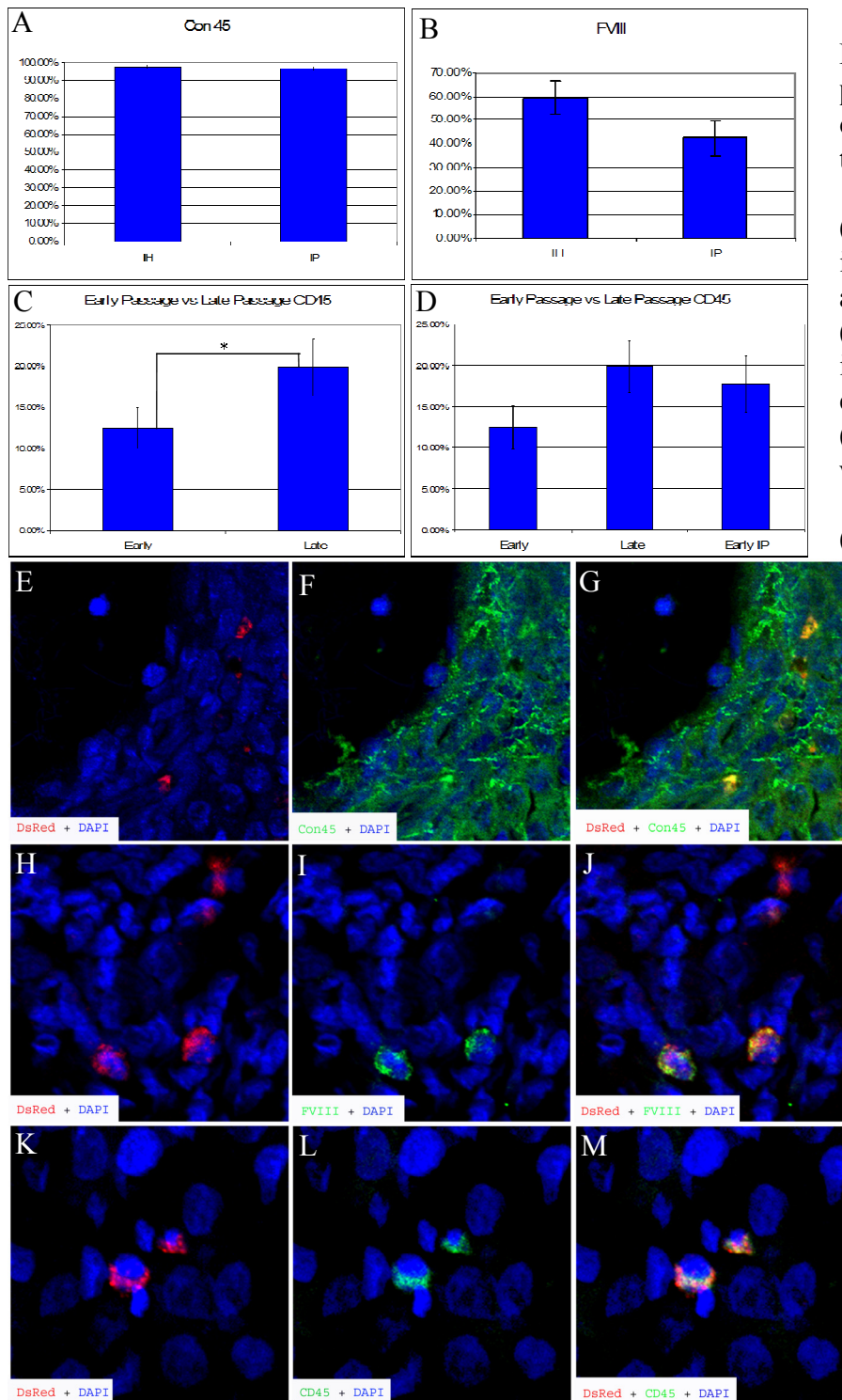


Figure 2.4. EPC participate in the cytoarchitecture of the chimeric liver.

97.56%±1.41% (n=4) of the IH injected animals and 96.32%±1.10% (n=9) of the IP injected animals expressed Con45 (A). Factor VIII was observed in 59.35%±6.86% (n=4) of the

DsRed+ cells in IH injected animals and 42.38%±7.39% (n=9) of the DsRed+ EPCs of IP injected animals (B). CD45 was expressed by 10.28%±2.49% (n=4) of the cells in IH injected animals and 18.85%±2.22% (n=9) of the cells in IP injected animals (C). Early passage EPCs in both routes of injection expressed CD45 at lower levels than early

passage IP injected cells alone, 12.44%±2.65% as compared to 17.70%±3.48%. (D) Representative images of connexin 45 (E,F,G), Factor VIII (H,I,J), and CD45 (K,L,M) positivity in the chimeric liver, respectively. Data represented as mean ± SEM, (*p<0.05).

Engrafted EPC contribute to liver development.

Engrafted EPCs contribute to the development of the functional liver. Ov6, a liver stem cell marker, positivity demonstrates that a small number of the engrafted EPCs do contribute to the further development of the liver in addition to contributing to vasculature. Overall, $4.05\% \pm 1.26\%$ ($n=14$) of the engrafted EPCs expressed Ov6 and this level of expression was found to be statistically significant against a background level of zero ($p=0.007$). However, the expression of Ov6 by engrafted EPCs was highly variable between animals. A consequence of the highly variable nature of the diminished expression of Ov6 was that it is not at significant enough levels to be studied in terms of the route of injection (data not shown). (fig. 2.5)

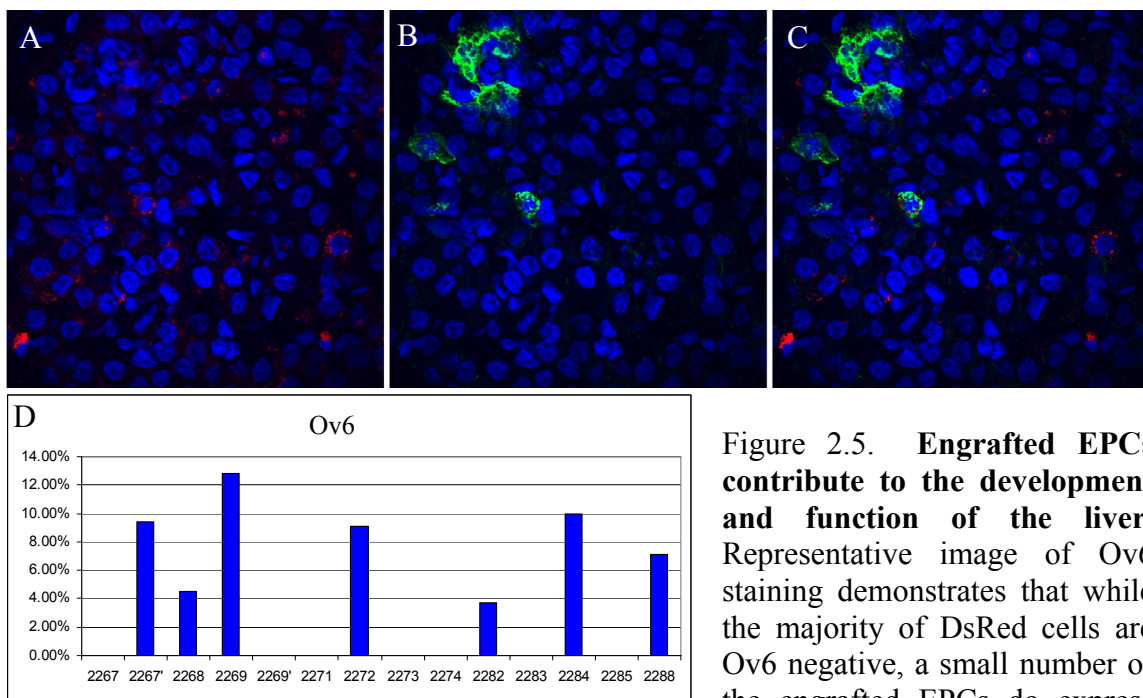


Figure 2.5. Engrafted EPCs contribute to the development and function of the liver. Representative image of Ov6 staining demonstrates that while the majority of DsRed cells are Ov6 negative, a small number of the engrafted EPCs do express

Ov6. (A,B,C) Expression of Ov6 is highly variable from animal to animal but overall $4.05\% \pm 1.26\%$ ($n=14$) of engrafted EPCs expressed Ov6 and this was significantly greater than a background level of zero ($p=0.007$). (D)

Discussion

In Utero injection of EPCs into the fetal sheep model results in the engraftment of these cells at low levels into the liver. Furthermore, upon engraftment, EPCs function to primarily contribute to the vasculature of the liver. (fig. 2.1) As compared to IP injection, IH injection of EPCs results in significantly reduced contribution to vasculature (fig. 2.1) in conjunction with significantly elevated expression of CD31 and vWF (fig. 2.2). Moreover, while IP injection of EPCs results in reduced CD31 and vWF expression (fig. 2.2) with increased contribution to vasculature (fig. 2.1), the IP injected cells exhibit a significantly higher expression of CD45. However, at least some of the diminished association with vasculature in IH injected animals as well as some of the diminished CD31 expression in IP injected animals and possibly the majority of diminished vWF expression in IP injected animals can be attributed to the effects of the later passage transplanted cells. (fig. 2.2)

Overall, this evidence indicates that IH injected cells differentiate less but do not contribute as much to the vasculature of the host. In contrast, IP injected cells contribute more to the vasculature of the host and are more differentiated. Furthermore, later passage EPCs are either more differentiated upon injection or differentiate more readily after injection. Further work is needed to elucidate the effects of *in vitro* culturing on EPCs. Both injection routes and both passages result in the majority of the engrafted cells actively forming tight junctions with the surrounding cells (fig. 2.3). Additionally, populations of EPCs in both injection methods express the important clotting protein, Factor VIII (fig. 2.3). There is not a significant change in the level of CD34 expression

between the two routes of injection suggesting that while some of the EPCs in both injection methods may be proceeding down a hematopoietic lineage there is likely a population of IP injected EPCs that are proceeding down a lymphatic lineage without becoming CD34+ (data not shown). However, in considering the elevated CD45 (fig. 2.3) levels in IP injected animals in conjunction with the CD34 expression levels; it is possible that a small population of the EPCs are differentiating down a hematopoietic lineage in the IP injected animals. Both injection routes result in small but observable populations of liver stem cells (fig. 2.4). In comparing the two routes of injection it appears that IP injection results in the greatest contribution to vasculature and the largest range of differentiative potential.

Methods and Materials

EPCs transduced with a retroviral vector carrying the DsRed gene were provided by Dr. Yoder. The cells were then injected either IP or IH in to the fetal sheep at 59days of gestation. At 143-145 days of gestation, tissue samples were collected from the fetal sheep. The tissue samples were embedded in frozen and paraffin mounting media for analysis via immunofluorescence and FISH. Peripheral blood and bone marrow samples were analyzed using flow cytometry (fig. 2.6).

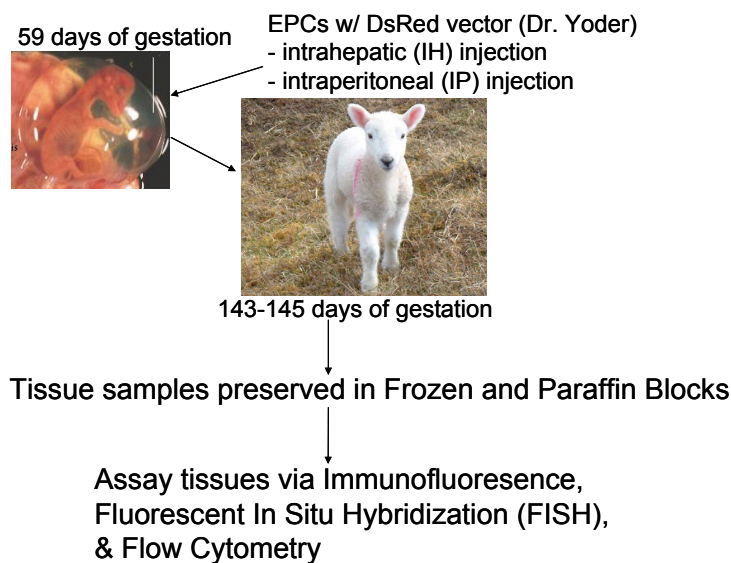


Figure 2.6 **Outline of experimental protocol.**

EPCs transduced with a retroviral vector carrying the DsRed gene were provided by Dr. Yoder. The cells were then injected either IP or IH into the fetal sheep at 59 days of gestation. At 143-145 days of gestation, tissue samples were collected from the fetal sheep. The tissue samples were embedded in frozen and paraffin mounting media for analysis via

immunofluorescence and FISH. Peripheral blood and bone marrow samples were analyzed using flow cytometry. (Images from: www.visitberneray.com/gallery/flora10/ & <http://www.vivo.colostate.edu/hbooks/pathphys/reprod/placenta/ovfetus.jpg>)

Cell culture

Cell culture was performed as previously described by Yoder et al. 2007.¹²

Flowcytometry

Flow cytometric analysis of PB and BM was performed using antibodies for CD105 (Serotec, Raleigh, NC), CD146 (Serotec, Raleigh, NC), CD45 (BD, San Jose, CA), and CD13 (Serotec, Raleigh, NC) that were used to stain the PB and BM for 15 minutes at room temperature. Both the PB and BM were lysed using FACs lysing solution; the cells were then spun at 1500rpm for 5 minutes. The cells were then washed with PBS (Gibco, Aukland, CA) with 0.1% sodium azide (Sigma, St. Louis, MO). Following a second spin at 1500 rpm for 5 minutes, the cells were fixed using 1% formaldehyde (Sigma, St. Louis, MO). Following staining, the samples were analyzed using a FACScan (Becton Dickinson Immunosystems, San Jose, CA).

In Situ Probe Production

The In situ probe was generated using PCR amplification with primers that generated a human specific probe (5'GAAGCTTA(A/T)(C/G)T(C/A)ACAGAGTT(G/T)AA3') & (5'GCTGCAGATC(A/C)C(A/C)AAG(A/T/C)AGTTTC3') (IDTDNA, San Diego, CA). The reaction conditions were as follows: 5µL 10X hi-fi PCR buffer (Roche, Pleasanton, CA), 3µL 25mM hi-fi MgCl₂ (Roche, Pleasanton, CA), 1µL each d(A,C,G)TP with 0.75µL dTTP 10mM (Invitrogen, Carlsbad, CA), 2.5µL 647nm dUTP 1mM (Invitrogen, Carlsbad, CA) 0.5µL Taq polymerase (Roche, Pleasanton, CA), 4µL 2.5ng/µL Human DNA, 2µL 30µM of each primer, and 27.25µL H₂O. The PCR conditions were as follows: 1min 30sec - 94⁰C, 40*(1min - 94⁰C, 1min - 55⁰C, 1min - 72⁰C), hold- 4⁰C. In both cases the PCR product was purified using PCR clean-up (QIAGEN, Germantown, MD). The 647nm probe was then diluted to 20ng/µL with in situ hybridization buffer (Biogenex, San Ramon, CA).

In Situ Hybridization

The probe was heated to 95⁰C for 10 min and then incubated for 1-3 hours at 37⁰C. Preserved cryoblocks were sectioned using a Lica Minotome in 8 micron thick sections and adhered to Superfrost/plus slides (Fisher Scientific, Santa Cruz, CA). The slides were then incubated at 37⁰C in 2X SSC for 30min. Following incubation the tissue was dehydrated via incubation in 70, 95, and 100% (twice) ETOH for 1-2min each. The slides were then digested using 20µg/mL proteinase K solution (Invitrogen, Carlsbad, CA) for 5min for the human sections and 7min for the sheep sections. The slides were then immersed in H₂O for 5min then in 2X SSC for 5min. The slides were then dehydrated

via incubation in ice cold 70, 95, and 100% ETOH for 1-2min each. The slides were then prehybridized for 3 min at 85⁰C in 70% Di-Formamide (Sigma, St. Louis, MO) and 2X SSC. The slides were then dehydrated via incubation in ice cold 70, 95, and 100% (twice) ETOH for 1-2min each. The tissues were then hybridized with a 647nm labeled human specific probe for 5min at 45⁰C then overnight at 42⁰C in In situ hybridization buffer (Biogenex, San Ramon, CA).

The following day all slides were washed in 45⁰C 2X SSC for 5 min then twice in 1X PBS (Gibco, Aukland, CA) + 0.1% Triton X (Sigma, St. Louis, MO) for 5min. Following these washing the slides were washed twice with 1X PBS (Gibco). The slides were then labeled with DAPI (Biogenex, San Ramon, CA) counterstain for 5min, washed with PBS (Gibco), dried, and covered using a glass cover slip with 2 drops of Cytoseal 60 (Fisher Scientific, Santa Cruz, CA).

Immunofluoresence

Preserved cryoblocks were sectioned using a Lica Minotome in 8 micron thick sections and adhered to Superfrost/plus slides (Fisher Scientific, Santa Cruz, CA). Following the sectioning the slides were washed with PBS (Gibco, Aukland, CA) followed by blocking with 10% NGS (Atlanta Biologicals, Lawrenceville, GA) in PBS. Following blocking, slides were incubated overnight in the following primary antibodies: CD31 (Biogenex, San Ramon, CA), Factor VIII related antigen (vWF) (Biogenex, San Ramon, CA), Connexin 45 (Chemicon, Temecula, CA), Factor VIII (Affinity Biologicals, Ontario, and CAN), and CD45 (Biogenex, San Ramon, CA), and Ov6 (R&D Systems, Minneapolis, MN). The following day the slides were washed in 2% NGS in PBS and then incubated in secondary antibody (Molecular Probes, Eugene, OR) for ~1 hour. Following

incubation, the slides were stained with DAPI (Biogenex, San Ramon, CA) to label the nuclei.

Microscopy

Immunofluorescent confocal microscopy imaging was performed using an Olympus Fluoview 1000 Confocal System. Immunohistochemistry microscopy imaging was performed using an Olympus BX60 microscope with an Olympus DP70 camera and DP controller software.

Statistical analysis

Standard two-tailed student's t-tests and ANOVA analysis were used in all comparative statistics. All regression analysis was performed using a modified step-wise regression analysis. The StatPro statistical analysis package (Palisade, Ithaca, NY) was used for all statistical analyses and tests.

References

1. Ingram DA, Mead LE, Tanaka H, et al. Identification of a novel hierarchy of endothelial progenitor cells using human peripheral and umbilical cord blood. *2004;104:2752-2760.*
2. Javed MJ, Mead LE, Prater D, et al. Endothelial Colony Forming Cells and Mesenchymal Stem Cells are Enriched at Different Gestational Ages in Human Umbilical Cord Blood. *Pediatric Research. 2008;64:68-73.*
3. Yoder MC. Hemangioblasts: of mice and men. *Blood. 2007;109:2667-2668.*
4. Matsumoto K, Yoshitomi H, Rossant J, Zaret KS. Liver Organogenesis Promoted by Endothelial Cells Prior to Vascular Function. *Science. 2001;294:559-563.*
5. Schmelzer E, Zhang L, Bruce A, et al. Human hepatic stem cells from fetal and postnatal donors. *Journal of Experimental Medicine. 2007;204:1973-1987.*
6. Roskams T, Desmet V. Embryology of Extra- and Intrahepatic Bile Ducts, the Ductal plate. *The Anatomical Record. 2008;291:628-635.*
7. Asahara T, Masuda H, Takahashi T, et al. Bone Marrow Origin of Endothelial Progenitor Cells Responsible for Postnatal Vasculogenesis in Physiological and Pathological Neovascularization. *Circulation Research. 1999;85:221-228.*
8. Asahara T, Murohara T, Sullivan A, et al. Isolation of Putative Progenitor Endothelial Cells for Angiogenesis. *Science. 1997;275:964-966.*
9. Hsieh PCH, Davis ME, Lisowski LK, Lee RT. ENDOTHELIAL-CARDIOMYOCYTE INTERACTIONS IN CARDIAC DEVELOPMENT AND REPAIR. *Annual Review of Physiology. 2006;68:51-66.*
10. Leor J, Guetta E, Feinberg MS, et al. Human Umbilical Cord Blood-Derived CD133+ Cells Enhance Function and Repair of the Infarcted Myocardium. *Stem Cells. 2006;24:772-780.*
11. Ribatti D. The discovery of endothelial progenitor cells: An historical review. *Leukemia Research. 2007;31:439-444.*
12. Yoder MC, Mead LE, Prater D, et al. Redefining endothelial progenitor cells via clonal analysis and hematopoietic stem/progenitor cell principals. *Blood. 2007;109:1801-1809.*
13. Gehling UM, Ergun S, Fiedler W. CFU-EC: how they were originally defined. *Blood. 2007;110:1073.*
14. Moll R, Zimbelmann R, Goldschmidt MD, et al. The human gene encoding cytokeratin 20 and its expression during fetal development and in gastrointestinal carcinomas. *Differentiation. 1993;53:75-93.*
15. Cogle CR, Theise ND, Fu D, et al. Bone Marrow Contributes to Epithelial Cancers in Mice and Humans as Developmental Mimicry. *Stem Cells. 2007;25:1881-1887.*
16. Roncalli JG, Tongers J, Renault M-A, Losordo DW. Endothelial progenitor cells in regenerative medicine and cancer: a decade of research. *Trends in Biotechnology. 2008;26:276-283.*
17. Bhagwat SV, Petrovic N, Okamoto Y, Shapiro LH. The angiogenic regulator CD13/APN is a transcriptional target of Ras signaling pathways in endothelial morphogenesis. *Blood. 2003;101:1818-1826.*

18. Young PP, Vaughan DE, Hatzopoulos AK. Biologic Properties of Endothelial Progenitor Cells and Their Potential for Cell Therapy. *Progress in Cardiovascular Diseases*. 2007;49:421-429.
19. Van Anh Nguyen CFPOHSNRNS. Endothelial cells from cord blood CD133⁺CD34⁺ progenitors share phenotypic, functional and gene expression profile similarities with lymphatics. *Journal of Cellular and Molecular Medicine*. 2008;9999.
20. Khakoo AY, Finkel T. Endothelial Progenitor Cells. *Annual Review of Medicine*. 2005;56:79-101.
21. Alvarez DF, Huang L, King JA, ElZarrad MK, Yoder MC, Stevens T. Lung microvascular endothelium is enriched with progenitor cells that exhibit vasculogenic capacity. *American Journal of Physiology - Lung Cellular and Molecular Physiology*. 2008;294:L419-430.
22. Urbich C, Dimmeler S. Endothelial Progenitor Cells: Characterization and Role in Vascular Biology. *Circulation Research*. 2004;95:343-353.
23. Salerno F, Gerbes A, Gines P, Wong F, Arroyo V. Diagnosis, prevention and treatment of hepatorenal syndrome in cirrhosis. *GUT*. 2007;56:1310-1318.
24. Grompe M. Principles of therapeutic liver repopulation. *Journal of Inherited Metabolic Disease*. 2006;29:421-425.
25. Fausto N. Liver regeneration: From laboratory to clinic. *Liver Transplantation*. 2001;7:835-844.
26. Fausto N, Campbell JS, Riehle KJ. Liver Regeneration. *Hepatology*. 2006;43:S45-53.
27. Oertel M, Shafritz DA. Stem cells, cell transplantation and liver repopulation. *Biochimica et Biophysica Acta (BBA) - Molecular Basis of Disease*. 2008;1782:61-74.
28. Vogel A, Muhsen IETvdB, Al-Dhalimy, et al. Chronic liver disease in murine hereditary tyrosinemia type 1 induces resistance to cell death. *Hepatology*. 2004;39:433-443.
29. Overturf K, al-Dhalimy M, Ou CN, Finegold M, Grompe M. Serial transplantation reveals the stem-cell-like regenerative potential of adult mouse hepatocytes. *Am J Pathol*. 1997;151:1273-1280.
30. Overturf K, Al-Dhalimy M, Tanguay R, et al. Hepatocytes corrected by gene therapy are selected in vivo in a murine model of hereditary tyrosinaemia type I. *Nature Genetics*. 1996;12:266-273.
31. Cho CH, Berthiaume F, Tilles AW, Yarmush ML. A new technique for primary hepatocyte expansion in vitro. *Biotechnology and Bioengineering*. 2008;101:345-356.
32. Lysy PA, Campard D, Smets F, Najimi M, Sokal EM. Stem cells for liver tissue repair: Current knowledge and perspectives. *World Journal of Gastroenterology*. 2008b;14:864-875.
33. Fausto N. Liver regeneration and repair: Hepatocytes, progenitor cells, and stem cells. *Hepatology*. 2004;39:1477-1487.
34. Camargo FD, Finegold M, Goodell MA. Hematopoietic myelomonocytic cells are the major source of hepatocyte fusion partners. *The Journal of Clinical Investigation*. 2004;113:1266-1270.

35. Chamberlain G, Fox J, Ashton B, Middleton J. Concise Review: Mesenchymal Stem Cells: Their Phenotype, Differentiation Capacity, Immunological Features, and Potential for Homing. *Stem Cells*. 2007;25:2739-2749.
36. Becker A, McCulloch E, Till J. Cytological Demonstration of the Clonal Nature of Spleen Colonies Derived from Transplanted Mouse Marrow Cells. *Nature*. 1963;197:452-454.
37. Siminovitch L, McCulloch E, Till J. The distribution of colony-forming cells among spleen colonies. *The Journal of Cellular and Comparative Physiology*. 1963;62:327-336.
38. Colletti EJ, Airey JA, Liu W, et al. Generation of tissue-specific cells from MSC does not require fusion or donor to host mitochondrial/membrane transfer. *Stem Cell Research*. 2009;2:125-138.
39. Chen L-B, Jiang X-B, Yang L. Differentiation of rat marrow mesenchymal stem cells into pancreatic islet beta-cells. *World J Gastroenterol*. 2004;10:3016-3020.
40. Chamberlain J, Yamagami T, Colletti E, et al. Efficient generation of human hepatocytes by the intrahepatic delivery of clonal human mesenchymal stem cells in fetal sheep. *Hepatology*. 2007;46:1935-1945.
41. Kolf CM, Cho E, Tuan RS. Biology of adult mesenchymal stem cells: regulation of niche, self-renewal and differentiation. *Arthritis Research & Therapy*. 2007;9:204.
42. Porada CD, Zanjani ED, Almeida-Porada G. Adult Mesenchymal Stem Cells: A Pluripotent Population with Multiple Applications. *Current Stem Cells Research & Therapy*. 2006;1:231-238.
43. Sato Y, Araki H, Kato J, et al. Human mesenchymal stem cells xenografted directly to rat liver are differentiated into human hepatocytes without fusion. *Blood*. 2005;106:756-763.
44. Barry FP, Murphy JM. Mesenchymal stem cells: clinical applications and biological characterization. *The International Journal of Biochemistry & Cell Biology*. 2004;36:568-584.
45. Debatin K, Wei J, Beltinger C. Endothelial progenitor cells for cancer gene therapy. *Gene Therapy*. 2008;15:780-786.
46. Fenno LE, Ptaszek LM, Cowan CA. Human embryonic stem cells: emerging technologies and practical applications. *Current Opinion in Genetics & Development*. 2008;18:1-6.
47. Iwami Y, Masuda H, Asahara T. Endothelial progenitor cells: past, state of the art, and future. *Journal of Cellular and Molecular Medicine*. 2004;8:488-497.
48. Beaudry P, Hida Y, Udagawa T, et al. Endothelial progenitor cells contribute to accelerated liver regeneration. *Journal of Pediatric Surgery*. 2007;42:1190-1198.
49. Nakamura T, Torimura T, Sakamoto M, et al. Significance and Therapeutic Potential of Endothelial Progenitor Cell Transplantation in a Cirrhotic Liver Rat Model. *Gastroenterology*. 2007;133:91-107.e101.
50. Taniguchi E, Kin M, Torimura T, et al. Endothelial Progenitor Cell Transplantation Improves the Survival Following Liver Injury in Mice. *Gastroenterology*. 2006;130:521-531.
51. Ueno T, Nakamura T, Torimura T, Sata M. Angiogenic cell therapy for hepatic fibrosis. *Medical Molecular Morphology*. 2006;39:16-21.

52. Patrick S. Kamath RHWMMWKTMTCLKGDAERDWRK. A model to predict survival in patients with end-stage liver disease. *Hepatology*. 2001;33:464-470.
53. Hayashi Y, Tsuji S, Tsujii M, et al. The Transdifferentiation of Bone-Marrow-Derived Cells in Colonic Mucosal Regeneration after Dextran-Sulfate-Sodium-Induced Colitis in Mice. *Pharmacology*. 2007;80:193-199.
54. Khalil PN, Weiler V, Nelson PJ, et al. Nonmyeloablative Stem Cell Therapy Enhances Microcirculation and Tissue Regeneration in Murine Inflammatory Bowel Disease. *Gastroenterology*. 2007;132:944-954.

Chapter 3:
Human Endothelial Progenitor Cells:
A Novel and Promising Cellular Therapy for
Regenerating Intestinal Mucosa

Abstract

Abnormal or inadequate vasculogenesis, local inflammation and severe epithelial damage are common features of both inflammatory bowel disease (IBD) and irradiation injury after pelvic or abdominal cancer treatment. Previous studies have shown that adult bone marrow-derived stem cells, upon transplantation, home to the damaged digestive tissue and facilitate mucosal repair in both IBD and radiation injury. However, despite increasing evidence that endothelial progenitor cells (EPC) represent a promising tool for ischemic cardiac and vascular repair, few have investigated whether transplanted EPC can contribute to the intestinal vasculogenic process and/or the stem or mature epithelial cell pool. In order to study the intrinsic ability of human EPC to contribute to the epithelial or vascular bed of the small intestine, we transplanted 13 pre-immune 55-60 day old fetal sheep with $0.5\text{-}2.6 \times 10^6$ human EPC/fetus and examined the contribution of these cells to the intestinal architecture. CB-derived EPC were obtained as previously described (Ingram et al. Blood:104,2004) and transduced with a retroviral vector expressing DsRed. Recipients were evaluated at 85 days post-transplant for the presence of donor (human)-specific cell types by confocal microscopy. We found that within the intestine, EPC, as detected by DsRed positivity, localized preferentially to the mucosal layer above the muscularis mucosa in the area of the crypts of Lieberkühn. The overall levels of EPC engraftment positively correlated with the cell dose administered ($p < 0.05$) such that the levels of DsRed positive cells found within the mucosal layer of animals in each transplant group were as follows: $7.6 \pm 0.5\%$ in the animal transplanted with 5×10^5 cells; $8 \pm 0.3\%$ in those transplanted with 1.5×10^6 cells ($n=8$), and $10.9 \pm 0.5\%$ in sheep transplanted with 2.6×10^6 cell/fetus ($n=4$). Immunostaining with vWF and CD31

demonstrated that only 0.7-1.7% of the DsRed cells retained an EPC phenotype, thus suggesting that the majority of the transplanted cells had adopted an alternative fate. Double positivity for DsRed and Cytokeratin 20, a major cellular protein present in mature enterocytes, was found in $1.12 \pm 0.02\%$ of the cells, all of which were found in the villi area. Colocalization of DsRed cells with expression of Musashi a putative marker for intestinal stem cells was also evaluated. These analyses revealed that $23.45 \pm 1.65\%$ of the cells within the crypt region were DsRed positive and thus donor derived. Furthermore, $37.66 \pm 3.33\%$ of the donor derived cells expressed Musashi. Expression of this marker was not observed in any DsRed positive cells in any other location within the intestine. In addition to their direct contribution to the stem cell pool, donor derived cells were found to contribute to the stem cell niche supporting, myofibroblasts population. Coexpression of vimentin and smooth muscle actin was found in $25.56 \pm 1.10\%$ of the donor derived cells. Furthermore, $9.46 \pm 0.69\%$ of the donor derived cells were found to contribute to the interstitial cells of cajal population through the expression of CD117 without the coexpression of CD45. Finally, small percentages ($<1\%$) of the donor derived cells were also found to contribute to the epithelial and enteroendocrine cell population through the expression of cytokeratin 20 and chromogranin A, respectively. In addition DsRed positive cells that did not co-express any of the markers tested thus far were found in the stromal layer adjacent to the crypts. In conclusion, these are the first studies, to our knowledge, to show that EPC can contribute significantly to the developing intestinal mucosa and the intestinal stem cell pool, and EPC may thus represent a valuable cell source for intestinal regeneration and repair.

Introduction

Endothelial Progenitor Cells (EPCs) are derived from the precursor hemangioblast that gives rise to both the EPCs and to the hematopoietic stem cells (HSCs) that are responsible for the creation of the blood and immune systems.¹ EPCs give rise to the endothelium and are responsible for *de novo* blood vessel synthesis which is now termed “vasculogenesis.” Endothelium controls the delivery of hormones, vasoactive autocooids, proliferative signals and circulating cells to the appropriate targets.² Endothelium also forms a continuous layer between blood and tissue and the endothelial cells are thought to turnover every 1-3 years in major vessels.² When Ashara and colleagues reported the isolation of EPCs from human peripheral blood in 1997, they found evidence that hemangioblasts may be present in blood.³ While scientific evidence has demonstrated that the hemangioblast exists during embryonic development, its existence is disputed in adult tissues.^{1,3} While a great deal of indirect evidence has supported the existence of the hemangioblast, mostly based on expression of endothelial and hematopoietic markers during development, no *In vivo* evidence that directly identifies the hemangioblast has been observed.^{4,5} For this reason the existence of the hemangioblast is disputed.^{1,3} As an alternative, EPCs are proposed to originate from the angioblast which is simply a primitive cell on the periphery of the embryonic blood islands that gives rise to EPCs.⁵

Initially, EPCs cells were thought only to exist in the developing embryo as the vast majority of new blood vessel synthesis occurs during this stage. However, in the 1990's a population of adult circulating EPCs was discovered and first characterized by Ashara and colleagues.⁶ Ashara also found that the adult populations of EPCs are

derived from the bone marrow. Since their discovery, EPCs have been shown to be in umbilical cord blood at highest levels from 33-36 weeks of gestation.⁷ EPCs can also be isolated from bone marrow (BM) or peripheral (PB) in addition to cord blood (CB).^{8,9} Their availability and neovasculogenic potential mean that EPCs represent a promising tool for the development of novel cell therapies.⁸⁻¹⁰ These cells have also been shown to be critically involved in the budding of a variety of organs including heart, lung, liver, and gut.^{2,11-16}

Originally, EPCs were discovered and shown to contribute to vasculogenesis following post ischemic injury and other vessel impacting damage.^{6,17-19} In 1985 and 1987, two separate studies concluded that endothelial cells are derived from blood cells as opposed to the cells composing the blood vessel walls.³ In 1994, Scott *et al.* found that a population of circulating cells with possible stem cell characteristics left polytetrafluoroethylene pieces covered with endothelial cells, smooth muscle cells, macrophages, monocytes, and capillary-like structures while studying the pieces following suspension in the aorta of dogs.³ Further controversy has surrounded EPC research in the form a dispute over the culturing techniques. A commercially available kit became commonly used for the isolation of EPCs from bone marrow mononuclear cells separate by centrifugation on a ficoll density gradient. In the commercially available method the mononuclear cells were then plated on fibronectin coated plates and the non-adherent cells were collected and replated. In a Blood 2007 paper by Yoder *et al.*, these cells were termed colony forming unit-endothelial cells (CFU-EC). Yoder *et al.* then clearly demonstrates that these cells give rise to fibroblasts and macrophages but do not give rise to endothelial cells. This finding is consistent with the clinical evidence

observed as a short benefit in the patients blood system is seen but no long term benefit nor blood vessel formation was found.²⁰ However, it should be noted that the author's who coined the term "CFU-EC" dispute that what they defined as CFU-EC are in fact a population of EPCs and while they do not dispute the findings Yoder et al. makes, they argue that the cells isolated from the commercial kit should be named after the kit's designer and thus should be named CFU-Hill to avoid confusion with what they define as CFU-ECs.²¹

In contrast to CFU-EC, Yoder et al. defines a population of endothelial colony forming cells (ECFCs). ECFCs are derived using the same mononuclear cell layer described in the isolation of CFU-ECs, but these cells are instead plated on collagen I. The non-adherent cells are then removed and the adherent cells form colonies and compose the ECFCs. Yoder et al. not only demonstrates that ECFC express all of the classic endothelial cell markers, but form chimeric blood vessels when transplanted *In vivo* as well.²⁰ EPCs have also been shown to be in higher circulation levels during the angiogenic phases of invasive breast cancer and pathways for their role in cancer related angiogenesis have been proposed.²²⁻²⁶ While there is a great deal of evidence for the role of EPCs in vasculogenic processes, there is little research as to the capabilities of EPCs in the small intestine or any other gut associated tissue.^{2,6,24,26,27}

The small intestine is primarily responsible for the absorption of nutrients through an epithelial cell layer. There are also a large number of Peyer's and immune related tissues and cells in the small intestine.²⁸ Additionally, mucosal cells, smooth muscle cells, enteroendocrine cells, goblet cells and a host of other cell types can be found in the small intestine. To maintain these cell populations, two suspected populations of stem cells are

thought to exist in the small intestine. The crypt base stem cell (CBSC) is a slow dividing stem cell that exists in an interdigitated manner with the paneth cells at the base of the crypts of Lieberkühn.^{29,30} These cells divide rather slowly and are both chemo- and radiation therapy resistant.^{29,30} Upon injury, these cells divide more rapidly in both a symmetric and asymmetric manner giving rise to: more stem cells, the epithelial columnar cells, and the supporting parenchymal cells of the small intestine.²⁹ However, the small intestine experiences a large amount of natural turnover particularly in the form of columnar epithelial cells as they mature up from the crypts and progress towards the villi. This large turnover is a natural result of the harsh physiological environment in the small intestine. Replenishing this supply of cells is thought to be the responsibility of a second population of stem cells located at the +4 region of the crypt walls.²⁹ These stem cells divide much more rapidly in both a symmetric and asymmetric manner enabling them to constantly resupply the columnar epithelial cell population but this also renders them much more sensitive chemo- and radiation therapy as well as sensitive to other assaults on the cell population in the form of diseases such as inflammatory bowel disease (IBD).^{29,31-34} These two stem cell populations are thought to maintain the intestine following injury or under normal conditions of cell turnover, respectively. Stem cell niches have long been reported to be important to the maintenance of various stem cell populations ranging from HSCs to intestinal stem cells (ISCs).^{15,35} ISCs and their supporting niche are of particular interest because of their ability to repopulate the epithelium of the small intestine following chemo- and radiation therapy as well as during certain gastrointestinal conditions like inflammatory bowel disease (IBD).³⁵⁻³⁷

Gastrointestinal malignancies are among the most common types of cancer found and lead to the highest cancer related mortality rates world wide.^{38,39} Adenocarcinomas of the small bowel are less common with 2840 men and 2580 women diagnosed with cancer of the small bowel in 2005.⁴⁰ Furthermore, IBD encompasses a large number of diseases but the primary forms are ulcerative colitis and Crohn's disease. In the United States approximately 1 million people have IBD and 30,000 new cases are diagnosed each year.⁴¹ Treatment in severe cases of bowel disorders includes partial removal and transplantation. However, transplantation often results in further complications particularly related to immune rejection of grafts.⁴² Furthermore, the proven treatment of total parenteral nutrition is associated with morbidity and mortality in the long term.⁴³ Cell therapy has the potential to regenerate the intestinal epithelium in IBD patients or following chemo-radio therapy with little to no immune response compared to transplant.⁴³⁻⁴⁷ Furthermore, MSCs are readily available in the bone marrow and populations of EPCs have been found circulating in the peripheral blood which results in a readily available supply of stem cells that can be expanded *ex vivo* creating the opportunity for autologous transplant.⁴³⁻⁴⁸

Autologous hematopoietic stem cell transplant, using HSCs that are readily available in the bone marrow, is currently being developed for the treatment of immune related IBD disorders such as Crohn's disease.⁴⁹ Mesenchymal stem cells have been shown to contribute to the expansion of intestinal cells and in tissue regeneration.^{44,46,47,50} While MSCs have been demonstrated in tissue regeneration, the sustained delivery of VEGF has also been shown to enhance to proliferation generation of engineered intestine.⁴³ EPCs have already been proven to be capable of vasculogenesis and

demonstrated to secrete VEGF and in addition to the promise of mesenchymal stem cells; are a promising cell therapy in regenerative medicine in their own right.^{9,10,24,27,43,44,51,52}

In this paper, we will demonstrate that upon xenotransplantation EPCs not only engraft into the small intestine but do so in a preferential manner in the area containing the crypts of Lieberkühn (above the muscularis mucosa and below the crypt-villus junction). Upon transplantation, these cells actively engraft and differentiate into both ISCs and into the supporting cell types of the ISC niche as well as mature cells of the intestinal parenchyma.

Results

EPCs preferentially engraft between the muscularis mucosa and the crypt-villi junction

The small intestine is composed of five major regions: the smooth muscle, the sub-mucosa, the muscularis mucosa, the crypt region, and the villus region. (fig. 3.1A) Following transplantation, $81.89 \pm 2.21\%$ (n=13) of the donor derived cells preferentially engrafted in and around the crypts of Lieberkühn. (fig. 3.1B) Two separate injection routes, intra-hepatic (IH) and intra-peritoneal (IP), were employed but no significant difference in engraftment in either the entire intestine or the CPT region was found. Furthermore, two different cell doses of IH injected animals were tested. The largest cell IP (2.6×10^6 cells) dose was found to have a higher average engraftment in both the overall intestine tissue ($10.89 \pm 1.92\%$, n=4) and the CPT region ($26.71 \pm 3.75\%$, n=4) when compared to the smallest cell dose (1.3×10^6 cells) in the overall intestine ($8.64 \pm 1.47\%$, n=4) and the CPT region ($23.30 \pm 3.35\%$, n=4). (fig. 3.1C,D,E) However, the difference in engraftment was not significant.

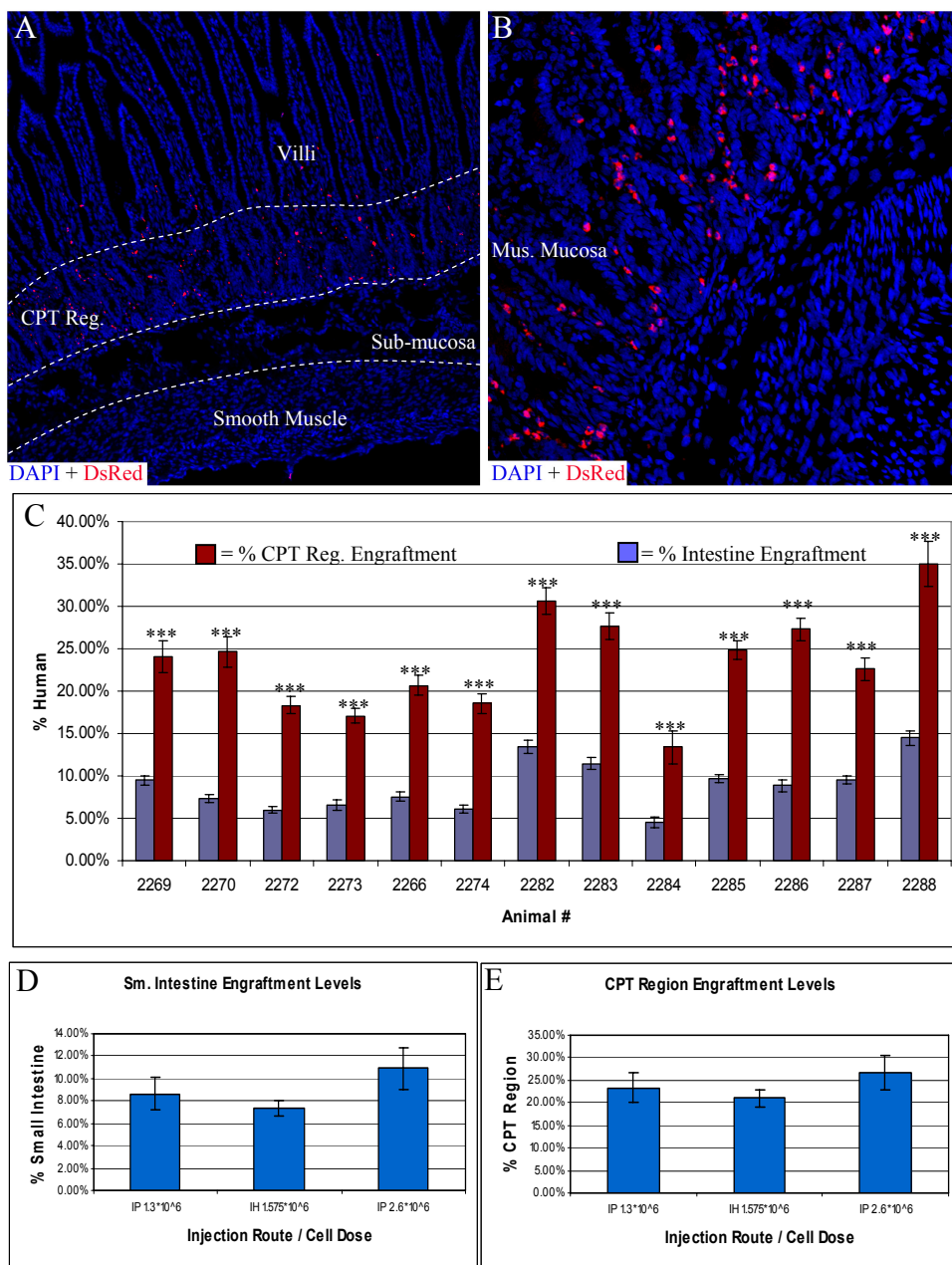


Figure 3.1. EPCs retain DsRed expression and preferentially engraft near the crypts of Lieberkühn. 81.89±2.21% (n=13) of the donor derived cells preferentially engrafted in and around the crypts of Lieberkühn (A,B,C). ($p < 0.001$, using a two-tailed student's t-test.) Two separate injection routes, intra-hepatic (IH) and intra-peritoneal (IP), were employed but no significant difference in engraftment in either the entire intestine or the CPT region was found. The largest cell IP (2.6×10^6 cells) dose was found to have a higher average engraftment in both the overall intestine tissue ($10.89 \pm 1.92\%$, n=4) and the CPT region ($26.71 \pm 3.75\%$, n=4) when compared to the smallest cell dose (1.3×10^6 cells) in the overall intestine (8.64 ± 1.47 , n=4) and the CPT region ($23.30 \pm 3.35\%$, n=4). The difference in engraftment was not significant using two-tailed student's t-tests. (D,E)

Donor derived cells are human retain expression of EPC markers

In Situ labeling with a human specific probe was performed in order to ensure the DsRed cells were human in origin and therefore donor derived. Human specific In Situ labeling labels all nuclei in fetal human intestine and no nuclei in sheep fetal control intestine (fig. 3.2A,B). Human specific In Situ labeling labels DsRed positive engrafted EPCs in chimeric In Situ (fig. 3.2C,D). Immunofluorescent labeling with an anti-DsRed antibody was employed to confirm the expression of DsRed by the donor derived cells. (fig 2 E,F,G) Furthermore, $91.88 \pm 1.82\%$ (n=12) of donor derived cells continued to express the EPC marker CD133. (fig. 3.2 H,I,J)

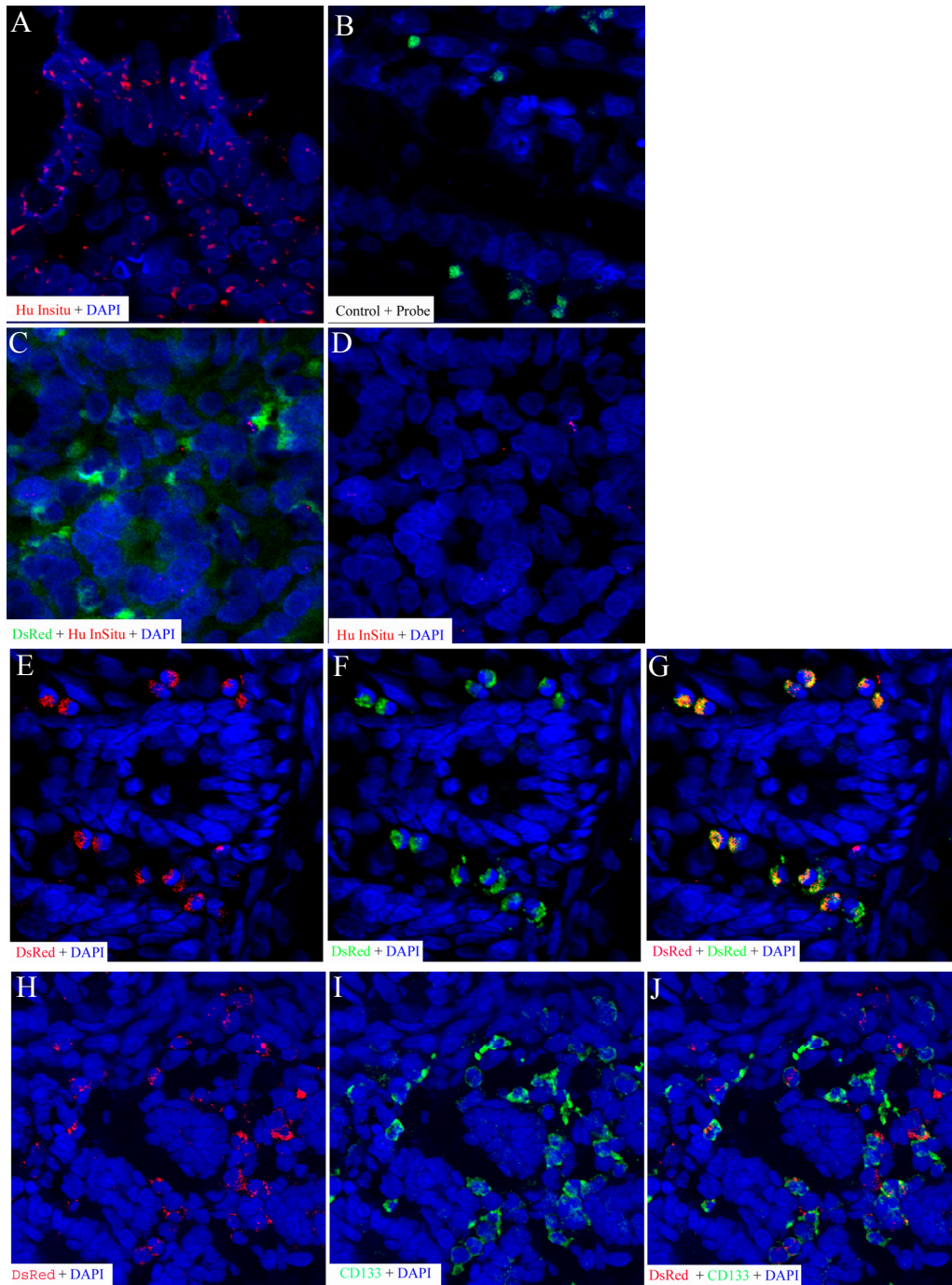


Figure 3.2. In Situ Labeling of Engrafted EPCs. Human specific In Situ labeling labels all nuclei in fetal human intestine and no nuclei in sheep fetal control intestine (A,B). Human specific In Situ labeling labels DsRed positive engrafted EPCs in chimeric In Situ (C,D). Immunofluorescent labeling with an anti-DsRed antibody was employed to confirm the expression of DsRed by the donor derived cells. (E,F,G) Furthermore, $91.88 \pm 1.82\%$ ($n=12$) of donor derived cells continued to express the EPC marker CD133. (H,I,J)

EPCs contribute to the Crypts of Lieberkühn as ISCs

During development, expression of the intestinal stem cell marker (ISC), Musashi was found to label the crypts in the small intestine. Overall, $37.66 \pm 3.33\%$ ($n=12$) of the donor derived cells expressed the ISC marker Musashi. Furthermore, the Musashi positive donor derived ISC composed $10.79 \pm 1.00\%$ ($n=12$) of the entire Musashi positive ISC population. (fig. 3.3A,B,C) At the highest IP injected cell dose (2.6×10^6 cells), $12.36 \pm 2.39\%$ ($n=4$) of the ISC were from donor derived cells which was not significantly different from $12.67 \pm 1.31\%$ ($n=3$) of the ISCs at the lowest cell dose of 1.3×10^6 cells. However, the injection route did have a significant impact on the contribution of donor derived cells to the ISC population. Following IH injection of 1.6×10^6 EPCs, donor derived cells composed only $8.19 \pm 0.51\%$ ($n=4$) of the ISC population which was found to be significantly lower than the comparable cell dose following IP injection (fig. 3.3D). Furthermore, while cell dose did not play a role in CD133 expression, there was a significant difference in CD133 expression based on injection route. $82.38 \pm 2.83\%$ ($n=4$) of donor derived cells retained CD133 expression following IH injection of 1.6×10^6 cells while only $68.02 \pm 5.05\%$ ($n=3$) of donor derived cells retained CD133 expression following IP injection of 1.3×10^6 cells (fig. 3.3E). Combined this evidence indicates that IH injected EPCs are less likely to differentiate into ISCs than IP injected EPCs.

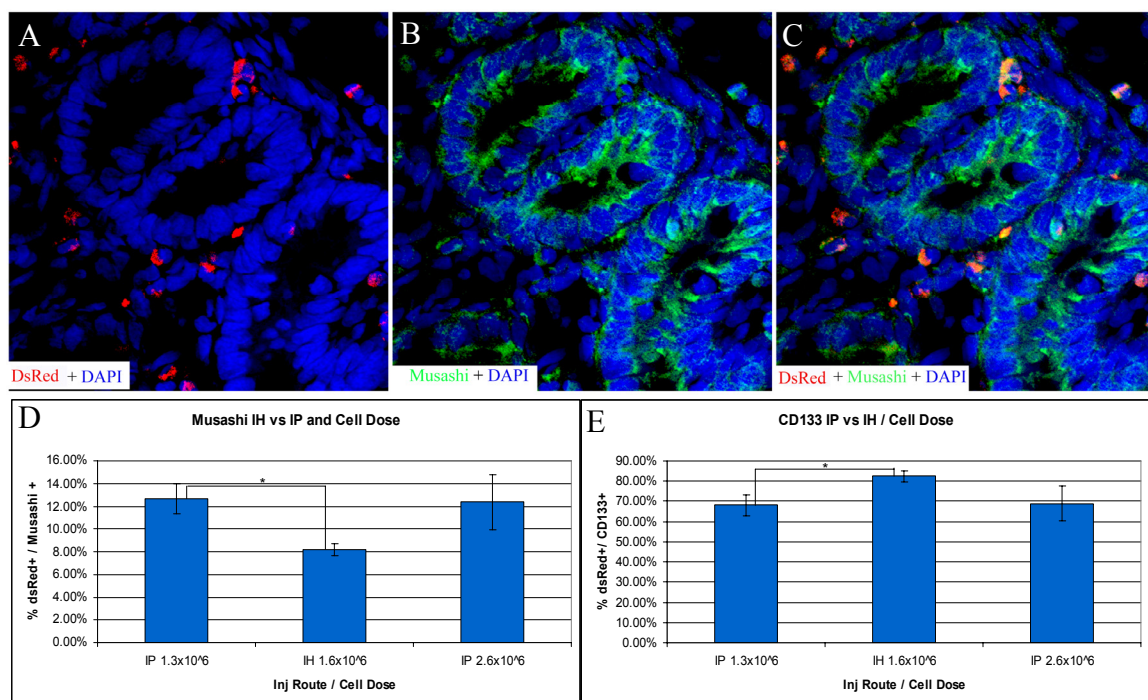


Figure 3.3. EPCs contribute to the intestinal stem cell (ISC) population. 37.66±3.33% (n=12) of the donor derived cells expressed the ISC marker Musashi. The Musashi positive donor derived ISC composed 10.79±1.00% (n=12) of the entire Musashi positive ISC population. (A,B,C) At the highest IP injected cell dose, 2.6*10⁶ cells 12.36±2.39% (n=4) of the ISC were from donor derived cells which was not significantly different from 12.67±1.31% (n=3) of the ISCs at the lowest cell dose of 1.3*10⁶ cells. Injection route did have a significant impact on the contribution of donor derived cells to the ISC population. Following IH injection of 1.6*10⁶ EPCs, donor derived cells composed only 8.19±0.51% (n=4) of the ISC population which was found to be significantly lower than the comparable cell dose following IP injection. (D) 82.38±2.83% (n=4) of donor derived cells retained CD133 expression following IH injection of 1.6*10⁶ cells while only 68.02±5.05% (n=3) of donor derived cells retained CD133 expression following IP injection of 1.3*10⁶ cells. (F) (*p<0.05)

EPCs contribute to the intestinal stem cell niche

The stem cell niche in the small intestine is primarily composed of myofibroblasts which are responsible for supporting the ISC population. Classically, myofibroblasts are identified via coexpression of vimentin and smooth muscle actin. 25.37±1.30% (n=11) of donor derived cells express both smooth muscle actin and vimentin. Furthermore, the donor derived myofibroblasts compose 28.51±1.06% (n=11) of the myofibroblast

population in the small intestine. (fig. 3.4) In order to confirm the expression of both cellular markers by a single cell, Z-stack analysis of a $1\mu\text{M}$ thick stack of images was employed to confirm expression of both smooth muscle actin and vimentin by a single nucleus. (fig. 3.4F)

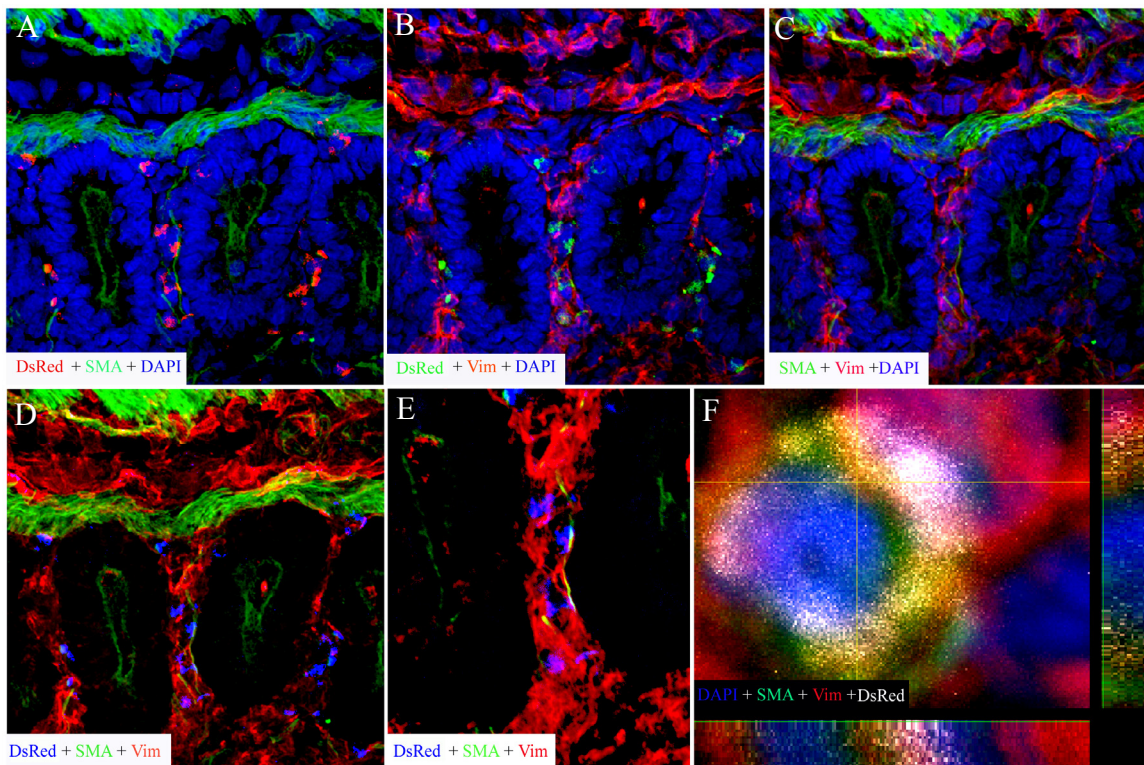


Figure 3.4. **EPCs contribute to the intestinal stem cell niche.** $25.37\pm 1.30\%$ ($n=11$) of donor derived cells express both smooth muscle actin and vimentin. The donor derived myofibroblasts compose $28.51\pm 1.06\%$ ($n=11$) of the myofibroblast population in the small intestine. (A-E) Z-stack analysis of a $1\mu\text{M}$ thick stack of images confirms expression of both smooth muscle actin and vimentin by a single nucleus. (F)

EPCs contribute to the developing intestinal cell population.

Beyond the contribution to the myofibroblast population, EPCs also contributed to the interstitial cell population as well as the epithelial, and enteroendocrine cell populations. Overall, $9.46\pm 0.69\%$ ($n=12$) of donor derived cells expressed the interstitial cell marker, CD117. (fig. 3.5A,B,C) While the majority of the donor derived cells

engrafted in and around the CPT region, $13.63 \pm 1.66\%$ ($n=12$) of the cells engrafted in the villi region of the small intestine. Some of these cells expressed CD117 and contribute to the interstitial cell population. Additionally, a small number of these cells ($>1\%$) expressed the epithelial cell marker, cytokeratin 20 (fig. 3.5D,E,F). Furthermore, a small number of the donor derived cells expressed the enteroendocrine marker, chromogranin A. (fig. 3.5G,H,I).

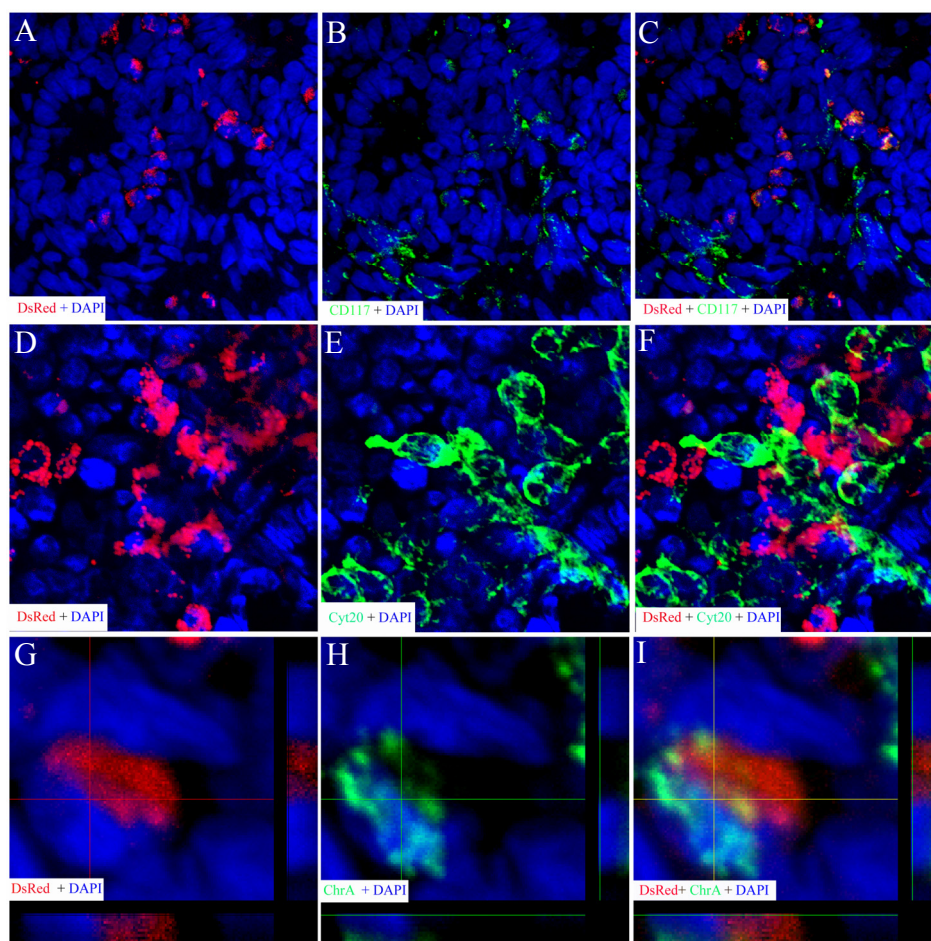


Figure 3.5. EPCs contribute to the intestinal cell population. $9.46 \pm 0.69\%$ ($n=12$) of donor derived cells expressed the interstitial cell marker, CD117. (A,B,C) $13.63 \pm 1.66\%$ ($n=12$) of the cells engrafted in the villi region of the small intestine. Some of these cells expressed CD117 and contribute to the interstitial cell population. Additionally, a small number of these cells ($<1\%$) expressed the epithelial cell marker, cytokeratin 20 (fig 5D,E,F). Furthermore, a small number of the donor derived cells ($<1\%$) expressed the enteroendocrine marker, chromogranin A. (G,H,I).

Discussion

Following transplantation EPCs engraft preferentially into the CPT region of the small intestine. Following transplantation, $81.89 \pm 2.21\%$ ($n=13$) of the donor derived cells preferentially engrafted in and around the crypts of Lieberkühn. Two separate injection routes, intra-hepatic (IH) and intra-peritoneal (IP), were employed but no significant difference in engraftment in either the entire intestine or the CPT region was found. Furthermore, two different cell doses of IH injected animals were tested. The largest cell IP (2.6×10^6 cells) dose was found to have a higher average engraftment in both the overall intestine tissue and the CPT region when compared to the smallest cell dose but was not significant.

In Situ labeling with a human specific probe was performed in order to ensure the DsRed cells were human in origin and therefore donor derived. Human specific In Situ labeling labels all nuclei in fetal human intestine and no nuclei in sheep fetal control intestine as well as the DsRed positive engrafted EPCs in chimeric In Situ. Immunofluorescent labeling with an anti-DsRed antibody also confirmed the presence of donor derived cells as measured through DsRed expression. (fig. 3.2)

$91.88 \pm 1.82\%$ ($n=12$) of donor derived cells continued to express the EPC marker CD133. (fig 2) Expression of the intestinal stem cell marker (ISC), Musashi was found to label the crypts in the small intestine. Overall, $37.66 \pm 3.33\%$ ($n=12$) of the donor derived cells expressed the ISC marker Musashi. While cell dose was insignificant to the contribution to the ISC population, the injection route did have a significant impact on the contribution of donor derived cells to the ISC population. Following IH injection of 1.6×10^6 EPCs, donor derived cells composed only $8.19 \pm 0.51\%$ ($n=4$) of the ISC

population which was found to be significantly lower than the comparable cell dose following IP injection. (fig. 3.3D) Furthermore, while cell dose did not play a role in CD133 expression, there was a significant difference in CD133 expression based on injection route (fig. 3.3). Combined, this evidence indicates that IH injected EPCs are less likely to differentiate into ISCs than IP injected EPCs. Contribution to the stem cell population demonstrates the ability of engrafted EPCs to contribute directly to intestinal regeneration following engraftment.

The stem cell niche in the small intestine is primarily composed of myofibroblasts which are responsible for supporting the ISC population. Classically, myofibroblasts are identified via coexpression of vimentin and smooth muscle actin. $25.37 \pm 1.30\%$ (n=11) of donor derived cells express both smooth muscle actin and vimentin. Furthermore, the donor derived myofibroblasts compose $28.51 \pm 1.06\%$ (n=11) of the myofibroblast population in the small intestine (fig. 3.4). Contribution by the EPCs to the supporting stem cell niche demonstrates their ability to support intestinal regeneration in our non-injury model.

Beyond the contribution to the myofibroblast population, EPCs also contributed to the interstitial cell population as well as the epithelial, and enteroendocrine cell populations. Overall, $9.46 \pm 0.69\%$ (n=12) of donor derived cells expressed the interstitial cell marker, CD117. While the majority of the donor derived cells engrafted in and around the CPT region, $13.63 \pm 1.66\%$ (n=12) of the cells engrafted in the villi region of the small intestine. Some of these cells expressed CD117 and contribute to the interstitial cell population. Additionally, a small number of these cells ($>1\%$) expressed the epithelial cell marker, cytokeratin 20. Furthermore, a small number of the donor derived

cells expressed the enteroendocrine marker, chromogranin A. (fig. 3.5) Contribution to the mature cell population by the donor derived cells was limited and time course data will be needed to determine if the limits to contribution are due to the developmental stage of the fetal model or some other underlying factor. In any case, human EPCs have been shown to functionally engraft into the small intestine following *In Utero* transplantation. Additionally, the donor derived EPCs and their progeny have been shown to contribute to the ISC population as well as the supporting stem cell niche and the mature cell population. While this is a non-injury model, the potential for EPCs to be used in cell therapy in the small bowel has been successfully demonstrated.

Methods and Materials

EPCs transduced with a retroviral vector carrying the DsRed gene were provided by Dr. Yoder. The cells were then injected either IP or IH into the fetal sheep at 59 days of gestation. At 143-145 days of gestation, tissue samples were collected from the fetal sheep. The tissue samples were embedded in frozen and paraffin mounting media for analysis via immunofluorescence and FISH (fig. 3.6)

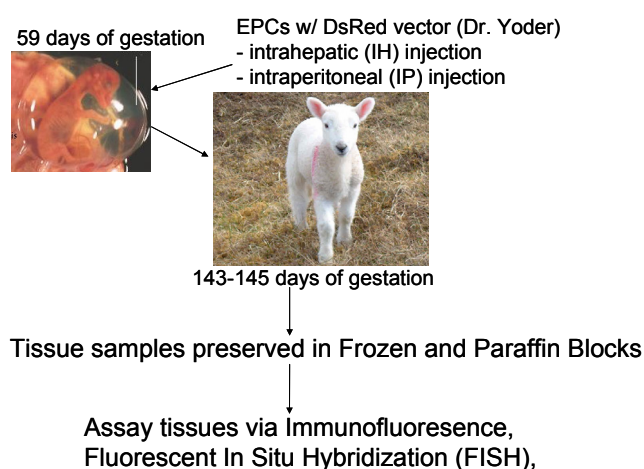


Figure 3.6 Outline of experimental protocol. EPCs transduced with a retroviral vector carrying the DsRed gene were provided by Dr. Yoder. The cells were then injected either IP or IH into the fetal sheep at 59 days of gestation. At 143-145 days of gestation, tissue samples were collected from the fetal sheep. The tissue samples were embedded in frozen and paraffin mounting media for analysis via immunofluorescence and FISH.

(Images from: www.visitberneray.com/gallery/flora10/ & <http://www.vivo.colostate.edu/hbooks/pathphys/reprod/placenta/ovfetus.jpg>)

Cell culture

Cell culture was performed as previously described.²⁰

Immunofluorescence

Preserved cryoblocks were sectioned using a Lica Minotome in 8 micron thick sections and adhered to Superfrost/plus slides (Fisher Scientific, Santa Cruz, CA). Following the sectioning the slides were washed with PBS (Gibco, Aukland, CA) followed by blocking with 10% NGS (Atlanta Biologicals, Lawrenceville, GA) in PBS. Following blocking, slides were incubated overnight in the following primary antibodies: CD31 (Biogenex, San Ramon, CA), Factor VIII related antigen (vWF) (Biogenex, San Ramon, CA), Musashi-1 (R&D Systems, Minneapolis, MN), Cytokeratin 18 (Biogenex, San Ramon, CA), Cytokeratin 19 (Biogenex, San Ramon, CA), Cytokeratin 20 (Biogenex, San Ramon, CA) and DsRed (Clonotech, Mountain View, CA). The following day the slides were washed in 2% NGS in PBS and then incubated in secondary antibody (Molecular Probes, Eugene, OR) for ~30 minutes. Following incubation, the slides were stained with DAPI (Biogenex, San Ramon, CA) to label the nuclei.

In Situ Probe Production

The In situ probe was generated using PCR amplification with primers that generated a human specific probe (5'GAAGCTTA(A/T)(C/G)T(C/A)ACAG-AGTT(G/T)AA3') & (5'GCTGCAGATC(A/C)C(A/C)AAG(A/T/C)AGTTTC3') (IDTDNA, San Diego, CA). For the 647nm labeled probe the reaction conditions were as follows: 5µL 10X hi-fi PCR buffer (Roche, Pleasanton, CA), 3µL 25mM hi-fi MgCl₂ (Roche, Pleasanton, CA), 1µL each d(A,C,G)TP with 0.75µL dTTP 10mM (Invitrogen, Carlsbad, CA), 2.5µL 647nm dUTP 1mM (Invitrogen, Carlsbad, CA) 0.5µL Taq

polymerase (Roche, Pleasanton, CA), 4 μ L 2.5ng/ μ L Human DNA, 2 μ L 30 μ M of each primer, and 27.25 μ L H₂O. The DIG probe was generated using the same conditions with the exception that no 647nm dUTP was used and 1 μ L instead of 0.75 μ L of dTTP was used. The PCR conditions were as follows: 1min 30sec - 94⁰C, 40*(1min - 94⁰C, 1min - 55⁰C, 1min - 72⁰C), hold- 4⁰C. In both cases the PCR product was purified using PCR clean-up (QIAGEN, Germantown, MD). The 647nm probe was then diluted to 20ng/ μ L with in situ hybridization buffer (Biogenex, San Ramon, CA). The DIG probe was then labeled using the DIG High Prime kit (Roche, Pleasanton, CA).

In Situ Hybridization

Preserved paraffin blocks were sectioned using a Shandon Finesse Microtome (Thermo Fisher, Santa Cruz, CA) in 4 micron thick sections and adhered to Superfrost/plus slides (Fisher Scientific, Santa Cruz, CA). The slides were then baked for 45min at 60⁰C in a slide oven (Thermo Fisher, Santa Cruz, CA). The tissue was then washed twice in Xylene (Sigma Aldrich, St. Louis, MO) for 10 min followed by rehydration in 100, 95, then 70% ETOH followed by distilled water for 1-2min each. Antigen retrieval was then performed twice for 10min each at 94⁰C in 1X Dako Target Retrieval Solution (Dako, Via Real Carpinteria, CA). The slides were then cooled to room temperature and then digested using 20 μ g/mL proteinase K solution (Invitrogen, Carlsbad, CA) for 30min for the human sections and 45min for the sheep sections. Both sets of slides were then prehybridized for 5 min at 85⁰C in 50% Di-Formamide (Sigma, St. Louis, MO) and 2X SSC. The human sections were then hybridized with a DIG labeled human specific probe and the sheep / chimeric slides were labeled with a 647nm

labeled human specific probe for 5min at 45⁰C then overnight at 42⁰C in In Situ hybridization buffer (Biogenex, San Ramon, CA).

The following day all slides were washed in 37⁰C 2X SSC for 5 min then twice in 1X PBS (Gibco, Aukland, CA) + 0.1% Triton X (Sigma, St. Louis, MO) for 5min. Following these washing both sets of slides were washed twice with 1X PBS (Gibco). The slides that received the 647nm labeled probe were labeled with DAPI (Biogenex, San Ramon, CA) counterstain for 5min, washed with PBS (Gibco), dried, and covered using a glass cover slip with 2 drops of Cytoseal 60 (Fisher Scientific, Santa Cruz, CA) The DIG labeled slides were blocked with 10% NGS (Atlanta Biologicals, Lawrenceville, GA) in PBS following the PBS wash. Following blocking, slides were incubated overnight in 250 μ L of rabbit anit-DIG antibody (Dako, Via Real Carpinteria, CA). The following day the slides were washed in 2% NGS in PBS and then incubated in 647nm goat anti-rabbit secondary antibody (Molecular Probes, Eugene, OR) for 30 minutes. Following incubation, the slides were washed in 2% NGS in PBS. Following these washes slides were washed with 1X PBS (Gibco), labeled with DAPI (Biogenex, San Ramon, CA) counterstain for 5min, washed with PBS (Gibco), dried, and covered using a glass cover slip with 2 drops of Cytoseal 60 (Fisher Scientific, Santa Cruz, CA)

Microscopy

Immunofluorescent confocal microscopy imaging was performed using an Olympus Fluoview 1000 Confocal System. Immunohistochemistry microscopy imaging was performed using an Olympus BX60 microscope with an Olympus DP70 camera and DP controller software.

Statistical analysis

One-tailed and two-tailed student's t-tests were used in all comparative statistics. All regression analysis were performed using a modified step-wise regression analysis. The StatPro statistical analysis package (Palisade, Ithaca, NY) was used for all statistical analysis and tests.

References

1. Yoder MC. Hemangioblasts: of mice and men. *Blood*. 2007;109:2667-2668.
2. Alvarez DF, Huang L, King JA, ElZarrad MK, Yoder MC, Stevens T. Lung microvascular endothelium is enriched with progenitor cells that exhibit vasculogenic capacity. *American Journal of Physiology - Lung Cellular and Molecular Physiology*. 2008;294:L419-430.
3. Ribatti D. The discovery of endothelial progenitor cells: An historical review. *Leukemia Research*. 2007;31:439-444.
4. Eguchi M, Masuda H, Asahara T. Endothelial progenitor cells for postnatal vasculogenesis. *Clin Exp Nephrol*. 2007;11:18-25.
5. Jin S-W, Patterson C. The Opening Act: Vasculogenesis and the Origins of Circulation. *Arterioscler Thomb Vasc Biol*. 2009;29:00-00.
6. Asahara T, Murohara T, Sullivan A, et al. Isolation of Putative Progenitor Endothelial Cells for Angiogenesis. *Science*. 1997;275:964-966.
7. Javed MJ, Mead LE, Prater D, et al. Endothelial Colony Forming Cells and Mesenchymal Stem Cells are Enriched at Different Gestational Ages in Human Umbilical Cord Blood. *Pediatric Research*. 2008;64:68-73.
8. Nguyen VA, Fürhapter C, Obexer P, Stössel H, Romani N, Sepp N. Endothelial cells from cord blood CD133⁺CD34⁺ progenitors share phenotypic, functional and gene expression profile similarities with lymphatics. *Journal of Cellular and Molecular Medicine*. 2008;9999.
9. Iwami Y, Masuda H, Asahara T. Endothelial progenitor cells: past, state of the art, and future. *Journal of Cellular and Molecular Medicine*. 2004;8:488-497.
10. Khakoo AY, Finkel T. Endothelial Progenitor Cells. *Annual Review of Medicine*. 2005;56:79-101.
11. King J, Hamil T, Creighton J, et al. Structural and functional characteristics of lung macro- and microvascular endothelial cell phenotypes. *Microvascular Research*. 2004;67:139-151.
12. Illa-Bochaca I, Montuenga LM. The regenerative nidi of the locust midgut as a model to study epithelial cell differentiation from stem cells. 2006;209:2215-2223.
13. Roskams T, Desmet V. Embryology of Extra- and Intrahepatic Bile Ducts, the Ductal plate. *The Anatomical Record*. 2008;291:628-635.
14. Schmelzer E, Zhang L, Bruce A, et al. Human hepatic stem cells from fetal and postnatal donors. *Journal of Experimental Medicine*. 2007;204:1973-1987.
15. Yen T-H, Wright N. The gastrointestinal tract stem cell niche. *Stem Cell Reviews*. 2006;2:203-212.
16. Matsumoto K, Yoshitomi H, Rossant J, Zaret KS. Liver Organogenesis Promoted by Endothelial Cells Prior to Vascular Function. *Science*. 2001;294:559-563.
17. Asahara T, Masuda H, Takahashi T, et al. Bone Marrow Origin of Endothelial Progenitor Cells Responsible for Postnatal Vasculogenesis in Physiological and Pathological Neovascularization. *Circulation Research*. 1999;85:221-228.
18. Hsieh PCH, Davis ME, Lisowski LK, Lee RT. ENDOTHELIAL-CARDIOMYOCYTE INTERACTIONS IN CARDIAC DEVELOPMENT AND REPAIR. *Annual Review of Physiology*. 2006;68:51-66.

19. Leor J, Guetta E, Feinberg MS, et al. Human Umbilical Cord Blood-Derived CD133+ Cells Enhance Function and Repair of the Infarcted Myocardium. *Stem Cells*. 2006;24:772-780.
20. Yoder MC, Mead LE, Prater D, et al. Redefining endothelial progenitor cells via clonal analysis and hematopoietic stem/progenitor cell principals. *Blood*. 2007;109:1801-1809.
21. Gehling UM, Ergun S, Fiedler W. CFU-EC: how they were originally defined. *Blood*. 2007;110:1073.
22. Moll R, Zimbelmann R, Goldschmidt MD, et al. The human gene encoding cytokeratin 20 and its expression during fetal development and in gastrointestinal carcinomas. *Differentiation*. 1993;53:75-93.
23. Cogle CR, Theise ND, Fu D, et al. Bone Marrow Contributes to Epithelial Cancers in Mice and Humans as Developmental Mimicry. *Stem Cells*. 2007;25:1881-1887.
24. Roncalli JG, Tongers J, Renault M-A, Losordo DW. Endothelial progenitor cells in regenerative medicine and cancer: a decade of research. *Trends in Biotechnology*. 2008;26:276-283.
25. Bhagwat SV, Petrovic N, Okamoto Y, Shapiro LH. The angiogenic regulator CD13/APN is a transcriptional target of Ras signaling pathways in endothelial morphogenesis. *Blood*. 2003;101:1818-1826.
26. Young PP, Vaughan DE, Hatzopoulos AK. Biologic Properties of Endothelial Progenitor Cells and Their Potential for Cell Therapy. *Progress in Cardiovascular Diseases*. 2007;49:421-429.
27. Urbich C, Dimmeler S. Endothelial Progenitor Cells: Characterization and Role in Vascular Biology. *Circulation Research*. 2004;95:343-353.
28. Lyscom N, Brueton MJ. Intarephthelial, lamina propria and Peyer's patch lymphocytes of the rat small intestine: isolation and characterization of immunoglobulin markers and receptors for monoclonal antibodies. *Immunology*. 1982;45:775-783.
29. Scoville DH, Sato T, He XC, Li L. Current View: Intestinal Stem Cells and Signaling. *Gastroenterology*. 2008;134:849-864.
30. Barker N, van Es JH, Kuipers J, et al. Identification of stem cells in small intestine and colon by marker gene *Lgr5*. *Nature*. 2007;449:1003-1007.
31. Haydont V, Vozenin-Brotans M-C. Maintenance of radiation-induced intestinal fibrosis: Cellular and molecular features. *World Journal of Gastroenterology*. 2007;13:2675-2683.
32. Brittan M, Alison MR, Schier S, Wright NA. Bone Marrow Stem Cell-Mediated Regeneration in IBD: Where Do We Go From Here? *Gastroenterology*. 2007;132:1171-1173.
33. Khalil PN, Weiler V, Nelson PJ, et al. Nonmyeloablative Stem Cell Therapy Enhances Microcirculation and Tissue Regeneration in Murine Inflammatory Bowel Disease. *Gastroenterology*. 2007;132:944-954.
34. Hayashi Y, Tsuji S, Tsujii M, et al. The Transdifferentiation of Bone-Marrow-Derived Cells in Colonic Mucosal Regeneration after Dextran-Sulfate-Sodium-Induced Colitis in Mice. *Pharmacology*. 2007;80:193-199.

35. Walker MR, Stappenbeck TS. Deciphering the 'black box' of the intestinal stem cell niche: taking direction from other systems. *Current Opinion in Gastroenterology*. 2008;24:115-120.
36. Jones DL, Wagers AJ. No place like home: anatomy and function of the stem cell niche. *Nat Rev Mol Cell Biol*. 2008;9:11-21.
37. Ishuzuya-Oka A. Regeneration of the amphibian intestinal epithelium under the control of stem cell niche. *Development, Growth & Differentiation*. 2007;49:99-107.
38. Crew KD, Neugut AI. Epidemiology of upper gastrointestinal malignancies. *Seminars in Oncology*. 2004;31:450-464.
39. Mosolits S, Ullenhag G, Mellstedt H. Therapeutic vaccination in patients with gastrointestinal malignancies. A review of immunological and clinical results. *Annals of Oncology*. 2005;16:847-862.
40. Swartz MJ, Hughes MA, Frassica DA, et al. Adjuvant Concurrent Chemoradiation for Node-Positive Adenocarcinoma of the Duodenum. *Archives of Surgery*. 2007;142:285-288.
41. Stephen BH. Inflammatory bowel disease: Epidemiology, pathogenesis, and therapeutic opportunities. *Inflammatory Bowel Diseases*. 2006;12:S3-S9.
42. Ruiz P, Kato T, Tzakis A. Current Status of Transplantation of the Small Intestine. *Transplantation*. 2007;83:1-6.
43. Rocha FG, Sundback CA, Krebs NJ, et al. The effect of sustained delivery of vascular endothelial growth factor on angiogenesis in tissue-engineered intestine. *Biomaterials*. 2008;29:2884-2890.
44. Baksh D, Song L, Tuan RS. Adult mesenchymal stem cells: characterization, differentiation, and application in cell and gene therapy. *Journal of Cellular and Molecular Medicine*. 2004;8:301-316.
45. Nakamura T, Torimura T, Sakamoto M, et al. Significance and Therapeutic Potential of Endothelial Progenitor Cell Transplantation in a Cirrhotic Liver Rat Model. *Gastroenterology*. 2007;133:91-107.e101.
46. Weil B, Markel T, Herrmann J, Abarbanell A, Meldrum D. 204. Mesenchymal Stem Cells Enhance the Proliferation of Human Fetal Intestinal Cells Following Hypoxic Injury via Paracrine Mechanisms. *Journal of Surgical Research*. 2009;151:264-264.
47. Zhang ZL, Tong J, Lu RN, Scutt AM, Goltzman D, Miao DS. Therapeutic potential of non-adherent BM-derived mesenchymal stem cells in tissue regeneration. *Bone Marrow Transplant*. 2008;43:69-81.
48. Ingram DA, Mead LE, Tanaka H, et al. Identification of a novel hierarchy of endothelial progenitor cells using human peripheral and umbilical cord blood. 2004;104:2752-2760.
49. Al-toma A, Visser OJ, van Roessel HM, et al. Autologous hematopoietic stem cell transplantation in refractory celiac disease with aberrant T cells. *Blood*. 2007;109:2243-2249.
50. Moore KA, Lemischka IR. Stem Cells and Their Niches. *Science*. 2006;311:1880-1885.
51. Ingram DA, Mead LE, Moore DB, Woodard W, Fenoglio A, Yoder MC. Vessel wall-derived endothelial cells rapidly proliferate because they contain a complete hierarchy of endothelial progenitor cells. 2005;105:2783-2786.

52. Phinney DG, Prockop DJ. Concise Review: Mesenchymal Stem/Multipotent Stromal Cells: The State of Transdifferentiation and Modes of Tissue Repair Current Views. *Stem Cells*. 2007;25:2896-2902.

Chapter 4:
Retroviral Integration Site Analysis
of HIV and MSCV in MSCs & EPCs

Abstract

The ability of mesenchymal stem cells (MSC) to give rise to cells of other seemingly unrelated tissue has now been demonstrated by several researchers.¹⁻³ As currently defined, Mesenchymal Stem Cells are characterized as Stro-1⁺, CD45⁻, & Gly⁻A⁻.³ However, the possibility that the currently defined MSC population is a heterogeneous mixture of cells with varying potential remains. Thus, the argument remains as to whether or not a single parent MSC can give rise to multiple tissue types.⁴ To address this question we employed linear amplification mediated (LAM) and linker mediated (LM) PCR techniques to track the unique retroviral integration sites in MSCs. A single integration site was sequenced in *In vitro* cultured MSCs using LAM-PCR and several integration sites were sequenced in *In vitro* cultured MSCs using LM-PCR. However, identification of integration sites remained elusive in chimeric samples. Following discovery of much higher engraftment of Endothelial Progenitor Cells in the chimeric intestine of transplanted sheep, LM-PCR was employed to identify any engraftment sites in these samples. While electrophoresis following LM-PCR did not reveal any bands, the chimerism of the DNA has been confirmed using human specific PCR probes.

Introduction

The ability of mesenchymal stem cells (MSC) to give rise to cells of other seemingly unrelated tissue has now been demonstrated by several researchers.¹⁻³ We have previously reported the ability of MSC populations to give rise to several tissue sources.¹ A concise study of the *In vivo* potential of clonal MSC populations is needed. A method for studying the *In vivo* potential of individual cells came from the first real

success for gene therapy. In this trial, several children were cured of X-linked severe combined immunodeficiency (X-SCID) by gene therapy using an Moloney Murine Leukemia Virus (MMLV) derivative.⁵⁻⁷ In the trial, the MMLV vector was used to integrate the gene for the γ -common chain for the interleukin 2 receptor (which is absent in X-SCID patients) into the genome of the patients. While the disorder was corrected in all but one patient, leukemia developed as a result of integration upstream and subsequent activation of the LMO2 oncogene. Following the development of leukemia by some of the children enrolled in the French X-SCID gene therapy trial, techniques allowing accurate and relatively rapid integration site analysis of retroviral markers became necessary and were developed.^{2,8-15}

Human immunodeficiency virus (HIV) is another retrovirus that has been modified to eliminate its T-cell destroying effects and used as a gene therapy vector for over a decade.¹⁶ The HIV-based vectors possess multiple advantages over MMLV including the ability to infect both dividing and non-dividing cells.^{15,17,18} In contrast to HIV vectors, Murine Stem Cell Virus (MSCV) based vectors are also retroviral vectors and are only able to infect dividing cells.¹⁹ Since retroviral integration into the host cell genome is considered to be a semi-random process, each cell that has been transduced with a retroviral vector has a unique integration site, thus providing a molecular marker that is unique to each cell.^{18,20} By identifying the retroviral integration sites in a population of cells you have identified the cells in that population. Consequently, if the same integration sites are identified in multiple tissues following transplantation of those cells, then those cells have produced daughter cells that engrafted into those tissues.

Previous sequence analysis techniques required 100 to 1,000 copies of the flanking DNA region for sequencing reactions. Linear Amplification Mediated (LAM)-PCR uses a series of enzymatic reactions and amplifications to detect several unique integrations sites.² As little as a single integration site can be detected by this method of amplification followed by sequencing. The method relies on an initial linear amplification using a biotinylated primer that is specific to the LTR region of the viral vector employed for cell marking so that a Streptavidin-labeled magnetic bead can then be used to purify the product/amplicon. The linear product is then randomly primed and a complementary strand is synthesized using a Klenow reactoin. A linker cassette with nested primers is bound to allow double stranded PCR extension and sodium hydroxide is used to cleave the magnetic bead. Nested PCR is used to amplify the purified product exponentially. (fig. 4.1)

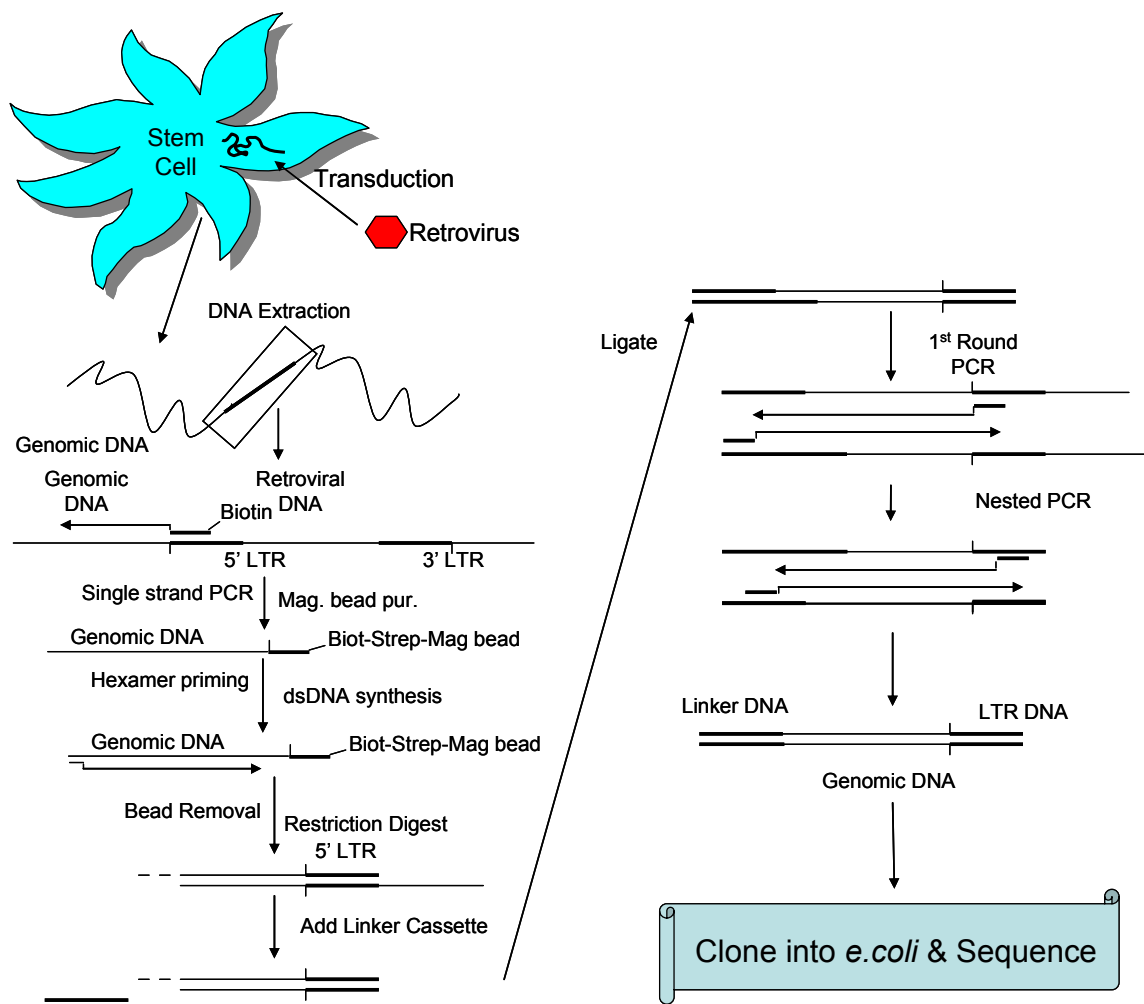


Figure 4.1. **Linear amplification mediated (LAM)-PCR.** The 5' biotinylated primer binds ~100bp from the 5' (or 3') terminus on the lagging strand LTR and amplifies for a variable distance into the genomic DNA. Streptavidin-coated magnetic beads (blue) are used to pull out the Biotinylated products/amplicons. These products are then randomly primed using random hexamers and extended using Klenow. A linker cassette with nested primer sites is then ligated following a restriction digestion and sodium hydroxide is used to cleave the biotin and accompanying magnetic bead. Nested PCR is then used to amplify the purified products which are then separated using gel electrophoresis. The samples are then gel-extracted and ligated into a TOPO[®] vector; which is transformed into competent *E. coli* cells and plated in the presence of Ampicillin and X-Gal. The appropriately transformed white colonies are then cultured in the presence of Ampicillin. Plasmids are then purified from these cultures and sequenced to identify the site of genomic integration.

However, LAM-PCR has been argued by several researchers to prefer certain integration sites over others given the nature of the PCR of the first linear strand. To

reduce the bias in the protocol, reduce the complexity, and the expense, linker mediated (LM) PCR was developed. LM-PCR employs an initial digestion step that cleaves the sample DNA in random locations using a 4-base pair cutter. A second endonuclease is then employed to cleave the undesired long terminal repeated region (LTR) of the integrated retrovirus to reduce non-specific amplicons. Following cleavage, a linker cassette is ligated to the amplicon using the overhanging cleaved DNA. The attached linker cassette, along with the LTR, is then used as primer binding sites in a nested PCR reaction (fig. 4.2).

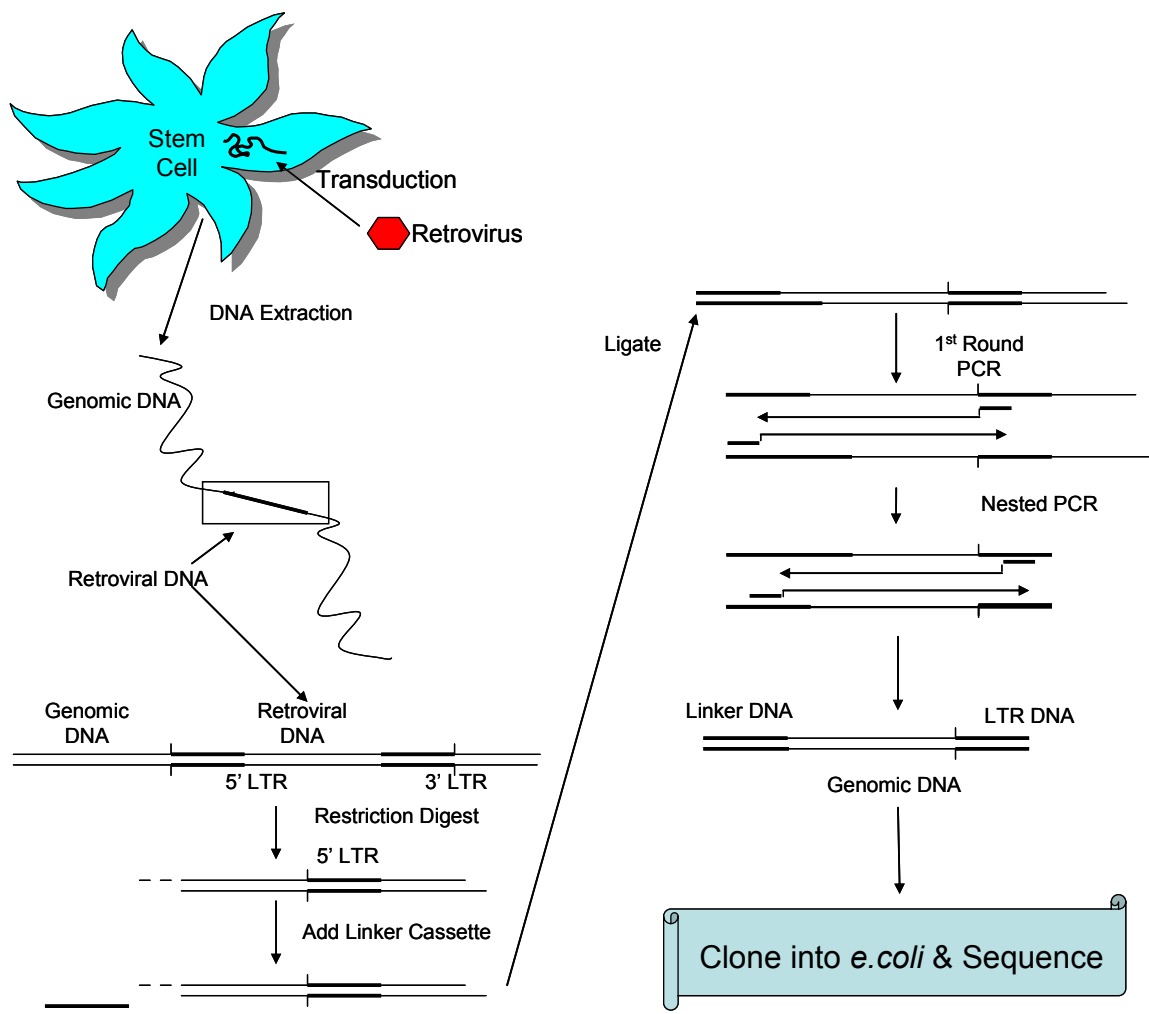


Figure 4.2. **Linker Mediated (LM)-PCR.** The genomic DNA is digested using enzymes that cleave specific DNA sequences. A linker cassette with nested primers is then ligated. Nested PCR is then used to amplify the purified products which are then separated using gel electrophoresis. The samples are then gel-extracted and ligated into a TOPO[®] vector; which is transformed into competent *E. coli* cells and plated in the presence of Ampicillin and X-Gal. The appropriately transformed white colonies are then cultured in the presence of Ampicillin. Plasmids are then purified from these cultures and sequenced to identify the site of genomic integration.

Following nested PCR amplification, the protocol is identical for both LM-PCR and LAM-PCR. The individually amplified products are separated using gel electrophoresis. The gel purified samples are then ligated into a TOPO[®] vector allowing individual colony selection carrying the 5' sequence and an individual insertion event.

The TOPO[®] vector is then transformed into chemically competent *E. coli* cells and plated in the presence of Ampicillin and X-Gal. The Ampicillin resistance gene is encoded on the plasmid, so only bacteria carrying a plasmid will survive on the plate. Furthermore, the ligation of the integration site interrupts the β galactosidase gene so only colonies that contain plasmid with an insert will be white. Colonies with a plasmid that does not contain an insert will react with the X-Gal and turn blue. The development of LAM-PCR and LM-PCR thus allows a relatively simple method of analyzing integration sites and is now commonly employed for this purpose (fig. 4.3).^{13,21,22}

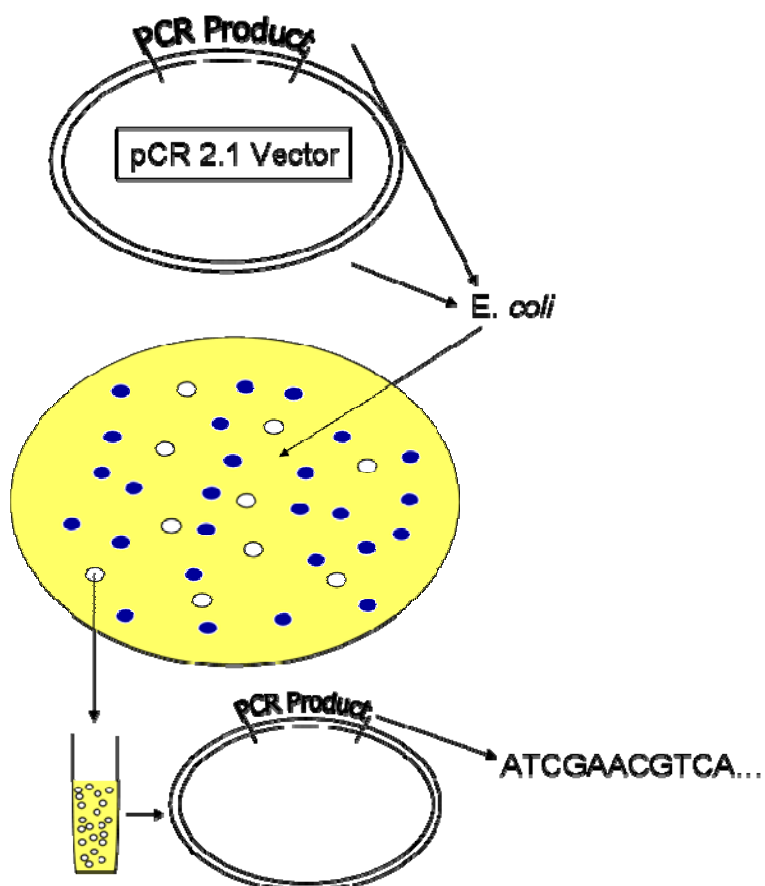


Figure 4.3. **TOPO cloning of 2nd Nested PCR products.** Following the 2nd nested PCR in either LAM or LM-PCR, the products are ligated into the pCR 2.1 TOPO vector. The vector is then transduced into chemically competent One-Shot TOP10 cells and the cells are plated on agar plates with Ampicillin and X-GAL. Only cells containing the vector can survive the Ampicillin. Furthermore, the PCR product interrupts the β -galactosidase gene so plasmids carrying inserts will not express β -galactosidase. These colonies will therefore not react with the X-GAL and

remain white. Colonies that contain plasmids but not inserts will express β -galactosidase and this will react with the X-GAL to turn blue. The white colonies are then grown in liquid cultures and the plasmids are extracted. The inserts in the extracted plasmids are then sequenced at the Nevada Genomics Center.

The LAM and LM-PCR techniques allow us to track the engraftment of individual MSCs following transplantation. Detection of the MSCs and their subsequent progenitors from the same cell lineage in multiple tissue types provides direct evidence that a single MSC is capable of giving rise to cells with the ability to engraft in multiple tissue types. This evidence would provide support for the argument that what is currently defined as an MSC population (isolated using Stro-1⁺, CD45⁻, & Gly-A⁻)³ is in fact a homogenous mixture of cells with equal potentials. In contrast, the detection of completely unique integration sites in multiple tissue types would indicate the possibility of a heterogeneous mixture of cells in the currently defined MSC population. In this chapter LAM-PCR is used to successfully identify an integration site in a positive control sample. Following the discovery of bias in the LAM-PCR protocol, the LM-PCR protocol is used to successfully identify several integration sites in positive control samples. Further testing on an experimental sample reveals the presence of chimeric DNA in the sample and successful amplification of integration sites in this sample is pending further investigation.

Results

Sequence analysis of an HIV vector integration site using LAM-PCR

The LAM-PCR system we employed was used to identify HIV-based vector integration sites. To demonstrate the functionality of the system, DNA from *In vitro* cultured cells that were transfected with the HIV-based vector was purified and analyzed. Along side the positive control, several samples from chimeric animals were also

analyzed using the LAM-PCR system. DNA from bone marrow was the primary source attempted to identify vector integration sites. Figure 4.4 is an image of the gel following LAM-PCR & electrophoresis. The sample order in the gel from left to right is: 100bp ladder, Positive control, 1925-1, 2560-1, empty lane, negative control, water control, 100bp ladder. 1925-1 is DNA from bone marrow that is from Dr. Chamberlain's samples. 2560-1 is DNA from bone marrow from my own samples. The positive control is DNA from BM-MSCs transfected with the HIV-1 vector. The bands that appear in the gel are DNA as indicated by the green color given by the GelStar stain as opposed to gel artifacts that appear in orange (fig. 4.4A). There appears to be three strong bands in the positive control sample that may be integration sites. The bands appear at ~380, 420, and 550bp in the positive control sample (fig. 4.4B). These three samples appear to be strong enough, and long enough (>280bp) to allow for gel extraction and successful sequencing. There are bands that appear in the two chimeric bone marrow samples that were too weak to be successfully extracted from the gel. The band that appears in the negative control is also too faint to be gel extracted but may be a non-specific product amplified using LAM-PCR. The smear that appears in the water control appears to be related, though not completely explained by, the magnesium concentration in the PCR reaction as varying this concentration varied the intensity of the smear (data not shown) (fig. 4.4).

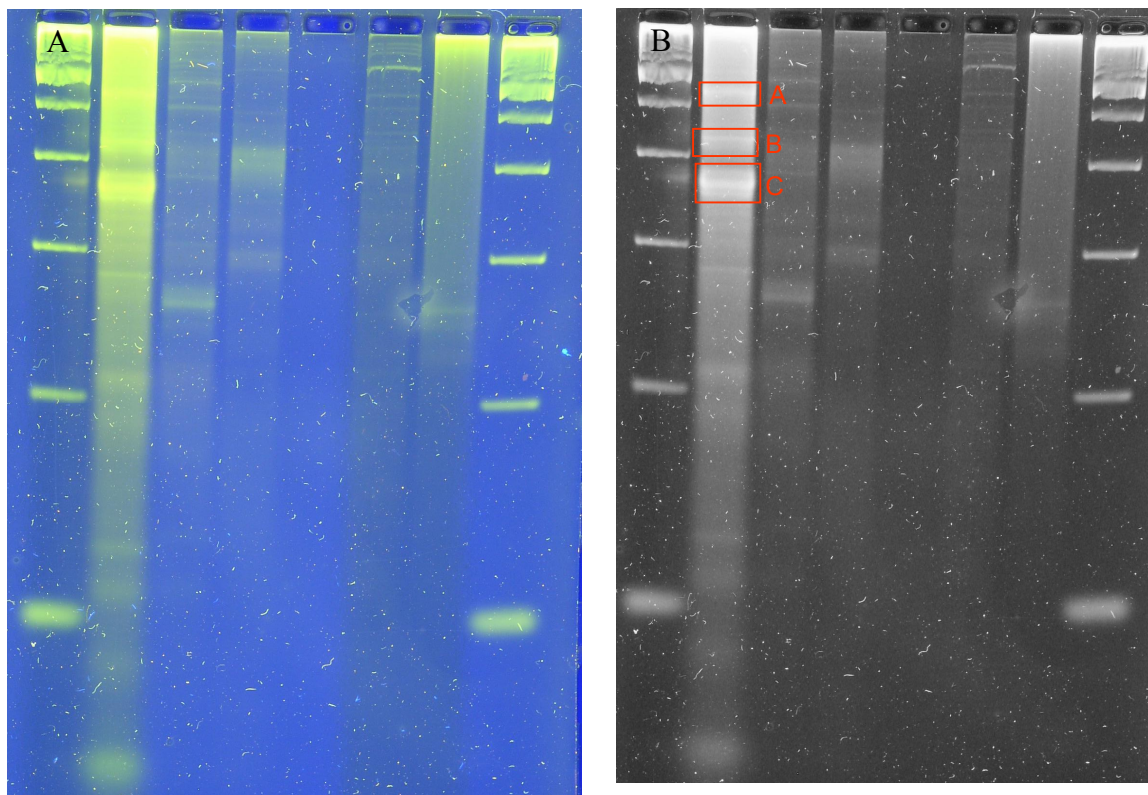


Figure 4.4 **Bands identified in the positive control sample to be TOPO cloned.** A color image of the gel (A) and a black and white image of the same gel (B) demonstrate the bands are in fact dsDNA given their green color using GelStar stain(A) and that the bands are significantly brighter than any background staining (B). The gel layout from left to right is: 100bp ladder, Positive control, 1925-1, 2560-1, space, negative control, water, 100bp ladder. 1925-1 is DNA from bone marrow that is from Dr. Chamberlain's samples. 2560-1 is DNA from bone marrow from my own samples. The positive control is DNA from BM-MSCs transfected with the HIV-1 vector. There appears to be three strong bands in the positive control sample that may be integration sites. The bands appear at ~380, 420, and 550bp in the positive control sample. These three samples appear to be strong enough, and long enough (>280bp) to allow for gel extraction and successful sequencing. Bands appear in the two BM samples but are too weak to be extracted. There are some bands in the negative control but again are far too weak to be extracted or sequenced, there is also an unknown smear in the water control that may be an Mg smear.

Following gel extraction and TOPO cloning, the positive control sample was quantitated and sent to the Nevada Genomic Center (NGC) for sequencing. Following sequencing, the first pass analysis was performed using the Chloroplast tool available

from the Nevada Bioinformatics Core. The sequences that contained human DNA sequences were then individually analyzed using the Blast website. The TOPO vector sequence was identified visually and using the BlastN function and highlighted in grey. The HIV-based vector sequence was then identified visually and using the BlastN function. The primer binding sequence was then identified visually and both the vector and the primer binding sequence were highlighted in red and fuchsia, respectively. The sequence of DNA that was found between the TOPO vector and the HIV LTR sequence was then screened against the *Bos Taurus* genome and the portion of the *Ovis Aries* genome that has been published. Non-specific amplification of the sheep genomic DNA (*Ovis Aries*) blasts with greater identity to cow (*Bos Taurus*). Sequences that were negative in the sheep and cow blasts were blasted against the human genome sequence using the Blast website. Further analysis revealed the human sequences to be on chromosome 17 between 43872895bp – 43873059bp. The integration site appears to be at base pair 43873059. One clone with an e-value of $5e^{-89}$ was found and 9 clones with an e-value of $1e^{-21}$ were found. These 10 clones successfully identify the integration site in this positive control. The identities were between 98-99% and there were no gaps in the sequences analyzed. (fig. 4.5)

>JAW-A16-M13F

```
GCTCGAGCGGCCGCCAGTGTGATGGATATCTGCAGAATTCGCCCTTGTACACCTAACTGC
TGTGCCACCAACCTTGTGACCTAGGGCAAGTCATTTAACCTCCAACCTTCAACATCTTC
ACTCCAAGGAGAAAATGCCTGGGAAAGGGAAGGCCAAGGGCTTCCAAAGTCCGCAATTT
AAGATGGTACCCAATAATGGTTAATGTGAGGATCCTCCCACCCCTCTGTGGATCTACCAC
ACACAAGGCTACTTCCCTGATTGGCAGAACTACACACCAGGGCCAGGGATCAGATATCC
ACTGACCTTTGGA TGGTGCTACAAGCTAGTACC AAGGGCGAATTCCAGCACACTGGCGG
CCGTTACTAGTGGATCCGAGCTCGGTACCAAGCTTGGCGTAATCATGGTCATAGCTGTT
```

NNN = Human DNA Sequence

NNN = HIV-1 Vector Sequence

NNN = Primer Binding Site

NNN = TOPO Vector Sequence

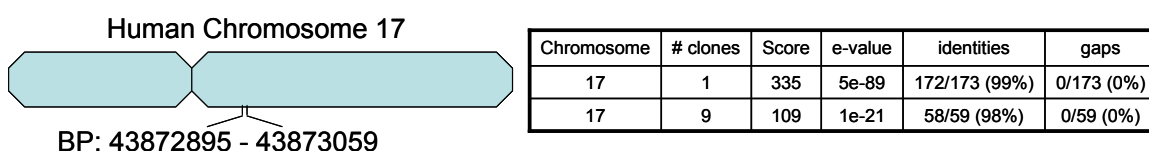


Figure 4.5. Positive control HIV-based vector positive control vector integration site. Following extraction from the gel and TOPO cloning, several samples were submitted to the genomics center for sequencing. A representative sequence above depicts the TOPO vector (grey) flanking the human sequence (yellow) and the HIV-based vector along with nested primer binding site (red & fuchsia). Further analysis revealed the human sequence to be on chromosome 17 between 43872895bp – 43873059bp. The integration site appears to be at base pair 43873059. One clone with an e-value of $5e^{-89}$ was found and 9 clones with an e-value of $1e^{-21}$ were found. These 10 clones successfully identify the integration site in this positive control. The identities were between 98-99% and there were no gaps in the sequences analyzed.

Sequence analysis of HIV vector integration site using LM-PCR

Following analysis of the positive control using LAM-PCR, LM-PCR was employed to identify the vector integration sites in a positive control sample. The protocol was used as previously described. Following nested PCR samples were analyzed using gel electrophoresis and a smear containing faint bands were identified in the positive control while no other smears or bands were identified in any other lanes including the sheep negative control and the water control. Unfortunately, no bands or smears were identified in the chimeric experimental samples.

Due to the large spread and faint nature of the bands, gel extraction was not employed. Instead, 10 μ L of nested PCR product was TOPO cloned as described previously. The resulting white colonies were selected and cultured in the 96-well plate format, the plasmids were then isolated and sequenced. In a similar analysis method to LAM-PCR, the sequences were extracted and ran in batch against the cow, sheep, and human genomes as previously described. The sequences that were a positive match to the human genome and a negative match to the sheep and cow genomes were formatted in a Microsoft Word document. The TOPO sequence was identified and highlighted in grey, the linker cassette in green, and the HIV-based vector sequence in red. (data not shown) The DNA sequence that was located between a linker cassette and an HIV-based vector was blasted and the resulting sequences that were found to be human with an e-value of $10e^{-19}$ or lower were accepted as true integration sites. There were other sites but these were too short or too inaccurate to be accepted. Each sequence was identified in more than one clone and integration sites were found on chromosomes: 1, 2, 9, 10, 11, 12 (two), 14, and 21 at base pairs: 148928361, 110248786, 85466327, 119556989, 14310371, 12470013, 120155475, 102391175, and 46451192, respectively. (fig. 4.6)

Chromosome	E-value	Bp Start	Bp End
14	2.00E-43	102391175	102391265
12	6.00E-36	120155475	120155558
12	2.00E-28	12470013	12470085
2	1.00E-27	110248786	110248849
21	2.00E-26	46451192	46451253
10	9.00E-26	119556989	119556959
11	1.00E-24	14310371	14310429
1	2.00E-23	148928361	148928417
9	9.00E-19	85466327	85466383

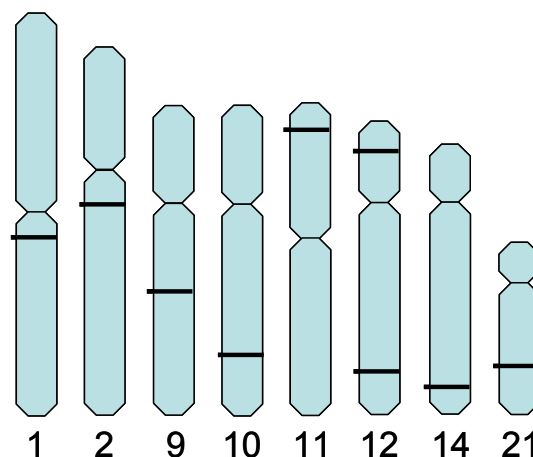
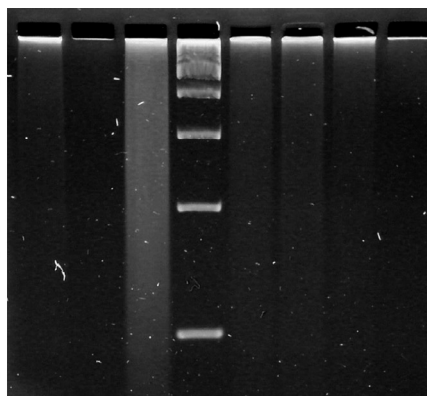
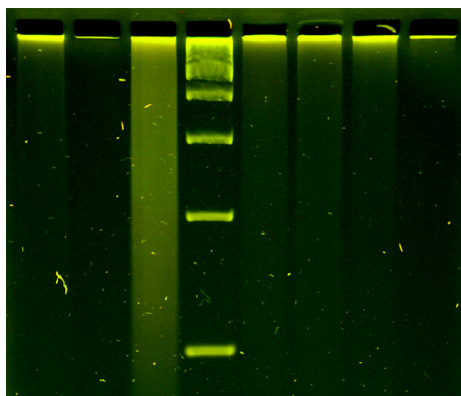


Figure 4.6. **Vector integration sites identified using LM-PCR on the HIV-based positive control MSC DNA.** The DNA sequence that was located in between a linker cassette and an HIV-based vector was blasted and the resulting sequences that were found to be human with an e-value of $10e^{-19}$ or lower were accepted as true integration sites. There were other sites but these were too short or too inaccurate to be accepted. Each sequence was identified in more than one clone and integration sites were found on chromosomes: 1, 2, 9, 10, 11, 12 (two), 14, and 21 at base pairs: 148928361, 110248786, 85466327, 119556989, 14310371, 12470013, 120155475, 102391175, and 46451192, respectively.

LM-PCR of MSCV transfected cells

The inability to identify vector integration sites in the experimental animals indicated that the system as it exists was not sensitive enough to detect these low levels of engraftment. However, we found much higher levels of engraftment in the small intestine of chimeric sheep that had been transplanted with EPCs. These EPCs carried integrations from and MSCV vector. LM-PCR for the detection of MSCV transfected cells from *In vitro* cell cultures was previously developed by Chris Clark in our lab. In order to increase the chance of detecting human cells in a chimeric animal, LM-PCR for MSCV was employed in the analysis of the EPC transplanted intestine for chimeric animal 2288. Analysis revealed that the positive control DNA (MSC DNA from transfected cells) produced a smear following electrophoresis analysis as was previously

observed in prior experiments (data not shown). However, LM-PCR of the chimeric animal revealed no smears or bands. In the gel image below (fig. 4.7), the sample order from left to right is: 2288 Intestine DNA, space, positive control DNA, 100bp ladder, human DNA, sheep DNA, water control-1, and water control-2. DNA was extracted from paraffin embedded intestine from animal 2288 using the QIAGEN DNA extraction kit. As can be seen, no bands or smears were detected. The positive control DNA is DNA extracted from MSC transfected with MSCV and as can be seen, a smear resulted and appears to be DNA as indicated by the green color (as opposed to an orange artifact) (fig. 4.9A). Furthermore, the smear is observably brighter than background levels (fig. 4.9B). The sheep and human control DNA presents no bands or smears. There is a slight difference between the water control-1 which went through the entire LM-PCR protocol and the water control-2 which only went through the nester PCR protocol. In either case



there are no bands or smears in either water control sample (fig. 4.7).

Figure 4.7. LM-PCR of MSCV positive control and chimeric samples. The sample order from left to right is: 2288 Intestine DNA, space, positive control DNA, 100bp ladder, human DNA, sheep DNA, water control-1, and water control-2. DNA was extracted from paraffin embedded intestine from animal 2288 using the QIAGEN DNA extraction kit. As can be seen, no bands or smears were detected. The positive control DNA is DNA extracted from MSC transfected with MSCV and as can be seen, a smear resulted. The sheep and human control DNA presents no bands or smears. There is a slight difference between the water control-1 which went through the entire LM-PCR protocol and the water control-2 which only went through the nester PCR protocol. In either case there are no bands or smears in either water control sample.

LM-PCR of EPCs

PCR analysis to determine the presence of human DNA was employed. Using human specific primers for the β 2-microglobulin gene, two of the four DNA samples were found to be chimeric (fig. 4.8A). Given the lack of bands in the electrophoresis results following LM-PCR of the chimeric intestine sample (animal 2288), further analysis using PCR primers for the house keeping gene, β -actin, were employed. PCR analysis with the β -actin primers confirmed the presence of amplifiable DNA in four separate samples (fig. 4.8B).

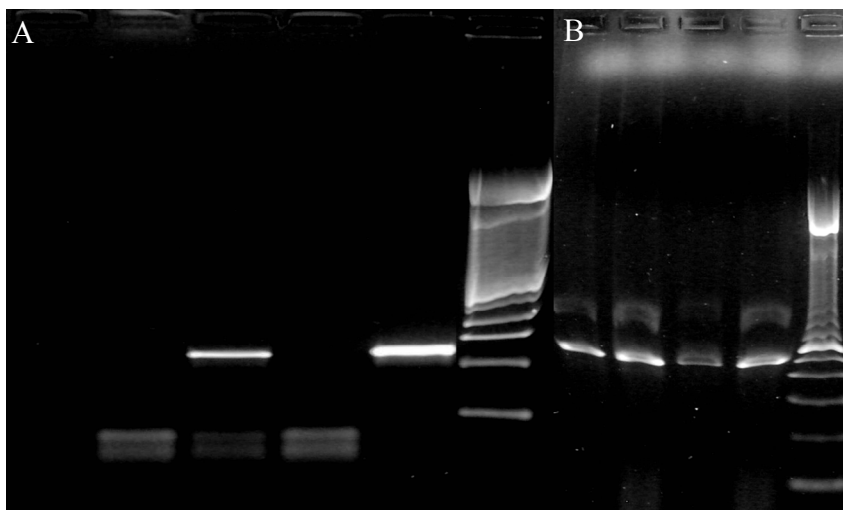


Figure 4.8. 2288 Intestine DNA can be amplified and is chimeric. Four separate samples of intestine DNA from animal 2288 were extracted from paraffin embedded tissue. Following extraction, PCR amplification using the human specific

primers for the factor 8 gene was employed to demonstrate the chimerism of the samples. The gel layout from left to right contains the four 2288 intestine DNA samples (one of which successfully amplified Factor 8), human control, 100bp ladder (A). PCR amplification of the β -actin housekeeping gene was employed to confirm intact and amplifiable DNA in all four samples. The gel layout from left to right is the beta actin gene amplified from the four 2288 intestine samples followed by the 100bp ladder (B).

Discussion

LAM-PCR was initially employed in our lab to identify the vector integration sites of HIV based vectors in transplanted MSCs. Analysis using LAM-PCR was able to

successfully identify only one vector integration site in DNA from MSCs that were cultured *In vitro*. Further analysis revealed this sequence to be on chromosome 17. (fig. 4.4) Following the discovery of bias in the LAM-PCR protocol, the much less complicated and less biased LM-PCR protocol was employed to identify vector integration sites in the same control DNA analyzed via LAM-PCR. The result of these experiments was a lack of bands in the chimeric samples and detection of multiple integration sites in the positive control DNA (fig. 4.6). However, the same integration site on chromosome 17 that was found using LAM-PCR was not found using LM-PCR. This evidence suggests that both LM and LAM-PCR are insufficient at detecting all of the integration sites present in a DNA sample. Thus, some level of bias or detection threshold still exist. Operating under the hypothesis that the engraftment level in the chimeric samples was below the detection threshold of the LM-PCR system a much higher engraftment sample was found.

During my studies of EPC engraftment in fetal sheep, particularly high engraftment rate was discovered in the intestine of EPC transplanted animals. However, the EPC transplanted in this case carry integrations from an MSCV based vector. Since LM-PCR for MSCV integration sites had previously been developed, this system was employed to study the integration sites. DNA was extracted from 10 μ m sections of the paraffin embedded small intestine of chimeric animal 2288. Quantitation by the NGC confirmed the presence of DNA. Furthermore, LM-PCR analysis revealed a smear in the positive control cells following electrophoresis as had been previously observed by Chris Clark and others. Since this positive result had been previously observed in our lab and given the lack of results in the chimeric sample, this smear has not been TOPO cloned or

sequenced to date (fig. 4.7). Further analysis using PCR primers for the house keeping gene, beta actin, confirmed the presence of amplifiable DNA. Additionally, a set of primers designed by Chad Sanada for human specific PCR to amplify the Factor VIII gene demonstrates the chimerism of the DNA (fig. 4.8). It remains possible that there is amplified integration sites in the nested PCR samples from chimeric animals but that the intensity of the resulting smear is simply too faint to be detected. Sequencing of these samples and the positive control samples will be employed in future experiments.

While these studies have been ongoing there have been advances in the field of vector integration site sequencing and in tracking the clonal populations of MSCs. The invention of pyrosequencing allows the sequencing of genomes at 100-fold higher throughput. The sequencing of the whole genome eliminates any biases that LM and LAM-PCR have and the high throughput allows the rapid detection of several integration sites across multiple DNA sources.^{23,24} Pyrosequencing is cost prohibitive however and would require collaboration and funding for our lab to apply this technology to the current studies. Furthermore, clonal analysis of adipose derived adult stem cells which are similar in surface and adhesion markers have been shown to differentiate into at least two different tissue types at the clonal level.²⁵ This study suggests that MSCs are likely to be homogenous in nature as well. However, the debate continues on this research and future findings in this project will continue to be pertinent.

Materials and Methods:

DNA Source

MSCs were transfected with either an HIV or an MSCV based vector and culture in the presence of antibiotic selection. *In utero* transplantation of MSCs that was then performed at 55 days of gestation. At 120 - 140 days of gestation the fetal tissue was collected. DNA extraction from both the transfected cells and the chimeric tissue was then performed using a Qiagen DNeasy Kit (QIAGEN sciences, MD).

LAM-PCR

To perform LAM-PCR, the purified DNA from each tissue source was first concentrated to yield 50ng/uL, so that 2uL of each sample contained 100ng of DNA for the initial PCR amplifications. The initial amplifications employed a standard 50μL reaction mixture (41 μL H₂O, 5 μL 10X Roche[®] PCR Buffer Mix, 10⁻⁵nmol of each dNTP, 10⁻⁵ μmol primer, and 2.5U Taq polymerase) with a biotinylated primer “Green-1” or “Orange” (fig 9, step 1) that binds ~100bp from the end of the retroviral long terminal repeat (LTR). Amplification followed a standard thermocycler program (tbl. 4.1) for 50 cycles. Following the first amplification, an additional 2.5U of Taq polymerase was added to the reaction, and cycling was allowed to continue for another 50 cycles.

Step #	Temperature (°C)	Time (min:sec)
1	95°C	5:00
2	95°C	1:00
3	57°C	0:45
4	72°C	1:30
5	Go To Step 2, 49 Times	
6	72°C	10:00
7	4°C	---
8	Add Taq	
9	Repeat Steps 1-7	

Table 4.1. Standard PCR reaction program for LAM-PCR. The samples were amplified for two, 50 cycle reactions resulting in a total number of amplicons equal to X^{100} . This began with an initial denaturation of the DNA at 95°C for 5 minutes followed by a repeated denaturation at the same temperature for 1 minute. The annealing temperature for the primer varied from 57^o – 62^oC depending on whether the Green or Orange primer was in use. In both case annealing proceeded for 45 seconds. Extension of the DNA then proceeded for 1½ minutes at

72⁰C and the denature, anneal, extend cycles were repeated 49 times. A final extension at 72⁰C for 10 minutes was performed at which point the samples were stored at 4⁰C until additional Taq polymerase was added and the entire protocol was repeated.

Following the initial amplification, the biotinylated amplification products were captured with Streptavidin-beads and washed using a DYNAL[®] KiloBase magnetic capture system and clean-up protocol. The complementary strand was synthesized with random hexanucleotides using 0.2U of Klenow during a 60 minute incubation at 37⁰C before enzyme digestion using 0.5U of HinP1I or HpyCH4IV and addition of a 3' linker cassette using the FAST-Link DNA Ligation Kit (EPICENTRE[®]) (fig. 4.9, steps 2-6). The linker cassette is composed of two custom oligo's annealed together, HIV Link-38 and HIV Link-31. Following these modifications, the samples were separated from the magnetic beads using 0.1N NaOH.

Nested PCR was then employed to exponentially amplify the product using primers that were specific for the 5'LTR region described above (HIV-NesLTR-1 Orange option or Green Option and HIV-NesLTR2) and nested primers (HIV-LC-nes-1 and HIV-LC-nes-2) specific to the cassette annealed to the 3'terminus of the purified products. Primer sequences are as follows:

HIV-NesLTR-1 Orange Option 5'- GGTCATCCATTCCATGCAGG-3'

HIV-NesLTR-1 Green Option 5'-ACAAGCTGGTGTCTCTCCT-3'

HIV-NesLTR2 Orange or Green 5'-GGTACTAGCTTGTAGCACCA -3'

HIV-LC-nes-1 5'-CTGCGGCGTCTAGACTTAAGTC-3'

HIV-LC-nes-2 5'-GTCACCTAACTGCTGTGCC-3'.

Amplification using the first nested primer pair employed the reaction conditions described in Table 1 for 32 cycles. Preceding amplification using the second nested

primer, a QIAquick PCR purification kit[®] was employed. The second nested primer reaction again used similar reaction conditions to those described in tbl. 4.1 with 3 μ L of the nested product serving as a template for 38 cycles of amplification. (fig. 4.9, step 7)

Gel electrophoresis using a Spreadex 1200 EL Submerged Mini Gel System by ElChrom[®] was then used to separate the amplified products. 7 μ L of dual technical replicates for each sample was loaded and run at 120V for 60 minutes at 25⁰C. Gels were then stained overnight with the SYBR Gold[®] system according to manufacturer's recommendations (Molecular Probes (Invitrogen), Carlsbad, CA). The samples were then extracted from the gel using a QIAGEN[®] gel extraction protocol after splitting each lane into three separate samples. The only modification to the manufacturer's protocol was to incubate the samples in buffer QG overnight at 65⁰C as opposed to simple vortexing. This step was necessary because Spreadex Gel does not readily dissolve like agarose.

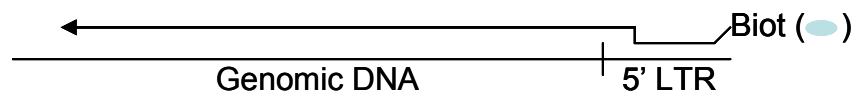
Linear Amplification Mediated (LAM)-PCR

1. Linear Amplification

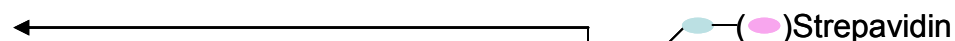
Possible Primers:

5'-Biot-ACCTCCACTCTAACACTTCTCTCTCC-3' "Green1"

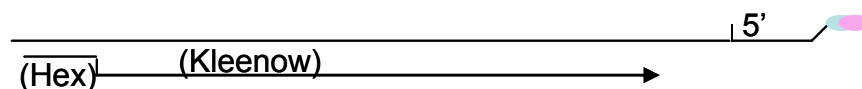
5'-Biot-CAGCAGTTCTTGAAGTACTCCGGATGCAG-3' (Hot) "Orange"



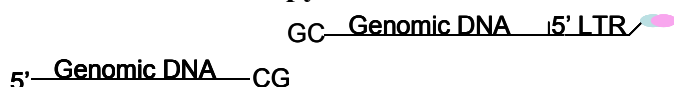
2. Magnetic Bead Binding



3. dsDNA Synthesis



4. Digestion w/ HinP1I or HpyCH4IV



5. Linker Cassettes

HIV-Link-38

5'-GGATTGACGACACGGTGACTTAAGTCTAGACGCCGCAG-3'

HIV-Link-31 5'-CTAGACTTAAGTCACCGTGTCGTCAATCCCG-3'

6. Ligation of Linker Cassette



7. 1st Nested Amplification

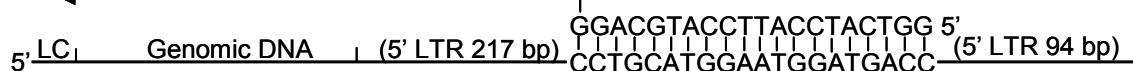
HIV-LC-nes-1 5'-CTGCGGCGTCTAGACTTAAGTC-3'

HIV-NesLTR-1 Orange Option 5'-GGTCATCCATTCCATGCAGG-3'

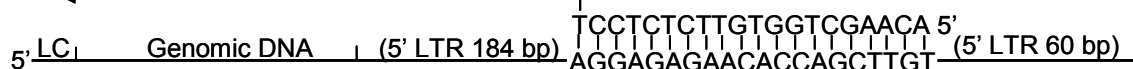
HIV-NesLTR-1 Green Option 5'-ACAAGCTGGTGTCTCTCCT-3'



Orange Option:



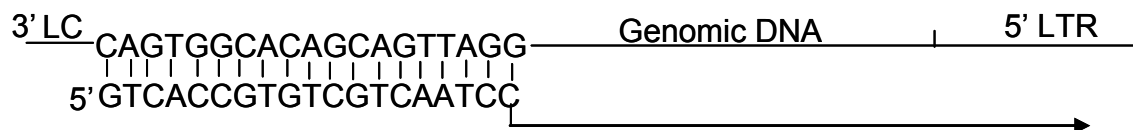
Green Option:



8. 2nd Nested Amplification

HIV-LC-nes-2 5'-GTCACCTAACTGCTGTGCC-3'

HIV-NesLTR2 Orange or Green 5'-GGTACTAGCTTGTAGCACCA-3'



Orange or Green Options:

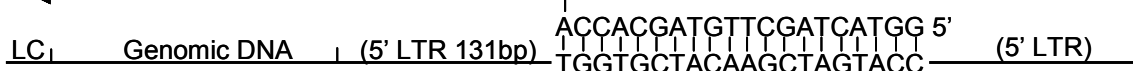


Figure 4.9. Outline of Linear Amplification Mediated (LAM)-PCR protocol. Amplification of the vector integration sites consists of several main steps. Biotinylated primers first synthesize several linear strands of DNA that originate in the 5' (or 3') LTR and proceed for an undetermined distance into the genomic DNA upstream of the integration site (step 1). These linear strands are then bound to magnetic beads via biotin (on the primer) binding strepavidin (on the bead). This allows the use of magnets to wash the products and exchange solutions without product loss (step 2). The complement to the linear DNA is then synthesized using random hexamer priming and Kleenow (step 3). The newly synthesized dsDNA is then digested with either *HinP1I* or *HpyCH4IV* (which should cleave any 3'LTR products from the orange option but may also cleave 5'LTR products non-specifically) both of which leave a hanging 3'GC (step 4). The linker cassette is a known sequence to allow priming of the 3' portion of the samples (which is unknown at this point) (step 5). The linker cassette has been designed with a complementary overhanging CG to ligate to the cleaved samples (step 6). The first nested amplification can then proceed using primers for the linker cassette and the 5'LTR (this system has been designed to anchor an overhanging region on the linker cassette, step 7). The second nested amplification then follows the first nested amplification and should generate sufficient quantities of each sample to allow sequencing (step 8). These samples can then be gel separated, extracted, TOPO cloned, and sequenced.

LM-PCR

To perform LAM-PCR, the purified DNA from each tissue source was first concentrated to yield 100ng/uL, so that 10uL of each sample contained 1µg of DNA for the initial digestion. The DNA was then digested with *MseI* and *PstI* (New England Biolabs) overnight at 37⁰C using the reaction mixture outlined in tbl. 4.2. Following overnight digestion, enzymes were heat inactivated for 20 min. at 65⁰C. (fig. 4.10, step 1)

Table 2: LM-PCR Digestion Reaction	
Component	Volume
10X NEB buffer 2	3µL
10X BSA	3µL
DNA	10µL (1µg)
<i>MseI</i>	1µL
<i>PstI</i>	1µL
H ₂ O	12µL
Total Vol	30µL

Table 4.2. Standard DNA digestion for LM-PCR. Sample DNA is concentrated to 100ng/µL allowing for an equal volume of 10µL of DNA to be added to each reaction mixture. 10X NEB buffer 3 along with 10X Bovine Serum Albumin (BSA), 20U of *MseI*, 20U of *PstI*, and 12µL of H₂O are all combined. Digestion of the DNA proceeds overnight at 37⁰C and heat inactivation of the enzymes occurs the following day during a 20 minute incubation at 65⁰C.

Following the initial digestion, assembly of the linker employs the DNA sequences Afl3-us-linker and Afl3-Is-linker (fig 10 step 2) at a concentration of 200 μ M each. 25 μ L of each linker is combined with 1 μ L of 50X STE (500mM Tris (pH 8.0), 2.5M NaCl, and 50mM EDTA) and the 51 μ L reaction is heated to 98 $^{\circ}$ C and cooled at a rate of 1 $^{\circ}$ C/min to a final temp of 4 $^{\circ}$ C. The annealed linker cassette is then ligated onto the overhanging MseI digested site using T4 DNA Ligase (high concentration) (New England Biolabs) overnight at 16 $^{\circ}$ C followed by warming to room temperature (23 $^{\circ}$ C) over 2½ hours and the reaction mixture outlined in table 3. (fig. 4.10, step 3)

Component	Volume
Digested DNA	15 μ L
10X NEB Ligase Buff.	2 μ L
100 μ M Linker Cassette	2 μ L
T4 DNA Ligase (high)	1 μ L
16 $^{\circ}$ C Overnight	
Warm to 23 $^{\circ}$ C	2.5 hours

Table 4.3. Standard Linker Cassette Ligation. 15 μ L of the digested DNA from the first step is combined with: 2 μ L of Ligase Buffer, 2 μ L of 100 μ M Linker Cassette, and 1 μ L of high concentration T4 DNA Ligase. The mixture is then incubated overnight at 16 $^{\circ}$ C and warmed to room temperature (23 $^{\circ}$ C) the following day over a period of 2½ hours.

Nested PCR was then employed to exponentially amplify the product using primers that were specific for the 5'LTR and linker cassette region described above (MseI 5'LTR Primer & AP1 Primer) along with nested primers (MseI 5'LTR nested Primer & Afl3 nested Primer) (fig. 4.10, steps 5-6) along with the PCR program outlined in tbl 4.4. PCR reaction components followed the protocol provided in the Platinum Taq package insert (Invitrogen). The first reaction and the nested reaction used 2 μ L of the ligated product and the first reaction, respectively. Primer sequences are as follows:

MseI 5'LTR Primer 5'-TAGCTTGCCAAACCTACAGGT-3'

AP1 Primer 5'-GTAATACGACTCACTATAGGGC-3'

MseI 5'LTR nested Primer 5'-ACCTACAGGTGGGGTCTTTCA-3'

Afl3 nested Primer 5'-AGGGCTCCGCTTAAGGGA -3'

Step #	Temperature (°C)	Time (min:sec)
1	95°C	2:00
2	95°C	:15
3	55°C	0:30
4	72°C	1:00
5	Go To Step 2, 24 Times	
7	4°C	----

Table 4.4. Standard PCR reaction program for LAM-PCR. The samples were amplified for two, 25 cycle reactions resulting in a total number of amplicons equal to X^{50} . This began with an initial denaturation of the DNA at 95°C for 2 minutes followed by a repeated denaturation at the same temperature for 15 seconds. The annealing temperature for the primer was 55°C for 30 seconds. Extension of the DNA then proceeded for 1 minute at 72°C and the denature, anneal, extend cycles were repeated 24 times. The

samples were stored at 4°C until the second nested reaction proceeded, following nested PCR samples were stored at -20°C.

Linker Mediated (LM)-PCR

1. Digestion w/ MseI and PstI

TA Genomic DNA | 5'LTR

2. Linker Cassettes

Afl3-us-Linker

5'-GTAATACGACTCACTATAGGGCTCCGCTTAAGGGAC-3'

Afl3-Is-Linker

5'- PO₄-TAGTCCCTTAAGCGGAG-NH₂-3'

3. Ligation of Linker Cassette

GTAATACGACTCACTATAGGGCTCCGCTTAAGGGACTA Genomic DNA | 5'LTR
 GAGGCGAATTCCTGAT

4. 1st Nested Amplification

MseI 5'LTR Primer 5'-TAGCTTGCCAAACCTACAGGT-3'

AP1 Primer 5'- GTAATACGACTCACTATAGGGC-3'

GTAATACGACTCACTATAGGGCTCCGCTTAAGGGACTA Genomic DNA | ACCTGTAGGTTTGGCAAGCTA
 TGGACATCCAACCGTTTCGAT

←

GTAATACGACTCACTATAGGGC
 CATTATGCTGAGTGATATCCCGAGGCGAATTCCTGAT Genomic DNA | TGGACATCCAACCGTTTCGAT
 5'LTR

5. 2nd Nested Amplification

MseI 5'LTR nested Primer 5'-ACCTACAGGTGGGGTCTTTCA-3'

Afl3 nested Primer 5'-AGGGCTCCGCTTAAGGGA -3'

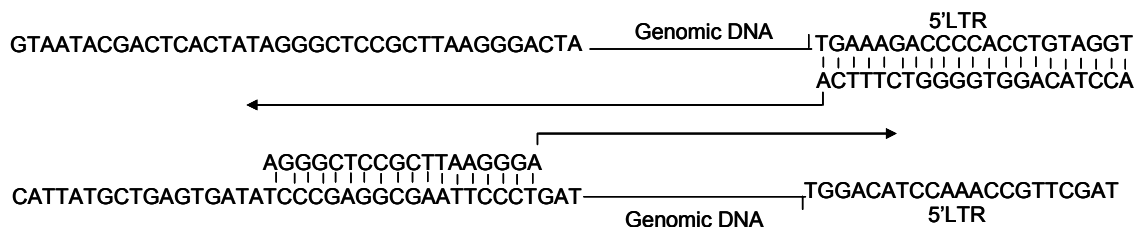


Figure 4.10. **Outline of Linker Mediated (LM)-PCR.** Unlike LAM-PCR, LM-PCR does not employ a biotinylation step but rather uses a control linker priming step. dsDNA is digested with MseI (which cleaves the genomic DNA at random intervals and the 5'LTR) and PstI (which cleaves the 3'LTR to avoid false positives) this cleavage leaves an overhanging TA in the human DNA (step 1). The linker cassette is a known sequence to allow priming of the 3' portion of the samples (which is unknown at this point) (step 2). The linker cassette has been designed with a complementary overhanging TA to ligate to the cleaved samples (step 3). The first nested amplification can then precede using primers for the linker cassette and the 5'LTR. The first round of PCR synthesizes the linker cassette primer binding site from the 5'LTR ensuring that amplicons containing LTR and linker cassette will out compete any non-specific ligations or primer binding (step 4). The second nested amplification then follows the first nested amplification and should generate sufficient quantities of each sample to allow sequencing (step 5). These samples can then be gel separated, extracted, TOPO cloned, and sequenced.

Sequencing

A modified TOPO protocol (Invitrogen) using the pCR[®] 2.1-TOPO[®] vector was employed to clone the gel-purified samples and non gel purified samples. The modified reaction mixture included 10µL of sample with 2µL each of salt solution and vector (with TOPO Isomerase). The ligated vector was then incubated for 1 hour in one reaction vial of TOP10 One Shot chemically competent *E. coli* (Invitrogen) cells at 37⁰C in a shaking incubator. 50-150µL of the transformed *E. coli* cell mixtures were then plated on Fast Media[®] LB plates with 50 µg/mL of Ampicillin and IPTG/X-Gal selection (Fermentas). The plates were then incubated 16-20 hours at 37⁰C.

Following incubation two possible selection and liquid culturing methods were employed. For LAM-PCR, white colonies were collected and cultured overnight in 5mL of Fast Media[®] Liquid LB Media with 50 µg/mL of Ampicillin (Fermentas) for 18-24 hours at 37⁰C in a shaking incubator. Plasmids were extracted using 4mL of culture and a QIAGEN[®] Plasmid Mini-Prep kit. 200ng of plasmid with 2pmol of forward sequencing primer were then sequenced by the Nevada Genomics Center using an Applied Biosystems (ABI) Prism 3730 DNA Analyzer. (fig 3) However, due to the better cost efficiencies and the potential for higher throughput when LM-PCR was developed, the culturing method was modified. White colonies were selected from the plates discussed above but were cultured in 1mL of Terrific Broth (Fermentas) in a 96 well-2mL plate with an AeraSeal breathable sealing film cover (Excel Scientific) at 37⁰C in a shaking incubator. The plasmids were then extracted using the QIAGEN 3000 bioRobot at the Nevada Genomics Center. 200ng of plasmid with 2pmol of forward sequencing primer were then used in the sequencing reaction at the NGC discussed above.

Sequence Analysis

Only sequences greater than 100bp and having acceptable Q20 values were analyzed. Sequences were batch analyzed in a multisequence FASTA file format against the NCBI Human Genome build 36 using the Nevada Bioinformatics Chloroplast site. Word size was set to 7 letters and only e-values less than 0.1 were kept. Positive results from the first screen were then batched into a Microsoft Word document and the retroviral and TOPO vector plasmid was identified and highlighted. The regions between the retroviral LTR and TOPO plasmid were then analyzed using megablast and blast

analysis through the NCBI website (www.ncbi.nlm.nih.gov/BLAST). Only sequences that were found to be uniquely human and with an e-value of 10^{-19} with at least a 98% identical match and few gaps were further analyzed. Further analysis investigated the location of the sequence on the chromosome and potential gene functions using the NCBI website.

Beta-actin screening

The beta-actin forward primer (5'- ACT CCT GCT TGC TGA TCC AC -3') and reverse primer (5'- TGG CTA CAG CTT CAC CAC C -3') were used in a 25 μ L PCR reaction with 1X Invitrogen buffer (w/o MgCl₂), 2mM MgCl₂, 0.2mM dNTP mix, 100ng of each primer, 1U Invitrogen Taq polymerase, 20ng of DNA, and PCR grade H₂O. The PCR mixture was then denatured for 4min. at 94⁰C followed by 30 cycles of 45sec. at 94⁰C, 30sec. at 55⁰C, and 45sec. at 72⁰C. The final extension was for 10min. at 72⁰C and the samples were stored at 4⁰C in the short term and -20⁰C long term.

Chimeric screening

The human specific, Factor VIII gene forward primer, FVIII 2a fwd, (5'- AGCTTTGAAACAATTCAGACTCC -3') and reverse primer, FVIII2a rev (5'- TACCTTTGCAATGGGTAATGG -3') were used in a 50 μ L PCR reaction with 1X Invitrogen buffer (w/o MgCl₂), 2mM MgCl₂, 0.2mM dNTP mix, 0.5 μ M primers, 1U Invitrogen Taq polymerase, 2.5ng of DNA, and PCR grade H₂O. The PCR mixture was then denatured for 4min. at 94⁰C followed by 53 cycles of 20sec. at 94⁰C, 20sec. at 55⁰C, and 30sec. at 72⁰C. The final extension was for 10min. at 72⁰C and the samples were stored at 4⁰C in the short term and -20⁰C in the long term.

References:

1. Almeida-Porada G, Chamberlain J, Frias AM, Porada C. Tissue of Origin Influences In Vivo Differentiative Potential of Mesenchymal Stem Cells. *Blood*. 2003;102.
2. Schmidt M, Kohn HGMWGHKOSSDCJFTCLHHCEDH-PKSKDB. Efficient Characterization of Retro-, Lenti-, and Foamyvector-Transduced Cell Populations by High-Accuracy Insertion Site Sequencing. *Annals of the New York Academy of Sciences*. 2003;996:112-121.
3. Colletti EJ, Airey JA, Liu W, et al. Generation of tissue-specific cells from MSC does not require fusion or donor to host mitochondrial/membrane transfer. *Stem Cell Research*. 2009;2:125-138.
4. Wagers AJ, Weissman IL. Plasticity of Adult Stem Cells. *Cell*. 2004;116:639-648.
5. Hacein-Bey-Abina S, Le Deist F, Carlier F, et al. Sustained Correction of X-Linked Severe Combined Immunodeficiency by ex Vivo Gene Therapy. *New England Journal of Medicine*. 2002;346:1185-1193.
6. Handgretinger R, Koscielniak E, Niethammer D, Cavazzana-Calvo M, Hacein-Bey-Abina S, Fischer A. Gene Therapy for Severe Combined Immunodeficiency Disease. *New England Journal of Medicine*. 2002;347:613-614.
7. Rosen FS. Successful Gene Therapy for Severe Combined Immunodeficiency. *New England Journal of Medicine*. 2002;346:1241-a-1243.
8. Baum C, von Kalle C, Staal FJT, et al. Chance or necessity? Insertional Mutagenesis in Gene Therapy and Its Consequences. *Mol Ther*. 2004;9:5-13.
9. Hacein-Bey-Abina S, Von Kalle C, Schmidt M, et al. LMO2-Associated Clonal T Cell Proliferation in Two Patients after Gene Therapy for SCID-X1. *Science*. 2003;302:415-419.
10. McCormack MP, Rabbitts TH. Activation of the T-Cell Oncogene LMO2 after Gene Therapy for X-Linked Severe Combined Immunodeficiency. *New England Journal of Medicine*. 2004;350:913-922.
11. Kaiser J. GENE THERAPY: Seeking the Cause of Induced Leukemias in X-SCID Trial. *Science*. 2003;299:495-.
12. Kohn D, Michel S, Glorioso J. Occurrence of Leukaemia Following Gene Therapy of X-Linked SCID. *Nature Reviews: Cancer*. 2003;7:477-488.
13. Woods N-B, Muessig A, Schmidt M, et al. Lentiviral vector transduction of NOD/SCID repopulating cells results in multiple vector integrations per transduced cell: risk of insertional mutagenesis. *Blood*. 2003;101:1284-1289.
14. Wu X, Li Y, Crise B, Burgess SM. Transcription Start Regions in the Human Genome Are Favored Targets for MLV Integration. *Science*. 2003;300:1749-1751.
15. Tan G, Gao Y, Shi M. SiteFinding-PCR: a simple and efficient PCR method for chromosome walking. *Nucleic Acids Research*. 2005;33:122.
16. Naldini L, Blomer U, Gallay P, et al. In Vivo Gene Delivery and Stable Transduction of Nondividing Cells by a Lentiviral Vector. *Science*. 1996;272:263-267.
17. Poeschla E, Corbeau P, Wong-Staal F. Development of HIV vectors for anti-HIV gene therapy. *PNAS*. 1996;93:11395-11399.

18. Schröder ARW, Shinn P, Chen H, Berry C, Ecker JR, Bushman F. HIV-1 Integration in the Human Genome Favors Active Genes and Local Hotspots. *Cell*. 2002;110:521-529.
19. Hawley RG, Lieu FHL, Fong AZC, Hawley TS. Versatile retroviral vectors for potential use in gene therapy. *Gene Therapy*. 1994;1:136-138.
20. Calmels B, Ferguson C, Laukkanen MO, et al. Recurrent retroviral vector integration at the Mds1/Evi1 locus in nonhuman primate hematopoietic cells. *Blood*. 2005;106:2530-2533.
21. Schmidt M, Zickler P, Hoffmann G, et al. Polyclonal long-term repopulating stem cell clones in a primate model. *Blood*. 2002;100:2737-2743.
22. Thrasher AJ, Hacein-Bey-Abina S, Gaspar HB, et al. Failure of SCID-X1 gene therapy in older patients. *Blood*. 2005;105:4255-4257.
23. Margulies M, Egholm M, Altman WE, et al. Genome sequencing in microfabricated high-density picolitre reactors. *Nature*. 2005;437:376-380.
24. Wang GP, Ciuffi A, Leipzig J, Berry CC, Bushman FD. HIV integration site selection: Analysis by massively parallel pyrosequencing reveals association with epigenetic modifications. *Genome Research*. 2007;17:1186-1194.
25. Farshid Guilak KELHAAQCKCHBFJMG. Clonal analysis of the differentiation potential of human adipose-derived adult stem cells. *Cellular Physiology*. 2006;206:229-237.

Chapter 5: **Conclusions**

The primary avenue of EPC research continues to be in the area of vasculogenesis and in therapy following cardiac complications. These cells are currently employed in clinical trials in this capacity. Levels of circulating EPCs are also being researched as a predictor of the risk of cardiac conditions such as infarction.¹ Research into the ability to vascularize ischemic kidney tissue following acute injury and revive kidney function is also being conducted. Advances in this area would result in novel therapies for the treatment of renal failure.² In addition to vasculogenesis related research, EPC populations are mobilized from the bone marrow of diabetic mice and are being researched as a potential source of insulin producing cells.³ Research is also being conducted as it relates to senescence of EPC populations by TNF α as a result of both aging and atherosclerosis.⁴

This dissertation provides evidence that EPCs actively engraft and contribute to the developing liver and small intestine. We first demonstrate that transplanted EPCs can be found in the bone marrow and peripheral blood of transplanted animals. We then show that engrafted EPCs compose 0.013% - 0.43% of the liver following transplantation. Furthermore, 91.69 – 98.70% of the donor derived EPCs engrafted in and around vasculature in the liver. The engrafted EPCs were found to actively participate in the liver cytoarchitecture through the formation of tight junctions, which was demonstrated by connexin 45 staining. The EPCs engrafted in the liver primarily functioned to support vasculogenesis and maintained expression of CD31 and vWF. In addition to these roles, engrafted cells also contributed to the liver parenchyma by expressing Factor VIII and CD45 in a small number of cases. EPCs even made minor contributions to the formation

of new liver as liver stem cells based on the expression of Ov6. Overall, the role of EPCs in the liver appears to primarily relate to vasculogenesis as they have been classically demonstrated to do in other organs such as the heart.

The role of donor derived EPCs in the small intestine are very different from that found in the liver. In the small intestine, 81.89% of donor derived cells were found to engraft in and around the crypts of Lieberkühn (CPT region) and 13.63% of donor derived cells engrafted in the villi region. The remaining population of cells were found in the muscularis mucosa (which is directly adjacent to the CPT region) and in the sub-mucosa region. In contrast to liver engrafted EPCs, only 0.7% - 1.7% of donor derived cells maintained expression of vWF and CD31. Senescence of these endothelial markers is evidence that differentiation away from the endothelial lineage has occurred. Furthermore, 37.66% of the engrafted EPCs expressed the intestinal stem cell (ISC) marker, Musashi. In addition to contribution to the ISC population, 25.37% of the donor derived cells expressed both vimentin and smooth muscle actin. This evidence demonstrates that the EPCs differentiated into both ISCs and ISC niche supporting myofibroblasts. Donor derived EPCs were also found to contribute to the interstitial cell population given CD117 expression in 9.46% of the donor derived cells. Some of the interstitial cells were found in the villi region as were donor derived epithelial and enteroendocrine cells. Less than 1% of the donor derived cells were found to express the epithelial cell marker, cytokeratin 20. Another small population of EPCs (<1%) were found to express the enteroendocrine marker, chromogranin A. While the contribution to the mature intestinal cell population is small, further studies are needed to demonstrate

whether this is a function of the developmental stage of the small intestine, a function of the cells themselves, or some other factor such as silencing of the DsRed gene in fully differentiated cells.

In the animals studied, two different injection routes were studied as were two different cell doses. Transplanted animals received comparable cell doses either intra-hepatically (IH, n=5) or intra-peritoneally (IP, n=10). Furthermore, a group of IH injected animals received 1.6×10^6 cells (n=4) each, a group of IP injected animals received 1.3×10^6 (n=4) cells each, and another group of IP injected animals received a higher cell dose of 2.6×10^6 (n=4) cells each. In the liver, IP injected animals had significantly higher vascular contribution and CD45 expression but significantly lower CD31 and vWF expression compared to IH injected animals. However, further investigation of the IP injected cell doses revealed that some of the cells were injected at a much lower passage number than other cell doses and vWF expression was significantly higher in lower passage (younger) EPCs than in later passage EPCs. While statistical significance was not found, CD31 expression was higher and CD45 expression was lower in early passage IP injected cells than in later passage IP injected cells. This evidence indicates that later passage EPCs may have already experienced some degree of differentiation before injection than earlier passage EPCs. However, this evidence does not entirely explain the significantly higher vascular contribution & CD45 expression in conjunction with significantly lower CD31 and vWF expression found in IP injected animals when analyzed in conjunction with comparable cell doses in IH injected animals.

Given this evidence, we conclude that donor derived cells in IP injected animals differentiate to a greater degree than IH injected animals in the liver.

The same injection route and cell dose characteristics also apply to the donor derived cell populations found in the small intestine. Contribution to the CPT region by donor derived cells did not vary significantly under different injection route or cell dose conditions. In contrast, contribution to the ISC population did vary based on injection route; significantly more donor derived cells expressed Musashi when injected IP than when injected IH. Furthermore, IH injected cells retained expression of the EPC marker, CD133, to a greater degree than IP injected cells. This evidence demonstrates that IP injected cells differentiated to a greater degree than IH injected cells and is in concurrence with the liver that IP injected cells demonstrate a greater capacity for differentiation than IH injected cells.

Recently, several sub-populations of EPCs have been identified and characterization of the EPC lineage is needed.⁵ Therefore, the possibility that some of the effects we are observing are due to a heterogeneous population of cells as opposed to the effects of injection route or cell dose. While successful sequencing of a chimeric sample has yet to be obtained, vector integration site analysis would successfully address the question of a heterogeneous population of EPCs as compared to a homogenous population just as it would for MSCs. LM-PCR of these samples would provide evidence of either a homogenous or heterogeneous population of cells. Despite the discovery of pyro-sequencing, both LAM-PCR and LM-PCR continue to be employed in vector

integration site analysis.^{6,7} The primary applications for both techniques continue to be related to safety studies of gene therapy and clonal analysis of transfected cells.

LAM-PCR was initially employed in our lab to identify the vector integration sites of HIV based vectors in transplanted MSCs. Analysis using LAM-PCR was able to successfully identify only one vector integration site in DNA from MSCs that were cultured *In vitro*. Further analysis revealed this sequence to be on chromosome 17. The LM-PCR protocol was then employed to identify vector integration sites in the same control DNA analyzed via LAM-PCR. While several integration sites were identified in positive control, the same integration site on chromosome 17 that was found using LAM-PCR was not found using LM-PCR. Operating under the hypothesis that the engraftment level in the chimeric samples were below the detection threshold of the LM-PCR system, the intestine of the EPC transplanted animals was employed in our analysis because of its higher engraftment level. However, the EPC carry integrations from an MSCV based vector as opposed to the HIV based vector we had initially been researching. LM-PCR for MSCV integration sites had previously been used in the lab so this system was employed to study the integration sites. LM-PCR analysis revealed a smear in the positive control cells following electrophoresis as had been previously observed by Chris Clark and others in our lab but no bands were detected in chimeric samples. Further analysis using PCR primers for the house keeping gene, beta actin, confirmed the presence of amplifiable DNA in the small intestine DNA. Additionally, a set of primers designed by Chad Sanada for human specific PCR to amplify the Factor VIII gene demonstrates the chimerism of the small intestine DNA. This result confirms the

presence of human DNA and sequencing of these samples and the positive control samples will be employed in future experiments.

While these studies have been ongoing, there have been advances in the field of vector integration site sequencing and in tracking the clonal populations of MSCs. The invention of pyrosequencing allows the sequencing of genomes at 100-fold higher throughput. The sequencing of the whole genome eliminates any biases that LM and LAM-PCR have and the high throughput allows the rapid detection of several integration sites across multiple DNA sources.^{8,9} However, pyrosequencing is cost prohibitive and would require collaboration and additional funding for our lab to apply this technology to the current studies. LAM-PCR and/or LM-PCR continue to be sufficient for the analysis of vector integration sites in many situations including our own. Furthermore, clonal analysis of adipose derived adult stem cells which are similar in surface and adhesion markers to MSCs have been shown to differentiate into at least two different tissue types at the clonal level.¹⁰ This study suggests that MSC populations are likely to be homogenous in nature. Despite this evidence, the debate continues on this research and future findings in this project will continue to be pertinent. In addition to the debate with MSCs, the questions of homogeneity vs. heterogeneity in EPCs populations are just beginning and analysis of the EPC transplanted animals is as pertinent of a question as the homogeneity of MSC populations.

The work presented in this dissertation advances our knowledge of EPCs and their differentiative capabilities. The demonstration of vascular contribution in the liver by EPCs shows the diversity of these cells and provides the potential for a future cell therapy

in the treatment of cirrhotic and other liver diseases. Very few researchers are looking at the role of EPCs in the small intestine and the vast majority of the work in this area relates to engineered small bowel as opposed to cell therapy. Our findings demonstrate the potential for EPCs to be developed as a clinical therapy for the regeneration of small intestine following a myriad of diseases and disorders. Finally, the research into the nature of the currently defined populations of MSCs and EPCs continues to progress and successful cloning of integration sites in these cell populations will answer questions related to their clonal nature as well as safety questions related to the gene therapy vectors employed in these studies.

References

1. Sven Möbius-Winkler RHGSVA. Endothelial progenitor cells: Implications for cardiovascular disease. *Cytometry*. 2009;75A:25-37.
2. Becherucci F, Mazzinghi B, Ronconi E, et al. The Role of Endothelial Progenitor Cells in Acute Kidney Injury. *Blood Purification*. 2009;27:261-270.
3. Cheen Peen Khoo MGVMBMRAGWUJMHPP. Characterization of endothelial progenitor cells in the NOD mouse as a source for cell therapies. *Diabetes Metabolism*. 2009;25:89-93.
4. Zhang Y, Herbert B-S, Rajashekhar G, et al. Premature senescence of highly proliferative endothelial progenitor cells is induced by tumor necrosis factor- α via the p38 mitogen-activated protein kinase pathway. *FASEB*. 2009;e-pub:fj.08-110296.
5. Alvarez DF, Huang L, King JA, ElZarrad MK, Yoder MC, Stevens T. Lung microvascular endothelium is enriched with progenitor cells that exhibit vasculogenic capacity. *American Journal of Physiology - Lung Cellular and Molecular Physiology*. 2008;294:L419-430.
6. Kustikova OS, Modlich U, Fehse B, Baum C. Genetic Modification of Hematopoietic Stem Cells Methods and Protocols. *Methods In Molecular Biology*. Vol. 506: Humana Press; 2009.
7. Schmidt M, Schwarzwaelder K, Bartholomae CC, Glimm H, Kalle Cv, Baum C. Detection of Retroviral Integration Sites by Linear Amplification-Mediated PCR and Tracking of Individual Integration Clones in Different Samples *Methods In Molecular Biology*. Vol. 506: Humana Press; 2009.
8. Margulies M, Egholm M, Altman WE, et al. Genome sequencing in microfabricated high-density picolitre reactors. *Nature*. 2005;437:376-380.
9. Wang GP, Ciuffi A, Leipzig J, Berry CC, Bushman FD. HIV integration site selection: Analysis by massively parallel pyrosequencing reveals association with epigenetic modifications. *Genome Research*. 2007;17:1186-1194.
10. Farshid Guilak KELHAAQCKCHBFJMG. Clonal analysis of the differentiation potential of human adipose-derived adult stem cells. *Cellular Physiology*. 2006;206:229-237.

Glossary of Cellular Proteins and Labels

Albumin

Albumin is produced in the liver by the hepatocytes and is then secreted into the blood stream. Albumin composes approximately half of the blood volume as in used to carry steroids, fatty acids, and thyroid hormones.¹ Immunofluorescent labeling for albumin labels the parenchyma of the liver.

Alpha Fetoprotein (α FP)

Alpha fetoprotein is a protein expressed in the developing liver and the yolk sac of the embryo. α FP is thought to be the embryonic equivalent to serum albumin.² Labeling for α FP in the fetal liver labels all parenchyma.

CD13

CD13 is an aminopeptidase N (APN) which is a metalloprotease (type II) that is only expressed on endothelium that is capable of angiogenesis. CD13 is involved in the Ras signaling pathway and is therefore involved in endothelial cell morphogenesis. Antibody labeling for CD13 therefore labels cells circulating endothelial cells that are capable of vasculogenesis.³

CD31 (PECAM-1)

Platelet endothelial cell adhesion marker-1 (PECAM-1) is an immunoglobulin super family molecule that is responsible for trafficking leukocytes across the endothelium. It also is involved in angiogenesis and removing aged neutrophils in the body. The ligand that binds the PECAM-1 receptor is CD38. Antibody stains against CD31 label endothelial cells, monocytes, macrophages, Kupffer cells, osteoclasts, and T/NK cells.⁴

CD34

CD34 is an intercellular adhesion protein and cell surface glycoprotein that may mediate attachment of stem cells to bone marrow, extracellular matrix, or stromal cells. Antibody stains against CD34 label endothelial cells, hematopoietic stem cells, hematopoietic lineage cells, dendritic interstitial cells.⁴

CD45

Leukocyte common antigen (CD45) is an essential regulator of T and B cells activation through receptor mediated antigen. This protein tyrosine phosphatase is also involved in thymic selection of T cells. Antibody stains against CD45 label most hematopoietic cells.⁴

CD117

CD117 is also known as KIT or the C-kit receptor and is a surface cytochromeratin receptor found classically on hematopoietic stem cells.⁵ CD117 is also used to identify interstitial cells of cajal, a pace maker cell type, in the small intestine.⁶ Immunofluorescent labeling for CD117 labels the smooth muscle and muscularis mucosa which lines the bottom of the crypt region and has projections up through the crypt and into the villi.

CD133

Initially named AC133, CD133 is a five transmembrane domain glycoprotein that is 120kDa in size. CD133 is expressed on CD34+ hematopoietic stem cells as well as endothelial progenitor cells and neural stem cells. The expression pattern resembles that of the prominin molecule in mice and it is sometimes referred to as prominin-like for this reason. Mutations in the CD133 gene have also been linked to retinal degeneration in

humans and thus the CD133 molecule is probably linked to proper retina structure and function as well.⁷

Connexin 43

Connexin 43 is a gap junction protein in the plasma membrane of vertebrate cells. Connexin 43 is involved in the formation of the gap junction between cells that allows cellular signals to be relayed between cells.⁸ Immunofluorescent labeling for connexin 43 labels the cell membrane in a punctuate manner.

Connexin 45

Connexin 45 is a gap junction protein in the plasma membrane of vertebrate cells. While the specific role of connexin 45 is not fully elucidated it is reported to be involved in the formation of vasculature and is related to the gap junction between endothelial cells.⁹

Cytokeratin 20

Cytokeratin 20 is an intermediate filament of the cytoskeleton and is responsible primarily responsible for structure and transport of vesicles within the cell. In the small intestine Cytokeratin 20 is found in the intestinal mucosa in mature enterocytes and goblet cells.¹⁰ Immunofluorescent labeling for Cytokeratin 20 labels the villi of the small intestine and is particularly bright on goblet cells.

Ephrin B2

The ephrins are receptor-like ligands bound to the cell membrane that are responsible for cell trafficking in the small intestine. The “B” family of ephrins is composed of transmembrane proteins as opposed to the “A” family which are tethered to the outer membrane.¹¹ Ephrin B2 is a ligand that is responsible for the location of the

maturing intestinal cell along the side wall of the crypt and is strongest at the base of the crypt on the +4 position intestinal stem cells.¹² Staining for the Ephrin B2 ligand labels the majority of the crypt region and resembles musashi labeling.

Factor VIII:C

Factor VIII:C (FVIII) is a blood coagulation protein that forms a complex with von Willebrand Factor during clotting.¹³ Additionally, Factor VIII:C is produced in the liver. Labeling for FVIII labeled specific cells within the parenchyma.

Hepar

Hepar is not very well defined but it is known to be an antigen contained within the mitochondrial fraction of liver hepatocytes. Hepar is also known to work best with paraffin embedded sections though it does work with frozen section as well.¹⁴ Immunofluorescent labeling within the liver labels rings around the human hepatocytes.

Lgr5

Lgr5 (GPCR-49) is a G-protein coupled receptor containing a leucine rich repeated region. Expression of Lgr5 is limited to the crypt region in the small intestine. Antibody labeling for Lgr5 labels crypt base columnar cells. Evidence indicates that this may be a slow dividing population of intestinal stem cells (ISC) located at the base of the crypt as opposed to a more rapidly dividing ISC population found around the +4 position from the base of the crypt.¹⁵

Musashi

The musashi gene was first identified in *Drosophila* where it was found to be necessary for asymmetric division of sensory organ precursor cells. In mammals the musashi-1 gene encodes an RNA binding product originally associated with asymmetric

divisions during differentiation of neural stem cells. Musashi labeling was then discovered to label adult intestinal stem cells in the dividing and regenerating region known as the crypt.¹⁶

Ov-6

Oval cell marker 6 (Ov-6) is expressed on adult liver stem cells. These hepatic stem cells can differentiate into hepatocytes in the liver.¹⁷ Antibody labeling with Ov-6 antibodies reveals small clusters near forming biliary ducts in the fetal liver.

Smooth muscle actin

Alpha-smooth muscle actin (SMA) is an active microfilament believed to be involved in contraction of smooth muscle cells. Antibody labeling for SMA therefore labels filaments in the cytoplasm of smooth muscle cells.¹⁸ Cells that are positive for both SMA and Vimentin in the area surrounding the crypt of the small intestine are myofibroblasts which support the intestinal stem cells (ISCs) and are part of the ISC niche (discussed in later chapters).¹⁹

STRO-1

Stro-1 is expressed on the cell surface of stromal cells primarily found in the bone marrow. Classic applications of stro-1 are to enhance selection of MSCs from isolated bone marrow mononuclear cells. Selection using stro-1 results in 100-fold enrichment of CFU-F in culture.²⁰

Transferrin

Transferrin is a major iron carrying protein. It primarily carries ferric iron from the intestine and liver parenchyma to the rest of the dividing cells of the body.²¹ Immunofluorescent labeling in the liver for transferrin labels the entire parenchyma.

Vimentin

Vimentin contains an alpha helical domain that coils into a dimer with the alpha domain of another vimentin molecule. The dimer then forms a tetramer and this tetramer serves as an intermediate filament in the cytoskeleton of the cell. Vimentin can serve as an active component of the cytoskeleton allowing the cell some flexibility particularly in fibroblasts.²² Antibody labeling for vimentin labels the filaments inside the cell.

von Willebrand Factor

von Willebrand Factor (vWF) is responsible for the adhesion of platelets to sites of vascular trauma. The protein itself is a blood glycoprotein that is ~250kDa as a monomer but subunits link to form multimers larger than 20,000kDa. vWF is also a carrier protein for the clotting protein factor VIII. Antibody labeling against vWF reveals its expression in the liver as well as by endothelial cells.²³

References

1. Abcam. Human Serum Albumin data sheet; 2009.
2. Entrez G. AFP alpha fetoprotein; 2009.
3. Bhagwat SV, Petrovic N, Okamoto Y, Shapiro LH. The angiogenic regulator CD13/APN is a transcriptional target of Ras signaling pathways in endothelial morphogenesis. *Blood*. 2003;101:1818-1826.
4. Pernick N. PathologyOutlines.com. Vol. 2009; 2008.
5. Linnekin D. Early signaling pathways activated by c-Kit in hematopoietic cells. *The International Journal of Biochemistry & Cell Biology*. 1999;31:1053-1074.
6. Seidal E. Expression of c-kit (CD117) and Ki67 provides information about the possible cell of origin and clinical course of gastrointestinal stromal tumours. *Histopathology*. 1999;34:416-424.
7. Miraglia SJ, Buck D. AC133 (CD133). *PROW*. 2001;2:4-8.
8. Musil LS, Goodenough DA. Multisubunit assembly of an integral plasma membrane channel protein, gap junction connexin43, occurs after exit from the ER. *Cell*. 1993;74:1065-1077.
9. Kruger O, Plum A, Kim JS, et al. Defective vascular development in connexin 45-deficient mice. *Development*. 2000;127:4179-4193.
10. Moll R, Zimbelmann R, Goldschmidt MD, et al. The human gene encoding cytokeratin 20 and its expression during fetal development and in gastrointestinal carcinomas. *Differentiation*. 2006;53:75-93.
11. Hafner C, Meyer S, Langmann T, et al. Ephrin-B2 is differentially expressed in the intestinal epithelium in Crohn's disease and contributes to accelerated epithelial wound healing in vitro. *World J Gastroenterol*. 2005;11:4024-4031.
12. Scoville DH, Sato T, He XC, Li L. Current View: Intestinal Stem Cells and Signaling. *Gastroenterology*. 2008;134:849-864.
13. Dictionary OM. Medical Dictionary Online; 2008.
14. Dakocytomation. Mouse anti human hepatocyte; 2002.
15. Barker N, van Es JH, Kuipers J, et al. Identification of stem cells in small intestine and colon by marker gene *Lgr5*. *Nature*. 2007;449:1003-1007.
16. Potten CS, Booth C, Tudor GL, et al. Identification of a putative intestinal stem cell and early lineage marker; *musashi-1*. *Differentiation*. 2003;71:28-41.
17. Biotech SC. Oval Cell Marker (OV-6). Vol. 2009: Santa Cruz Biotechnology Inc.; 2007.
18. Skalli O, Pelte MF, Pecelet MC, et al. Alpha-smooth muscle actin, a differentiation marker of smooth muscle cells, is present in microfilamentous bundles of pericytes. *Journal of Histochemistry and Cytochemistry*. 1989;37:315-321.
19. Yen T-H, Wright N. The gastrointestinal tract stem cell niche. *Stem Cell Reviews*. 2006;2:203-212.
20. Invitrogen. Mouse anti-STRO-1. Vol. 2009; 2008.
21. YANG F, LUM JB, MCGILL JR, et al. Human transferrin: cDNA characterization and chromosomal localization. *Proc Natl Acad Sci USA*. 1984;81:2752-2756.

22. Fuchs E, Weber K. Intermediate Filaments: Structure, Dynamics, Function and Disease. *Annual Reviews of Biochemistry*. 1994;63:345-382.
23. Sadler JE. BIOCHEMISTRY AND GENETICS OF VON WILLEBRAND FACTOR. *Annual Reviews of Biochemistry*. 1998;67:395-424.